Biodegradable Nanoparticles Based on Aliphatic Polyesters; Towards Targeted Intracellular Delivery of Protein Therapeutics

Neda Samadi

2014

The printing of this thesis was financially supported by:
Utrecht Institue for Pharmaceutical Sciences, Utrecht, The Netherlands

Biodegradable Nanoparticles Based on Aliphatic Polyesters; Towards Targeted Intracellular Delivery of Protein Therapeutics

Neda Samadi

Ph.D. Thesis

Department of Pharmaceutics, Utrecht Institute for Pharmaceutical Sciences (UIPS), Faculty of Science, Utrecht University, the Netherlands

ISBN: 978-90-393-6134-4

Cover

Erik Oude Blenke

Print

CPI Wohrman Print Service

Copy right © 2014 by Neda Samadi

All rights resrved. No parts of this book may be reproduced in any form or by any means without permission of the author.

Biodegradable Nanoparticles Based on Aliphatic Polyesters; Towards Targeted Intracellular Delivery of Protein Therapeutics

Biodegradeerbare nanodeeltjes gebaseerd op alifatische polyesters voor de doelgerichte afgifte van therapeutische eiwitten

(met een samenvatting in het Nederlands)

Proefschrift

ter verkrijging van de graad van doctor aan de Universiteit Utrecht op gezag van de rector magnificus, prof.dr. G.J. van der Zwaan, ingevolge het besluit van het college voor promoties in het openbaar te verdedigen op maandag 14 april 2014 des middags te 4.15 uur

door

Neda Samadi

geboren op 5 februari 1978 te Tehran, Iran

Promotor: Prof.dr. ir. W. E. Hennink

Co-promotoren: Dr. C. F. van Nostrum

Dr. M. Amidi

“The two hardest tests on the spiritual road are the patience to wait for the right moment and the courage not to be disappointed with what we encounter.”

Paulo Coelho, Veronika Decides to Die

To My Family

Contents

Chapter 1 General Introduction 10

Chapter 2 The Effect of Lauryl End-Group Capping on Protein Release and Degradation of Poly(D,L-lactic-co-glycolic acid) Particles 30

Chapter 3 Mechanistic Studies on the Degradation and Protein Release Characteristics of Poly(lactic-co-glycolic-co-hydroxymethylglycolic acid) Nanospheres 58

Chapter 4 Nanoparticles Based on a Hydrophilic Polyester with a Sheddable PEG Coating for Protein Delivery 88

Chapter 5 Nanobody-Targeted and RNase-Loaded Nanoparticles Based on a Hydrophilic Polyester Aimed for Cancer Therapy 118

Chapter 6 Summary and Discussion 148

Appendices Nederlandse samenvatting 158

Acknowledgments 165

Curriculum Vitae 171

List of Publications 173

1

General Introduction

1. Therapeutic peptide and proteins

1.1. General

Many proteins and peptides posses specific biological activity that makes them potentially suitable as therapeutic agents for the treatment of various severe chronic and life-threatening diseases such as cancer, diabetes, several viral infections, and rheumatoid arthritis. A considerable striking and, probably, the best investigated class of protein therapeutics is that of exogenous enzymes including enzymes that act by destroying certain amino acids required for tumor growth (asparaginase), enzymes for replacement therapy (usually digestive enzymes to treat patients suffering from metabolic disorders, enzymes for the treatment of lysosomal storage diseases, enzymes for thrombolytic therapy (streptokinase, tissue plasminogen activator), antibacterial and antiviral enzymes (callipeltins and quinoxapeptins) and anti-inflammatory enzymes (serratiopeptidase).

1.2. Pharmaceutical proteins and peptides for cancer therapy

Peptides such as somatostatin analogs (octreotide, lanreotide, vapreotide) have acquired clinical applications for the treatment of pituitary and gastrointestinal disorders and tumors. Anti-angiogenic peptides including endostatin are currently in different stages of clinical trials and show a great promise for the treatment of different cancers like metastatic prostate cancer [1, 2]. Depsipeptides, that are oligomers composed of hydroxy and amino acids linked by amide and ester bonds, have also potential anticancer effects and one compound, the histone deacetylase inhibitor depsipeptide (FK228), is currently in a phase II clinical trial [3]. Antibodies that bind to certain tumor-specific ligands are also clinically used as anticancer drugs [1, 4, 5].

1.2.1. Protein toxins

Some proteins, named toxins, are extremely cytotoxic by virtue of their ability to inhibit protein biosynthesis. They vary both in structure and mode of action and can be applied in cancer therapy because they are among the most potent cell-killing agents [6]. These toxins have enzymatic activity and only a small number of molecules need to enter the cytosol to cause cell death. It has even been reported that only one molecule of a toxin delivered into the cytoplasm of a cancer cell is lethal [7]. Well known protein toxins include Diphtheria toxin (DT), Pseudomonas exotoxin A (PE) and Shigella toxin (bacterial toxins) and Ricin (plant toxin), which consist of two subunits linked by disulfide bridges. The B-subunit facilitates the entry of the toxin by binding to the cell surface and the enzymatic activity is at the A-subunit [8, 9]. The internalization of these toxins by target cells always involves three typical steps. First, the toxin binds to the cell surface through its specific binding domain and subsequently enters the cells via endocytosis to end up in cellular compartments (endosome/lysosome and/or trans-Golgi network). Cells that lack the membrane protein that is recognized by the binding domain of a toxin, consequently are resistant to these proteins. In the second step, the internalized toxins are split by proteases into its individual A and B fragments. The acidity of the endosome causes fragment B to create pores in the endosome membrane, thereby triggering the release of fragment A into the cytoplasm. Fragment A inhibits the synthesis of proteins by different mechanisms. To be therapeutically applicable for cancer therapy, these toxins need to be targeted to cancer cells, then be internalized and ultimately reach the cell cytoplasm. To this end, toxins have been conjugated to ligands that selectively target cancer cells. Typically, toxins have been conjugated to growth factors or monoclonal antibodies specific for a receptor expressed on the cell population of interest. Targeted toxins containing antibodies or antibody fragments are called immunotoxins (ITs) [6, 10]. Although several ITs have reached clinical trials, their therapeutic efficacy has not been fully exploited because of immunogenicity of the conjugate and toxicity due to disposition in non-target tissues and organs [11]. Most toxins damage vascular endothelial cells, liver or renal cells directly or indirectly through the induction of inflammatory responses [11, 12]. Due to these undesirable side effects, attention was put on other cytotoxic proteins, such as those of the mammalian ribonuclease (RNase) superfamily.

1.2.2. Ribonucleases (RNases)

RNases are stable secretory proteins with different biological functions such as maintenance of the cellular RNA pool, aid in food digestion, host defense and angiogenesis [13-15]. Human RNases are present in extracellular fluids and are not immunogenic, but they can exhibit cytotoxic activities if these proteins enter cells. Host cells are protected from endogenous RNases by ribonuclease inhibitor (RI), a ubiquitous cytosolic protein present at relatively high concentrations in the cytosol of cells. RI binds the active sites of most mammalian RNases with high affinity and thereby protects cells against rogue RNases that access the cytosol [16, 17]. RNases exert their cytotoxic properties by enzymatic activity. They degrade RNA by removing terminal nucleotides from either the 5’ end or the 3’ end of the RNA molecule or cleave phosphodiester bonds within a polynucleotide chain. They are small (10–28 kDa) basic proteins and bind to negatively charged cell membranes, enter cells by endocytosis, translocate into cytosol and when evading RI they degrade RNA. The mechanism of endosomal escape of RNases is not fully known, but can be due to their strong positive charge in acidic environment of endo/lysosomes allowing interaction of these enzymes with endosomal membranes, resulting in membrane destabilization/permeabilization and translocation of these proteins. Particularly, members of the RNase A and RNase T1 superfamilies have shown promising cytotoxicity against cancer cells. Members of the RNase A family are homologous in amino acid sequence and tertiary structure, but vary considerably in cytotoxicity. Bovine pancreatic ribonuclease A (RNase A), was the first enzyme of this group tested for a possible anticancer activity *in vivo* and the results were contradicting [18]. Some authors did not observe any effect while others reported anticancer activity only when high doses of enzyme were employed e.g., milligrams injected into solid tumors of animals. Only two classes within this superfamily, frog RNases and bovine seminal RNase (BS-RNase), have shown to be highly toxic against cancer cells. BS-RNase is the only known RNase with a quaternary structure and it naturally occurs as a homodimer that consists of two identical subunits linked by two disulfide bonds and also by non-covalent interactions. Onconase (ONC), a frog homologue of RNase A, has been evaluated in Phase III clinical trials for the treatment of malignant mesothelioma. Phase I and Phase II trials showed that renal toxicity was dose limiting and that Onconase® was immunologically well tolerated even after repeated administration, most probably due to its structural similarity to human RNases [19]. As pointed out, for a ribonuclease to be cytotoxic it must evade RI. In contrast to human RNases, Onconase® has a low affinity for RI which is because many of the RI contact amino acid residues present in mammalian RNase A are absent or substituted in Onconase® [20]. BS-RNase escapes RI via a different mechanism, because the active site of BS-RNase is sterically inaccessible for this inhibitor due to its quaternary structure [21]. Although still debatable, rather than evasion from the RNase inhibitor, also different other mechanisms have been proposed for increased potency of Onconase®, such as its high binding to cell membranes due to the existence of specific receptors for Onconase® on mammalian cell surfaces, and its action as an intracellular catalyst for the generation of RNAi, which in turn can cause cell death [22-25]. In comparative studies of the cytotoxic properties of RNase A (RI sensitive) and Onconase®, it was shown that when these enzymes are conjugated to targeting ligands like antibodies, they exert similar cytotoxic efficacy [22, 26].

2. Delivery challenges for therapeutic protein and peptides

The use of proteins and peptides as therapeutic agents often fails due to rapid inactivation and rapid elimination from the circulation mostly because of renal filtration, and clearance by the reticuloendothelial system (RES). Also, they are deposited and accumulated in non-targeted organs and tissues which results in toxic side effects. Moreover, foreign proteins contain antigenic determinants that can trigger the immune response and subsequent inflammatory reactions. Most pharmaceutical proteins and peptides (e.g. insulin) as well as antibodies exert their action extracellularly by binding to receptors present on cell surfaces. Other proteins, as pointed out above, like bacterial toxins and RNases, however, have their targets inside the cell. Low permeability of cell membranes for biotherapeutics that have to be delivered intracellularly requires multiple administrations of high doses to reach the desirable concentration in the cell, which is however associated with undesirable side effects and patient discomfort. In many cases the proteins that are taken up by cells are subject to endosomal/lysosomal degradation, or in some cases are even translocated to the extracellular space [27, 28]. Protein toxins and ribonucleases are equipped with required structural features responsible for escape from endosome/lysosomal compartments to reach the cytoplasm. However, to be therapeutically useful, physical protection and targeting to specific sites/cells is required. In recent years, various carrier systems have been developed to optimize protein and peptides pharmacokinetic profiles, as shortly discussed in the next paragraph.

3. Protein/peptide carriers

Pharmaceutical carriers are used to increase the physicochemical stability of administered protein/peptide drugs, to improve their efficacy and decrease undesired side-effects and even to promote cellular association and internalization. Although the principles by which pharmaceutical carriers are designed depend on the protein and intended route of administration (systemic or local delivery), there are some general requirements that have to be fulfilled. Ideally, carrier systems should be non-cytotoxic, biocompatible and biodegradable. Further, a preparation method that does not affect the structural integrity of the protein, and thus its biological activity, should be available and the carrier should protect the protein from physical and chemical degradation. Preferably, the carriers have a high loading efficiency and tailorable release properties. Also, the carriers, particularly nanosystems, should have possibilities for surface modification to provide stealthness after i.v. administration. Finally, the protein-loaded carrier should target and be retained at the desired site in the body, and, importantly, protect the therapeutic proteins from lysosomal degradation in case of intracellular delivery. Ranging from nanometer to micrometer sizes, various systems based on lipids, conjugates or biodegradable polymers have been proposed and investigated for protein delivery. Liposomes and cell penetrating peptides (CPPs) are frequently studied carrier systems for intracellular delivery of peptide/proteins However, because in this thesis the focus is on biodegradable nanoparticles these systems are discussed in this Introduction; the reader is referred to some recent review papers [29-33]. NPs (NPs) based on biodegradable polymers meet many of the above mentioned requirements of delivery systems for intracellular protein/peptide delivery. NPs are not only able to target the drug to its site of action, but also maintain the drug concentrations at therapeutically relevant levels for a sustained period of time [34, 35].

4. Biodegradable polymers for protein/peptide delivery

4.1. Physicochemical properties

Biodegradable polymers of either natural or synthetic origin can be cleaved into low molecular weight product by enzymatical or chemical (mainly hydrolysis) degradation. When properly designed, the formed degradation products are non-toxic and eliminated by normal metabolic pathways or excreted by the kidneys. Besides biocompatibility, they have to meet several other requirements for use in pharmaceutical formulations, like suitable biodegradation kinetics, and ease of processing. Their chemical diversity enables the modulation of physicochemical properties for the aimed drug release profile (delayed, sustained, triggered). The use of polymers for protein delivery was first reported by Langer et al. [36]. After this publication, many other researchers have developed polymer formulations loaded with protein drugs and studied their release characteristics. So far, synthetic biodegradable polymers most frequently studied to deliver proteins are aliphatic poly esters like poly(lactic acid) (PLA), poly(glycolic acid) (PGA). In particular PLGA, a copolymer of D,L-lactic acid and glycolic acid (poly(D,L-lactic-co-glycolic acid) that degrades by bulk erosion through hydrolysis of its ester linkages [37, 38]has been investigated as matrix for the controlled of proteins. It has been shown that the degradation kinetics of PLGA based systems depends mainly on the lactic acid/glycolic acid ratio, molecular weight of the polymer, and on the morphology and size of the device [38-42]. Various PLGA devices like microspheres, NPs, pellets, implants, and films have been fabricated for the delivery of therapeutic proteins and peptides. The effect of polymer properties, geometry and morphology of the drug-loaded device on protein release [43-50], interaction between the protein and polymer, chemical degradation of the incorporated peptide/protein have been extensively studied [51-54]. Since proteins do not dissolve in hydrophobic polymeric matrices and also have a low (or absent) mobility in such matrices, their release from homogeneous (non-porous) systems is essentially governed by matrix degradation/erosion [49, 55]. So far, researchers have shown that by alteration of different factors (among which the molecular weight of the polymer, copolymer composition (lactide/glycolide ratio), and geometry of the device) different release patterns of the proteins, either sustained (zero-order) or pulsed, can be achieved. As mention, the degradation kinetics of PLGA depends on the copolymer composition with the fastest degradation for the 50/50 lactide/glycolide copolymer [56]. Interestingly, it has been shown that PLGA with capped carboxyl end groups (frequently lauryl alcohol is used as capping group) degraded slower than PLGA with free carboxyl end group (uncapped) [57]. The slower degradation is because this polymer is more hydrophobic than uncapped PLGA and therefore shows less water absorption. Besides the points addressed, the geometry of PLGA-based controlled drug delivery devices has been shown to also affect degradation kinetics [58]. Particularly, the rate at which the acidic polymer degradation products are neutralized and/or are extracted from the degrading matrix is dependent on the device geometry. Studies have demonstrated that in systems with a larger geometry accumulation of acidic degradation products occurs which in turn enhance the rate of polymer degradation [51, 59].

4.2. Drawbacks of PLGA polymeric devices for peptide/protein delivery

Interactions between PLGA and encapsulated proteins include covalent as well as non-covalent interactions (electrostatic, hydrophobic). Ionic interactions (when the protein and the polymer have opposite charge) between the protein and the COOH end group of uncapped PLGA will result in higher incorporation, while if the interaction between the protein/peptide and polymer is hydrophobic, polymers with hydrophobic capping groups will show a greater incorporation [59-62]. Investigation on the mechanisms of protein release form PLGA matrices has demonstrated that besides having effect on the release rate, such interactions can also lead to incomplete protein release or, more importantly, chemical modification due to reaction of lysine residues in proteins and ester group of PLGA resulting in acylated protein molecules, which may lead to protein inactivation and/or induction of undesired side effects and immunogenic reactions. Further, adsorption of the protein onto the polymer surface is one of the factors responsible for the frequently observed incomplete release of entrapped proteins from these matrices [49, 53, 60]. Besides acylation, in PLGA matrices, proteins/peptides can also undergo acid-catalyzed reactions, such as deamidation and chain cleavage [63-66]. Technologies have been developed to stabilize proteins and peptides in PLGA, to prevent protein-PLGA interactions and also to avoid/ minimize acidification of the degrading matrix. Entrapment of PEGylated or precipitated proteins [67, 68] and addition of excipients like urea or basic inorganic salts such as sodium bicarbonate, magnesium hydroxide or calcium carbonate (which neutralize acid degradation products) have been investigated in this respect [69-71]. Facilitating the extraction of acid degradation products from PLGA particles by either decreasing the diameter of the particles, by creating porosity and by incorporation of PEG are other strategies to increase water absorption of matrices and to favor extraction and thus avoid accumulation of acidic degradation products [72, 73].

4.2.1. PEGylation

PEG is a hydrophilic, flexible polymer with proven biocompatibility and is currently one of the most frequently used constituents of advanced drug delivery systems [74]. So far various types of block copolymers of polyesters with poly(ethylene glycol) (PEG) e.g. di-block (PLGA-PEG) or tri-blocks (PEG-PLGA-PEG and PLGA-PEG-PLGA) have been developed. Triblock copolymers of both the ABA and BAB type exhibit thermosensitive behavior and are able to form thermogels [75]. When properly designed, aqueous solutions of these copolymers are liquid at room temperatures and transform into gels at body temperature. These gels are used for the local delivery of drugs [76, 77]. Di-blocks of PEG-PLGA are mainly used in NP formulations to provide stealth behavior and render the particles long-circulating after i.v. administration due to the presence of a PEG layer at their surface. [78]. The PEG layer also provides opportunities to conjugate targeting ligands [79].

4.2.2. Functionalized polyesters

Functionalization of the polyesters is a relatively novel approach to design systems suitable for the delivery of biotherapeutics. Functionalized polyesters have basically the same backbone structure as other polyesters but with an increased hydrophilicity due to the introduction hydrophilic side groups. Delivery systems based on such polymers are more hydrophilic and have consequently a greater water absorbing capacity than e.g. PLGA based systems, which facilitates the release of formed acidic degradation products and thereby prevents a pH drop that is an important cause of peptide and protein inactivation [80-83]. Leemhuis et al. synthesized and characterized an aliphatic polyesters with pendant hydroxyl groups [81]. One representative is poly(D,L-lactic-co-hydroxymethyl glycolic acid) (PLHMGA), of which the hydrophilicity and degradation rate can be tailored by the copolymer composition [82]. Ghassemi et al. reported that microparticles based on this aliphatic polyester and loaded with proteins or a peptide (octreotide) showed tailorable release times between 20 and 60 days, mainly governed by the kinetics of degradation/erosion of the microparticles [83, 84]. It was further shown that these particles were hardly susceptible to acidification during degradation [85]. Therefore, these highly advantageous properties warrant further investigation of PLGHMGA (poly(lactic-co-glycolic-co-hydroxymethyl glycolic acid), copolymers containing hydrophilic HMG units but also glycolic acid units) for preparation of NPs that are potentially suitable for intracellular delivery of proteins. We selected PLGHMGA instead of PLHMGA for nanoparticle preparation for two reasons. First, by substitution of lactic acid by glycolic acid, a more hydrophilic polymer is obtained of which faster polymer degradation can be expected. This is particularly of interest for intracellular delivery of protein drugs for which a fast release is desirable. Second, the monomer benzyloxymethyl glycolide (BMG) used for the synthesis of PLGHMGA is an optically pure and crystalline compound which is obtained a relatively high yield. On the other hand, the monomer for PLHMGA (benzyloxymethyl methyl glycolide, BMMG) is, using our synthetic procedure, obtained as a mixture of diastereoisomers (the S,S and the S,R form), and only the S,S isomer is used for the synthesis of PLHMGA. The reason is that S, S monomer can be obtained in a purity needed for controllable ring-opening polymerization. But, the overall yield of this ‘pure’ monomer is rather low [81].

5. Internalization of PLGA NPs

The reticulo-endothelial system (RES) eliminates particles from the blood stream. This process is one of the most important biological barriers of NPs-based controlled drug delivery systems. Covering the surface with poly(ethylene glycol) (PEG) polymer is the most commonly used strategy to increase the circulation half-life of i.v. injected NPs. The PEG corona shields possible surface charges (e.g. originating from COO- end groups of polymers) and provides a hydrophilic layer which protects NPs against opsonization [86]. However, the benefit of PEG to increase the circulation half-life of NPs may adversely affect the uptake of NPs by target cells [87]. Also when the NPs are endocytosed, the PEG layer may prevent endosomal escape [88]. Therefore, the cellular internalization of sterically stabilized and drug-loaded NPs, and thus their efficacy, can be improved by means of PEG shedding after arrival of the NPs at the target site [87]. Surface charges of NPs have an important influence on their interaction with cells and hence on their uptake. PLGA NPs exhibit a negative surface charge at neutral pH due to the presence of uncapped end carboxylic acid groups of the polymer. Cellular uptake of PLGA NPs has shown to be cell type and surface charge dependent. It has been shown that PLGA-NPs are internalized either through fluid phase pinocytosis or clathrin-mediated endocytosis by vascular smooth muscle cells (VSMCs) and rat corneal epithelial cells, respectively [89, 90]. The main fraction of particles is recycled from the early endosomes to the cell surface, and only a small fraction undergoes endosomal escape and localizes in the cytosol [91]. With increasing incubation time and also NPs concentration the NPs uptake and retention in cells also increases [89]. A considerable cellular uptake and endosomal escape of these particles was achieved when the surface of particles was modified with a cationic polymer (poly(L-lysine) (PLL)) [89]. Furthermore, it is important to emphasize that ligand-conjugated NPs could have different intracellular trafficking pathways than unconjugated NPs [92]. Another factor (generally overlooked) that influence PLGA NPs uptake is surface associated PVA. It has been shown that even after multiple washing of NPs, PVA used in the formulation as stabilizer remains associated with the NPs surface [93]. This surface associated PVA can alter the physical properties e.g. hydrophilicity and the zeta potential of the particles and hence affect their cellular uptake. Panyam et al. reported that NPs with higher amounts of residual PVA showed relatively lower cellular uptake and endosomal escape than clean PLGA NPs [93].

6. Targeting

In general, NPs can target tumors via an active or passive process. Passive targeting takes advantage of the size and long-circulating behavior of (PEGylated) NPs and exploits the unique anatomical and pathological abnormalities of the tumor vasculature. NPs can accumulate in the interstitial space of tumors due to an enhanced permeability of tumor vasculature. Moreover, lymphatic vessels are ineffective or sometimes even absent in tumors, leading to inefficient drainage of the tumor tissue which contributes to an enhanced retention of deposited NPs. Together these two phenomena constitute the “Enhanced Permeability and Retention” (EPR) effect. [94]. To establish active targeting, ligands are grafted at the NPs surface and mostly conjugated to the distal ends of PEG chains. The ligand is selected to be selective for specific receptors overexpressed by cell population of interest (e.g. tumor cells) [86]. Ligands need to be optimally conjugated on NPs to preserve their binding affinity for the aimed receptor. Therefore, it is essential for the design of nanoparticulate systems to avoid shielding of targeting ligands with the PEG chains [95]. Targeting ligands so far used in pharmaceutical field include among others growth factors, monoclonal antibodies and antibody fragments ('nanobodies'). Nanobodies (VHHs or NBs) are targeting molecules that recently have raised tremendous attention in the pharmaceutical field. They are the smallest, naturally occurring, antigen binding fragments. These single variable domains of heavy chain only antibodies (HcAb) present in Camelidae and some sharks, have the high affinity and specificity of conventional antibodies, which features are essential for successful targeting [96]. Importantly, Nbs are smaller (12-15 kDa) than mAbs (150-160kDa), Fabs (60 kDa) or scFv (30 kDa) and have therefore the ability to recognize hidden or uncommon epitopes [97, 98]. They express low immunogenicity, are highly robust to tolerate hard manufacturing conditions and are easy to produce in bacteria and yeast [96].

7. Aim and outline of the thesis

In the present thesis, the suitability of PLGHMGA NPs for the controlled release and targeted intracellular delivery of (therapeutic) proteins is explored. Therefore, the main focus of this thesis (Chapters 3, 4 and 5) is on the preparation of NPs based on the functional polyester PLGHMGA and their application for protein delivery. Protein load NPs were prepared with a double emulsion solvent evaporation technique using model proteins (BSA and lysozyme) as well as a therapeutic protein (RNase A). In **Chapter 2** the effect of a specific and frequently used end group (lauryl alcohol) on the BSA release and degradation kinetics of poly(DL-lactic-co-glycolic acid) particles of different sizes (0.3, 1 and 20 µm) is explored.

Chapter 3 provides mechanistic insights into the effect of different formulation parameters, such as PLGHMGA polymer molecular weight and copolymer compositions on the degradation and release behavior of BSA-loaded NPs with the size of 400 to 700 nm.

Chapter 4 describes the preparation and characterization of PEGylated PLGHMGA NPs prepared from blends of PEG-PLGHMGA, with two different PEG chain lengths, and PLGHMGA, using bovine serum albumin (BSA) and lysozyme as model proteins. The effect of blend composition, i.e. type and amount of PEG-PLGHMGA copolymer in the mixture on nanoparticle properties (degradation and protein release) is investigated.

Chapter 5 reports on the in-vitro cytotoxic effects of stealth PLGHMGA NPs loaded with ribonuclease (RNase A), decorated with anti Her-2 nanobody as targeting ligand.

Chapter 6 summarizes the findings and conclusions of this thesis. In addition, perspectives and suggestions for future research are given.

References

1. Figg WD, Kruger EA, Price DK, Kim S, Dahut WD. Inhibition of angiogenesis: treatment options for patients with metastatic prostate cancer. *Invest New Drugs*. 2002;20:183-194.

2. Kerbel R, Folkman J. Clinical translation of angiogenesis inhibitors. *Nat Rev Cancer*. 2002;2:727-739.

3. Ballard CE, Yu H, Wang B. Recent developments in depsipeptide research. *Curr Med Chem*. 2002;9:471-498.

4. Harries M, Smith I. The development and clinical use of trastuzumab (Herceptin). *Endocr Relat Cancer*. 2002;9:75-85.

5. Marshall H. Anti-CD20 antibody therapy is highly effective in the treatment of follicular lymphoma. *Trends Immunol*. 2001;22:183-184.

6. Frankel AE, Kreitman RJ, Sausville EA. Targeted toxins. *Clin Cancer Res*. 2000;6:326-334.

7. Lord MJ, Jolliffe NA, Marsden CJ, et al. Ricin. Mechanisms of cytotoxicity. *Toxicol Rev*. 2003;22:53-64.

8. Wang BZ, Zou WG, Liu WY, Liu XY. The lower cytotoxicity of cinnamomin (a type II RIP) is due to its B-chain. *Arch Biochem Biophys*. 2006;451:91-96.

9. Moehring TJ, Moehring JM. Interaction of diphtheria toxin and its active subunit, fragment A, with toxin-sensitive and toxin-resistant cells. *Infect Immun*. 1976;13:1426-1432.

10. Pennell CA, Erickson HA. Designing immunotoxins for cancer therapy. *Immunol Res*. 2002;25:177-191.

11. Frankel AE. Reducing the immune response to immunotoxin. *Clin Cancer Res*. 2004;10:13-15.

12. Provoda CJ, Stier EM, Lee KD. Tumor cell killing enabled by listeriolysin O-liposome-mediated delivery of the protein toxin gelonin. *J Biol Chem*. 2003;278:35102-35108.

13. Shapiro R, Strydom DJ, Olson KA, Vallee BL. Isolation of angiogenin from normal human plasma. *Biochemistry*. 1987;26:5141-5146.

14. D'Alessio G, Di Donato A, Parente A, Piccoli R. Seminal RNase: a unique member of the ribonuclease superfamily. *Trends Biochem Sci*. 1991;16:104-106.

15. Hooper LV, Stappenbeck TS, Hong CV, Gordon JI. Angiogenins: a new class of microbicidal proteins involved in innate immunity. *Nat Immunol*. 2003;4:269-273.

16. Lee FS, Vallee BL. Expression of human placental ribonuclease inhibitor in Escherichia coli. *Biochem Biophys Res Commun*. 1989;160:115-120.

17. Vicentini AM, Kieffer B, Matthies R, et al. Protein chemical and kinetic characterization of recombinant porcine ribonuclease inhibitor expressed in Saccharomyces cerevisiae. *Biochemistry*. 1990;29:8827-8834.

18. Leland PA, Schultz LW, Kim BM, Raines RT. Ribonuclease A variants with potent cytotoxic activity. *Proc Natl Acad Sci U S A*. 1998;95:10407-10412.

19. Mikulski SM, Costanzi JJ, Vogelzang NJ, et al. Phase II trial of a single weekly intravenous dose of ranpirnase in patients with unresectable malignant mesothelioma. *J Clin Oncol*. 2002;20:274-281.

20. Boix E, Wu Y, Vasandani VM, et al. Role of the N terminus in RNase A homologues: differences in catalytic activity, ribonuclease inhibitor interaction and cytotoxicity. *J Mol Biol*. 1996;257:992-1007.

21. Lee JE, Raines RT. Cytotoxicity of bovine seminal ribonuclease: monomer versus dimer. *Biochemistry*. 2005;44:15760-15767.

22. Rybak SM. Antibody-onconase conjugates: cytotoxicity and intracellular routing. *Curr Pharm Biotechnol*. 2008;9:226-230.

23. Turcotte RF, Lavis LD, Raines RT. Onconase cytotoxicity relies on the distribution of its positive charge. *FEBS J*. 2009;276:3846-3857.

24. Altomare DA, Rybak SM, Pei J, et al. Onconase responsive genes in human mesothelioma cells: implications for an RNA damaging therapeutic agent. *BMC Cancer*. 2010;10:34-2407-10-34.

25. Ardelt B, Ardelt W, Darzynkiewicz Z. Cytotoxic ribonucleases and RNA interference (RNAi). *Cell Cycle*. 2003;2:22-24.

26. Newton DL, Ilercil O, Laske DW, Oldfield E, Rybak SM, Youle RJ. Cytotoxic ribonuclease chimeras. Targeted tumoricidal activity in vitro and in vivo. *J Biol Chem*. 1992;267:19572-19578.

27. Bruno BJ, Miller GD, Lim CS. Basics and recent advances in peptide and protein drug delivery. *Ther Deliv*. 2013;4:1443-1467.

28. Sanders LM. Drug delivery systems and routes of administration of peptide and protein drugs. *Eur J Drug Metab Pharmacokinet*. 1990;15:95-102.

29. Swaminathan J, Ehrhardt C. Liposomal delivery of proteins and peptides. *Expert Opin Drug Deliv*. 2012;9:1489-1503.

30. Moutinho CG, Matos CM, Teixeira JA, Balcao VM. Nanocarrier possibilities for functional targeting of bioactive peptides and proteins: state-of-the-art. *J Drug Target*. 2012;20:114-141.

31. Koren E, Torchilin VP. Cell-penetrating peptides: breaking through to the other side. *Trends Mol Med*. 2012;18:385-393.

32. Stewart KM, Horton KL, Kelley SO. Cell-penetrating peptides as delivery vehicles for biology and medicine. *Org Biomol Chem*. 2008;6:2242-2255.

33. Mae M, Langel U. Cell-penetrating peptides as vectors for peptide, protein and oligonucleotide delivery. *Curr Opin Pharmacol*. 2006;6:509-514.

34. Vasir JK, Labhasetwar V. Biodegradable nanoparticles for cytosolic delivery of therapeutics. *Adv Drug Deliv Rev*. 2007;59:718-728.

35. Panyam J, Labhasetwar V. Biodegradable nanoparticles for drug and gene delivery to cells and tissue. *Adv Drug Deliv Rev*. 2003;55:329-347.

36. Langer R, Folkman J. Polymers for the sustained release of proteins and other macromolecules. *Nature*. 1976;263:797-800.

37. Jalil R, Nixon JR. Biodegradable poly(lactic acid) and poly(lactide-co-glycolide) microcapsules: problems associated with preparative techniques and release properties. *J Microencapsul*. 1990;7:297-325.

38. Wu XS. Synthesis, characterization, biodegradation, and drug delivery application of biodegradable lactic/glycolic acid polymers: Part III. Drug delivery application. *Artif Cells Blood Substit Immobil Biotechnol*. 2004;32:575-591.

39. Cohen S, Alonso MJ, Langer R. Novel approaches to controlled-release antigen delivery. *Int J Technol Assess Health Care*. 1994;10:121-130.

40. Park TG. Degradation of poly (D, L-lactic acid) microspheres: effect of molecular weight. *J Control Release*. 1994;30:161–173.

41. Panyam J, Dali MM, Sahoo SK, et al. Polymer degradation and in vitro release of a model protein from poly(D,L-lactide-co-glycolide) nano- and microparticles. *J Control Release*. 2003;92:173-187.

42. Li S. Hydrolytic degradation characteristics of aliphatic polyesters derived from lactic and glycolic acids. *J Biomed Mater Res*. 1999;48:342-353.

43. Alexis F. Factors affecting the degradation and drug-release mechanism of poly(lactic acid) and poly[(lactic acid)-*co*-(glycolic acid)] *Polymer International*. 2005;54:36-46.

44. Blanco D, Alonso MJ. Protein encapsulation and release from poly(lactide-co-glycolide) microspheres: effect of the protein and polymer properties and of the co-encapsulation of surfactants. *Eur J Pharm Biopharm*. 1998;45:285-294.

45. Cohen S, Yoshioka T, Lucarelli M, Hwang LH, Langer R. Controlled delivery systems for proteins based on poly(lactic/glycolic acid) microspheres. *Pharm Res*. 1991;8:713-720.

46. Coombes AG, Yeh MK, Lavelle EC, Davis SS. The control of protein release from poly(DL-lactide co-glycolide) microparticles by variation of the external aqueous phase surfactant in the water-in oil-in water method. *J Control Release*. 1998;52:311-320.

47. Dunne M, Corrigan I, Ramtoola Z. Influence of particle size and dissolution conditions on the degradation properties of polylactide-co-glycolide particles. *Biomaterials*. 2000;21:1659-1668.

48. Frank A, Rath SK, Venkatraman SS. Controlled release from bioerodible polymers: effect of drug type and polymer composition. *J Control Release*. 2005;102:333-344.

49. Fredenberg S, Wahlgren M, Reslow M, Axelsson A. The mechanisms of drug release in poly(lactic-co-glycolic acid)-based drug delivery systems—A review. *Int J Pharm*. 2011;415:34-52.

50. Geng Y, Dalhaimer P, Cai S, et al. Shape effects of filaments versus spherical particles in flow and drug delivery. *Nat Nanotechnol*. 2007;2:249-255.

51. Zolnik BS, Burgess DJ. Effect of acidic pH on PLGA microsphere degradation and release. *J Control Release*. 2007;122:338-344.

52. Ye M, Kim S, Park K. Issues in long-term protein delivery using biodegradable microparticles. *J Control Release*. 2010;146:241-260.

53. van de Weert M, Hennink WE, Jiskoot W. Protein instability in poly(lactic-co-glycolic acid) microparticles. *Pharm Res*. 2000;17:1159-1167.

54. Schwendeman SP. Recent advances in the stabilization of proteins encapsulated in injectable PLGA delivery systems. *Crit Rev Ther Drug Carrier Syst*. 2002;19:73-98.

55. Sinha VR, Trehan A. Biodegradable microspheres for protein delivery. *J Control Release*. 2003;90:261-280.

56. Kitchell JP, Wise DL. Poly(lactic/glycolic acid) biodegradable drug-polymer matrix systems. *Methods Enzymol*. 1985;112:436-448.

57. Tracy MA, Ward KL, Firouzabadian L, et al. Factors affecting the degradation rate of poly(lactide-co-glycolide) microspheres in vivo and in vitro. *Biomaterials*. 1999;20:1057-1062.

58. Samadi N, Abbadessa A, Di Stefano A, et al. The effect of lauryl capping group on protein release and degradation of poly(d,l-lactic-co-glycolic acid) particles. *J Control Release*. 2013;172:436-443.

59. Mehta RC, Thanoo BC, Deluca PP. Peptide containing microspheres from low molecular weight and hydrophilic poly(d,l-lactide-co-glycolide). *J Controlled Release*. 1996;41:249-257.

60. Gasper MM, Blanco D, Cruz ME, Alonso MJ. Formulation of L-asparaginase-loaded poly(lactide-co-glycolide) nanoparticles: influence of polymer properties on enzyme loading, activity and in vitro release. *J Control Release*. 1998;52:53-62.

61. Blanco M, Alonso M. Development and characterization of protein-loaded poly(lactide-co-glycolide) nanospheres. *Eur J Pharm Biopharm*. 1997;43:287-294.

62. Jiang W, Schwendeman SP. Stabilization and controlled release of bovine serum albumin encapsulated in poly(D, L-lactide) and poly(ethylene glycol) microsphere blends. *Pharm Res*. 2001;18:878-885.

63. Crotts G, Park TG. Protein delivery from poly(lactic-co-glycolic acid) biodegradable microspheres: release kinetics and stability issues. *J Microencapsul*. 1998;15:699-713.

64. Wu F, Jin T. Polymer-based sustained-release dosage forms for protein drugs, challenges, and recent advances. *AAPS PharmSciTech*. 2008;9:1218-1229.

65. Jorgensen L, Moeller EH, van de Weert M, Nielsen HM, Frokjaer S. Preparing and evaluating delivery systems for proteins. *Eur J Pharm Sci*. 2006;29:174-182.

66. Houchin ML, Topp EM. Chemical degradation of peptides and proteins in PLGA: a review of reactions and mechanisms. *J Pharm Sci*. 2008;97:2395-2404.

67. Giteau A, Venier-Julienne MC, Marchal S, et al. Reversible protein precipitation to ensure stability during encapsulation within PLGA microspheres. *Eur J Pharm Biopharm*. 2008;70:127-136.

68. Jevsevar S, Kunstelj M, Porekar VG. PEGylation of therapeutic proteins. *Biotechnol J*. 2010;5:113-128.

69. Giteau A, Venier-Julienne MC, Aubert-Pouessel A, Benoit JP. How to achieve sustained and complete protein release from PLGA-based microparticles? *Int J Pharm*. 2008;350:14-26.

70. Diwan M, Park TG. Pegylation enhances protein stability during encapsulation in PLGA microspheres. *J Control Release*. 2001;73:233-244.

71. Zhu G, Mallery SR, Schwendeman SP. Stabilization of proteins encapsulated in injectable poly (lactide-co-glycolide). *Nat Biotechnol*. 2000;18:52-57.

72. Essa S, Rabanel JM, Hildgen P. Effect of polyethylene glycol (PEG) chain organization on the physicochemical properties of poly(D, L-lactide) (PLA) based nanoparticles. *Eur J Pharm Biopharm*. 2010;75:96-106.

73. Buske J, Konig C, Bassarab S, Lamprecht A, Muhlau S, Wagner KG. Influence of PEG in PEG-PLGA microspheres on particle properties and protein release. *Eur J Pharm Biopharm*. 2012;81:57-63.

74. Knop K, Hoogenboom R, Fischer D, Schubert US. Poly(ethylene glycol) in drug delivery: pros and cons as well as potential alternatives. *Angew Chem Int Ed Engl*. 2010;49:6288-6308.

75. Buwalda SJ, Perez LB, Teixeira S, et al. Self-assembly and photo-cross-linking of eight-armed PEG-PTMC star block copolymers. *Biomacromolecules*. 2011;12:2746-2754.

76. Yu L, Xu W, Shen W, et al. Poly(lactic acid-co-glycolic acid)-poly(ethylene glycol)-poly(lactic acid-co-glycolic acid) thermogel as a novel submucosal cushion for endoscopic submucosal dissection. *Acta Biomater*. 2013.

77. Yu L, Li K, Liu X, et al. In vitro and in vivo evaluation of a once-weekly formulation of an antidiabetic peptide drug exenatide in an injectable thermogel. *J Pharm Sci*. 2013;102:4140-4149.

78. Joralemon MJ, McRae S, Emrick T. PEGylated polymers for medicine: from conjugation to self-assembled systems. *Chem Commun (Camb)*. 2010;46:1377-1393.

79. Betancourt T, Byrne JD, Sunaryo N, et al. PEGylation strategies for active targeting of PLA/PLGA nanoparticles. *J Biomed Mater Res A*. 2009;91:263-276.

80. Seyednejad H, Ghassemi AH, van Nostrum CF, Vermonden T, Hennink WE. Functional aliphatic polyesters for biomedical and pharmaceutical applications. *J Control Release*. 2011;152:168-176.

81. Leemhuis M, vanNostrum CF, Kruijtzer JAW, et al. Functionalized poly (alpha-hydroxy acid)s via ring-opening polymerization: toward hydrophilic polyesters with pendant hydroxyl groups. *Macromolecules*. 2006;39:3500–3508.

82. Leemhuis M, Kruijtzer JA, Nostrum CF, Hennink WE. In vitro hydrolytic degradation of hydroxyl-functionalized poly(alpha-hydroxy acid)s. *Biomacromolecules*. 2007;8:2943-2949.

83. Ghassemi AH, van Steenbergen MJ, Talsma H, van Nostrum CF, Crommelin DJ, Hennink WE. Hydrophilic polyester microspheres: effect of molecular weight and copolymer composition on release of BSA. *Pharm Res*. 2010;27:2008-2017.

84. Ghassemi AH, van Steenbergen MJ, Talsma H, et al. Preparation and characterization of protein loaded microspheres based on a hydroxylated aliphatic polyester, poly(lactic-co-hydroxymethyl glycolic acid). *J Control Release*. 2009;138:57-63.

85. Liu Y, Ghassemi AH, Hennink WE, Schwendeman SP. The microclimate pH in poly(d,l-lactide-co-hydroxymethyl glycolide) microspheres during biodegradation. *Biomaterials*. 2012;33:7584-7593.

86. Danhier F, Feron O, Preat V. To exploit the tumor microenvironment: Passive and active tumor targeting of nanocarriers for anti-cancer drug delivery. *J Control Release*. 2010;148:135-146.

87. Romberg B, Hennink WE, Storm G. Sheddable coatings for long-circulating nanoparticles. *Pharm Res*. 2008;25:55-71.

88. Gao W, Langer R, Farokhzad OC. Poly(ethylene glycol) with observable shedding. *Angew Chem Int Ed Engl*. 2010;49:6567-6571.

89. Panyam J, Labhasetwar V. Dynamics of endocytosis and exocytosis of poly(D,L-lactide-co-glycolide) nanoparticles in vascular smooth muscle cells. *Pharm Res*. 2003;20:212-220.

90. Qaddoumi MG, Ueda H, Yang J, Davda J, Labhasetwar V, Lee VH. The characteristics and mechanisms of uptake of PLGA nanoparticles in rabbit conjunctival epithelial cell layers. *Pharm Res*. 2004;21:641-648.

91. Panyam J, Zhou WZ, Prabha S, Sahoo SK, Labhasetwar V. Rapid endo-lysosomal escape of poly(DL-lactide-co-glycolide) nanoparticles: implications for drug and gene delivery. *FASEB J*. 2002;16:1217-1226.

92. Furumoto K, Ogawara K, Yoshida M, et al. Biliary excretion of polystyrene microspheres depends on the type of receptor-mediated uptake in rat liver. *Biochim Biophys Acta*. 2001;1526:221-226.

93. Sahoo SK, Panyam J, Prabha S, Labhasetwar V. Residual polyvinyl alcohol associated with poly (D,L-lactide-co-glycolide) nanoparticles affects their physical properties and cellular uptake. *J Control Release*. 2002;82:105-114.

94. Matsumura Y, Maeda H. A new concept for macromolecular therapeutics in cancer chemotherapy: mechanism of tumoritropic accumulation of proteins and the antitumor agent smancs. *Cancer Res*. 1986;46:6387-6392.

95. Wang M, Thanou M. Targeting nanoparticles to cancer. *Pharmacol Res*. 2010;62:90-99.

96. Hassanzadeh-Ghassabeh G, Devoogdt N, De Pauw P, Vincke C, Muyldermans S. Nanobodies and their potential applications. *Nanomedicine (Lond)*. 2013;8:1013-1026.

97. De Genst E, Silence K, Decanniere K, et al. Molecular basis for the preferential cleft recognition by dromedary heavy-chain antibodies. *Proc Natl Acad Sci U S A*. 2006;103:4586-4591.

98. Stijlemans B, Conrath K, Cortez-Retamozo V, et al. Efficient targeting of conserved cryptic epitopes of infectious agents by single domain antibodies. African trypanosomes as paradigm. *J Biol Chem*. 2004;279:1256-1261.

2

The Effect of Lauryl End-Group Capping on Protein Release and Degradation of Poly(D,L-Lactic-co-Glycolic Acid) Particles

Neda Samadi [1]*
Anna Abbadessa [1]*
Antonio Di Stefano [2]
Cornelus F. van Nostrum [1]
Tina Vermonden [1]
Sima Rahimian [1]
Erik A. Teunissen [1]
Mies J. van Steenbergen [1]
Maryam Amidi [1]
Wim E. Hennink [1]

[1] *Department of Pharmaceutics, Utrecht Institute for Pharmaceutical Sciences, Utrecht University, Utrecht, The Netherlands*

[2] *Department of Pharmacy, University of "G. d'Annunzio", Chieti, Italy*

* Authors contributed equally

Journal of Controlled Release, 172(2):436-43 (2013)

Abstract

The aim of this study was to investigate the effect of a specific and frequently used end group (lauryl alcohol) on the protein release and degradation kinetics of poly(DL-lactic-co-glycolic acid) particles of different sizes. Lauryl-capped PLGA and uncapped PLGA (referred to as PLGA-capped and PLGA-COOH, respectively) particles (0.3, 1 and 20 µm) were prepared by a double emulsion solvent evaporation technique. Bovine serum albumin (BSA) was used as a model protein for release studies. During degradation (PBS buffer, pH 7.4 at 37 °C), a slower dry mass loss was observed for 0.3 µm particles than for particles of 1 and 20 µm. It was further shown that PLGA-capped particles showed slower mass loss likely due to its more hydrophobic nature. It was found that the ester bond hydrolysis rate was substantially slower for PLGA-capped particles and that the rate increased with particle size. Particles showed enrichment in lactic acid content (and thus a decrease in glycolic acid content) in time, and interestingly PLGA-capped particles showed also an enrichment of the lauryl alcohol content. No difference was observed in degradation kinetics between BSA loaded and blank particles. Independent of size, PLGA-COOH based particles showed, after a small burst, a sustained and nearly complete release of BSA during 60-80 days. On the other hand, particles based on PLGA-capped showed a much slower release and exhibited incomplete release, accompanied by the presence of an insoluble residue remaining even after 180 days. FTIR analysis of this residue showed that it contained both polymer and protein. Considering the polymer enrichment in lauryl alcohol, the incomplete release observed for PLGA-capped is likely attributed to interactions between the protein and the lauryl end group. In conclusion, since PLGA-COOH, in contrast to the capped derivative, shows complete degradation as well as quantitative release of an entrapped protein, this polymer is preferred for the design of protein formulations.

1. Introduction

Thanks to the growing advances in biotechnology, the number of recombinant proteins available for therapeutic purposes is increasing significantly [1, 2]. However a short biological half-life and low oral bioavailability are important drawbacks associated with peptide- and protein-based therapeutics for the treatment of chronic and life threatening diseases. Consequently, most of these products are commercialized in an injectable form and require frequent administrations, resulting in a low patient compliance [3]. Substantial research efforts have been focused to obtain a prolonged release and improved pharmacokinetic profiles of therapeutic proteins/peptides after injection [4, 5]. One of the most studied approaches is to entrap pharmaceutical proteins/peptides in polymeric micro- and nanoparticles that release the bioactive continuously due to the gradual erosion of their matrix after hydration and cleavage of hydrolytically sensitive bonds present in the polymer chains. Particularly, PLGA has gained tremendous attention over the last twenty-five years for the design of protein formulations because of its biocompatibility and biodegradability [6-12]. Since proteins do not dissolve in hydrophobic polymeric matrices and have a low (or absent) mobility in such matrices, their release from homogeneous (non-porous) systems is essentially governed by matrix degradation/erosion [13-17]. The erosion of matrices composed of PLGA and related aliphatic polyesters is dependent on the geometry of the device, crystallinity, glass transition temperature [18-23], molecular weight of the polymer and the copolymer composition [24-26]. The latter two parameters affect the capacity of the matrices to absorb water that in turn triggers the hydrolysis of ester bonds present in the polymer chains [19, 27]. For PLGA of the same molecular weight and copolymer composition it has been shown that the degradation can be affected by the presence and chemical nature of a capping group [28, 29]. It has been reported that microparticles based on acid terminated PLGA degrade 2-3 fold faster *in vitro* and 3-4 fold faster *in vivo* than those ones based on PLGA capped with aliphatic chains (ethyl or hexyl group), likely due to the higher hydrophilicity and consequently higher water-absorbing capacity of the uncapped polymer. Moreover, different degradation rates were observed for capped PLGA with similar molecular weights but bearing different end groups: PLGA with an ethyl capping group showed a slightly faster degradation rate than the polymer capped with a hexyl group [30]. Degradation kinetics of polymer matrices can also be influenced by the physico-chemical properties of the loaded drug(s). Previous studies have shown that hydrophilic drugs can facilitate water absorption that in turn leads to faster degradation. In contrast, lipophilic drugs can delay water diffusion into the system, slowing down polymer degradation [31]. Additional effects on the PLGA degradation kinetics have been reported when acidic and basic active agents are incorporated in polymer matrix, because ester hydrolysis is catalyzed by acids and bases [31-33]. Furthermore, it was shown that for peptides/proteins exhibiting interaction with PLGA, the nature of these interactions will determine the extent of incorporation. Ionic interactions between the protein and polymer will result in higher incorporation in the non-end-capped polymers while if the interaction between the peptide and polymer is hydrophobic, then the end-capped polymers will show a greater incorporation [28, 34, 35]. Besides the points addressed, the geometry of PLGA-based controlled drug delivery device has been shown to also affect degradation kinetics [36]. Particularly, the rate at which the acidic polymer degradation products are neutralized and/or are extracted from the degrading matrix is dependent on the device geometry. Previous studies have demonstrated that a decrease in micro-pH in systems with larger geometry can enhance the rate of polymer degradation [33, 34]. However, in a study on PLGA particles of different sizes (0.1, 1 and 10 µm) Panyam et al [37] demonstrated a relatively higher polymer degradation rate for nanoparticles as compared to the larger size microparticles. Despite these many and sometimes contradictory studies, a systematic study on the effect of particle size and PLGA end group on particle degradation behaviour and protein loading and release has not been carried out so far. Therefore, in this paper particles with different sizes (0.3, 1 and 20 µm) based on acid terminated-PLGA and ester terminated-PLGA bearing a long aliphatic tail, dodecanyl end group, were prepared and loaded with a model protein (bovine serum albumin, BSA) by a double emulsion solvent evaporation method. The protein release kinetics as well as particles' degradation characteristics were investigated.

2. Materials and methods

2.1. Materials

Peptide grade dichloromethane (DCM), tetrahydrofuran AR grade (THF) and acetonitrile HPLC-S grade were purchased from Biosolve (The Netherlands). Capped and uncapped PLGA (lactide/glycolide molar ratio 50:50, IV= 0.4 dl/g) were obtained from Purac, The Netherlands. The Polymers are further referred to as PLGA-capped and PLGA-COOH, respectively. BSA (fraction V, minimum 96%, lyophilized powder) was purchased from SAFC (USA) and polyvinylalcohol (PVA; average MW 30,000-70,000; 87-90 % hydrolyzed) was purchased from Sigma-Aldrich (USA). Disodium hydrogen phosphate (Na_2HPO_4) was obtained from Sigma Aldrich (Germany) and sodium dihydrogen phosphate (NaH_2PO_4) from Fluka (Germany). Sodium azide (NaN_3, Bio Ultra, ≥ 99.5%) was purchased from Sigma (Germany) and phosphate buffer saline (PBS, NaCl 8.2 g, $Na_2HPO_{4.}12H_20$ 3.1 g, $NaH_2PO_{4.}2H_20$ 0.3 g in 1L of water for injection, pH 7.4) from Braun (Melsungen AG, Germany). Bicinchoninic acid assay (BCA) reagents A and B were from Thermo Scientific, USA.

2.2. Identification of capping group

In order to identify the nature of the end group of the PLGA-capped this polymer was completely hydrolysed. PLGA-capped (2.5 g) was dissolved in 250 ml NaOH 10 M solution and the mixture was stirred for 4 days at 60 °C. Subsequently, an equal volume of DCM was added to extract the capping group from the water phase. The extraction was repeated three times and the capping group was collected after evaporation of DCM. The product was analyzed by ^{1}H-NMR using deuterated DMSO as solvent and by Differential Scanning Calorimetry (TA instrument, Q2000) to determine its melting point.

2.3. Preparation of PLGA nano- and microparticles with and without BSA loading

PLGA based nano- and microparticles were prepared by a double emulsion solvent evaporation technique as described in literature [29, 37, 38]. Specific formulation parameters and processing conditions applied for the preparation of the different sized particles are listed in Table 1. Briefly, for all sized particles a solution of BSA in reverse osmosis water (50 mg/ml) was emulsified in a solution of PLGA in DCM in an ice-bath using an ultra turrax (IKA® T10 basic ULTRA-TURRAX®, Germany) or ultrasonic homogenizer (LABSONIC P, B.Braun Biotech) to form a water-in-oil (w/o) emulsion. This w/o emulsion was subsequently emulsified into an external aqueous phase containing polyvinyl alcohol (PVA) and NaCl (0.9 % w/v) (filtered through 0.2 µm Millipore filter) in an ice-bath using an ultra turrax or ultrasonic homogenizer, which resulted in a water-in-oil-in-water (w/o/w) emulsion. Next, for 20 µm particles, the w/o/w emulsion was transferred into an additional external aqueous solution (20 ml) containing PVA 1% and NaCl 0.9 % (w/v) and stirred for 3 hrs to evaporate DCM and solidify the emulsified droplets. To obtain 1 and 0.3 µm sized particles, DCM was removed under reduced pressure for 30-45 minutes. After addition of 60 ml of an aqueous NaCl 0.9 % (w/v) solution, the nano- and microspheres were recovered by centrifugation at 10000 and 7000×g respectively, for 30 minutes at 4 °C (J-26XP, Beckman Colter, Avanti ®) and washed with 45 ml of PBS buffer. Finally, the particles were suspended in a certain volume of PBS buffer (NaCl 0.006 M, Na_2HPO_4 0.099 M, NaH_2PO_4 0.049 M, NaN_3 0.008 M, pH 7.4) to obtain a concentration of 4-6 mg of particles in 1 ml PBS buffer for release and degradation studies. Blank particles were also prepared according to the same procedure, using reverse osmosis water as internal water phase instead of an aqueous BSA solution.

2.4. Characterization of the nano- and microparticles

The average size and size distribution of the PLGA nanoparticles were measured using Dynamic Light Scattering (DLS; Zetasizer 4000, Malvern Instruments, Malvern, UK) at 25 °C at an angle of 90° (Z-average). A laser blocking technology (Accusizer 780, Optical particle sizer, Santa Barbara, California, USA) was used to measure the size of the PLGA microparticles.The morphology of the nano- and microparticles was studied by using Transmission Electron Microscopy (TEM, Tecnai 10, Philips, 100kV) and Scanning Electron Microscopy (SEM; Phenom™, FEI Company, The Netherlands), respectively. A diluted droplet of microparticle suspension was placed onto the 12 mm diameter aluminium stub, covered with conductive carbon paint (Agar scientific Ltd., England) and left overnight to dry. Samples were finally coated with palladium under vacuum using an ion coater. The samples for TEM visualization of the nanoparticles were prepared according to the following procedure: 25 µl of nanoparticle suspension was placed onto parafilm, and formvar/carbon-coated copper grids were placed on top of the sample droplets for 2 minutes. Excess liquid was removed by filter paper. Subsequently, the grids were negatively stained by placing them on top of 20 µl droplets of 2% uranyl acetate in demineralized water on parafilm for 2 minutes. Excess liquid was removed by filter paper and the grids were dried for 5 minutes at room temperature before the measurement.

2.5. Protein loading efficiency and loading percentage

BSA loading of nano- and microparticles was determined by dissolving about 10 mg of freeze-dried particles in 1 ml of DMSO. Next, 5 ml of a 0.05 M NaOH solution containing 0.5% (w/v) SDS (sodium dodecyl sulfate) was added, essentially as described by Hongkee *et al.* [39]. The resulting solution was then analyzed for protein content by a BCA protein assay. Loading efficiency (LE) is defined as the amount of protein entrapped divided by the nominal protein X 100%. Percent loading (L %) is expressed as the encapsulated amount of BSA divided by the dry weight of the loaded particles ×100%.

2.6. In vitro release

Freshly prepared particles were suspended in PBS (composition given in section 2.3) and samples of 1.5 ml of the homogeneous particle suspension were aliquoted into 1.5 ml eppendorf tubes. Four aliquots were immediately washed twice with reverse osmosis water (centrifuged for 20 minutes at 22000 X g at 4 °C; Hermle Z233MK-2 centrifuge) and the obtained pellets were freeze-dried and used to determine the exact particle concentration in release medium. All other eppendorf tubes were incubated at 37°C under mild agitation. At different time points, two tubes were taken and the particles were centrifuged at 22000×g for 20 min and the pH of supernatants was determined. The amount of BSA released in the supernatant was measured by UPLC (Acquity UPLC®) equipped with a BEH 300 C18 1.7 µm column. A gradient was run from the starting composition, acetonitrile/H_2O, (5/95%) / 0.1% TFA, to acetonitrile/ H_2O, (60/40%) / 0.1% TFA in 6 min. The mobile phase was delivered to the column at a flow rate of 0.250 ml/min. The injection volume was 7.5 µl, and detection was by measuring the UV absorbance at 280 nm. BSA standard solutions (10-300 µg/ml) were used for calibration. The amount of released protein is reported relative to the loaded amount of protein in present in the suspended particles.

2.7. In vitro degradation

Samples of 1.5 ml of BSA-loaded and placebo particles in PBS and at concentration of 4-6 mg/ml (section 2.4.) were transferred into eppendorf tubes. The samples were incubated at 37 °C while gently shaken. At different time points, two tubes were taken and the particles were collected after centrifugation at 22000 X g for 20 minutes and washed twice with reverse osmosis water. After freeze-drying, the remaining weight of the samples was measured. NMR, DSC, GPC and

FT-IR were used to analyze the remaining insoluble residues. ^{1}H-NMR analysis of the freeze dried insoluble residues dissolved in deuterated DMSO was performed using a Gemini-300 MHz spectrometer at 298 K. The molecular weights of the obtained polymers were determined using GPC (Waters Alliance system), with a Waters 2695 separating module and a Waters 2414 refractive index detector. Two PL-gel 5 µm Mixed-D columns fitted with a guard column (Polymer Labs, Mw range 0.2–400 kDa) were used and calibration was done using polystyrene standards with narrow molecular weight distributions. THF was used as the mobile phase (1 ml/min) [40]. The residues' thermal properties were measured using Differential Scanning Calorimetry (TA instrument, Q2000). A certain amount of freeze-dried residue (2-5 mg) was loaded into an aluminum pan, and after heating from room temperature to 120 °C, with a heating rate of 5 °C/min, the sample was cooled down to -50 °C. Thereafter, the sample was heated to 120 °C with temperature modulation of ±1 °C and a ramping rate of 2 °C/min. The second cycle was used to determine the glass transition temperature (T_g) of the material. FT-IR measurements were carried out only on the samples collected at the last time points (after 180 days for PLGA-capped particles) using a BIO-RAD FTS6000 FT-IR (BIO-RAD, Cambridge, MA, USA) and KBr disc [41]. The FTIR spectra were measured at room temperature and a total of 32 scans at a resolution of 2 cm^{-1} were averaged.

3. Results

3.1. Identification of capping group

The capping group was isolated after hydrolysis of PLGA in an aqueous solution and extraction with DCM. ^{1}H-NMR analysis showed that it consists of a long aliphatic chain alcohol (1-dodecanol) since the following chemical shifts were seen:

δ = 3.42 (m, 2H, $CH_3(CH_2)_9CH_2\underline{CH_2}OH$), 3.3 (s, H_2O), 2.5 (s, CH_3, DMSO), 1.45 (m, 2H, $CH_3(CH_2)_9\underline{CH_2}CH_2OH$), 1.30 (m, 18H, $CH_3\underline{(CH_2)}_9CH_2CH_2OH$), 0.92 (m, 3H, $\underline{CH_3}(CH_2)_9CH_2CH_2OH$) (Fig. 1).

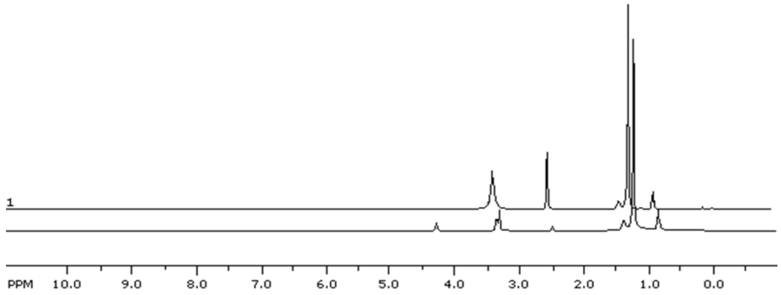

Figure 1: *1H-NMR spectrum of the isolated capping group of PLGA and 1-dodecanol in DMSO, δ: 3.42 (m, 2H, CH3(CH2)9CH2CH2OH), 3.3 (s, H2O), 2.5 (s, CH3, DMSO), 1.45 (m, 2H, CH3(CH2)9CH2CH2OH), 1.30 (m, 18H, CH3(CH2)9CH2CH2OH), 0.92 (m, 3H, CH3(CH2)9CH2CH2OH).*

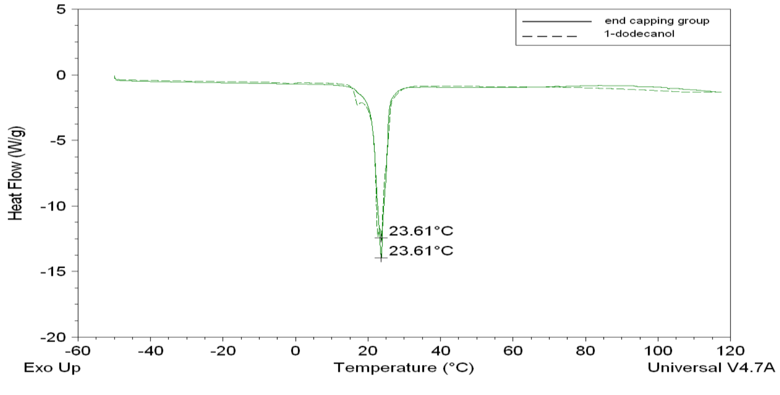

Figure 2: *DCS thermograms of the isolated capping group of PLGA and that of 1-dodecanol.*

DSC analysis showed that the isolated compound had a melting point of 24°C, which corresponds with that of 1-dodecanol (Fig. 2). NMR and DSC analysis therefore convincingly demonstrates that the capped PLGA used in this study contains a 1-dodecanol (or lauryl alcohol) terminus.

3.2. Preparation and characterization of PLGA nano- and microparticles with and without BSA loading

Nano- and microparticles based on PLGA-capped and PLGA-COOH with and without BSA loading were prepared by a double emulsion solvent evaporation technique. The formulation and processing parameters applied are given in Table 1 and the characteristics of the obtained particles are reported in Table 2. TEM and SEM analysis showed that, except a slight porosity that was observed for PLGA-COOH 20 µm particles, the particles were essentially non-porous and spherical with a smooth surface (Fig. 3). Table 2 shows that the BSA loading efficiency was between ~35 and 85 % and no clear effect of size and the type of polymer on loading was observed.

Table 1: *Preparation conditions of different size particles based on PLGA-capped and PLGA-COOH with and without BSA loading.*

Aimed particle size (µm)	Internal aqueous solution	PLGA solution in DCM	PVA solution	Energy source	Emulsification time (min.) First	second
0.3	300 µl	3 ml, 5% w/v	30 ml, 5% w/v	Ultrasonic homogenizer 40 % (first emulsification) and 60 % (second emulsification)	0.5	1
1	300 µl	3 ml, 10% w/v	30 ml, 5% w/v	Ultra turrax, 30000 rpm	1	2
20	200 µl	1 ml, 30% w/v	5 ml, 2.5% w/v	Ultra turrax, 15000 rpm	1	2

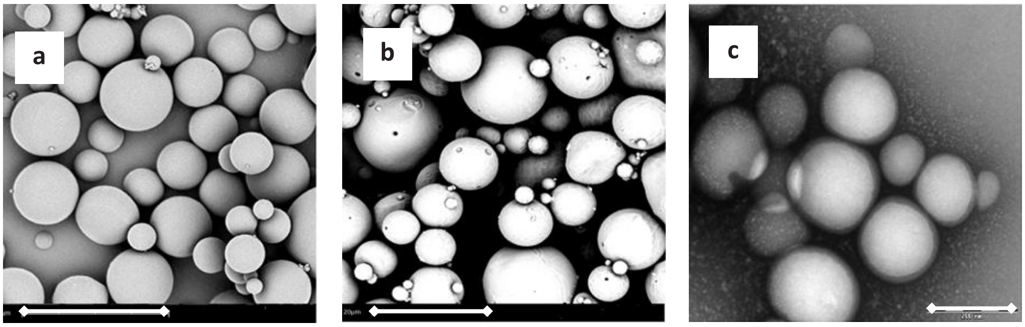

Figure 3: *SEM analysis of particles a) PLGA-capped 20* µm*, b) PLGA-COOH 20* µm*, c) TEM picture of PLGA-capped 0.3* µm *particles (scale bars show: a: 40µm; b=20* µm *and c=200 nm).*

Table 2: *Characteristics of BSA-loaded particles based on PLGA-COOH and PLGA-capped (n=3).*

Formulation	Size (µm)	PDI	LE (%)	L %	Yield (%)
PLGA-capped 20µm	19.5±1.6	--	68±4	3.4±0.2	71±4
PLGA-COOH 20µm	19.9±7.2	--	71±1	3.4±0.1	79±5
PLGA-capped 1µm	1.1±0.1	--	86±4	4.3±0.2	90±1
PLGA-COOH 1µm	1.0±0.1	--	57±7	2.8±0.3	76±10
PLGA-capped 0.3µm	0.32±0.18	0.09±0.04	35±4	3.5±0.4	58±6
PLGA-COOH 0.3µm	0.30±0.16	0.07±0.01	53±14	5.2±1.4	58±3

3.3. In vitro degradation of particles: effect of size and lauryl capping group

Figures 4 and 5 show the mass loss profiles for PLGA-COOH and PLGA–capped particles of different sizes. Irrespective of the polymer type these figures demonstrate a slower mass loss for 0.3 µm particles (lasting 100 and 180 days for PLGA-COOH and PLGA-capped respectively), as compared to 1 and 20 µm particles (which degraded in 70 days for PLGA-COOH and 100 days for PLGA-capped particles).

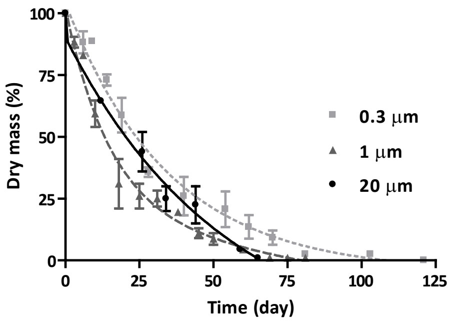

Figure 4: *Effect of particle size on dry mass loss for PLGA-COOH particles.*

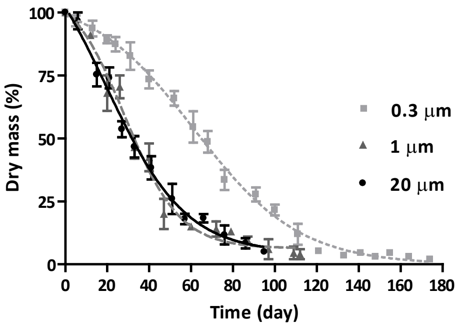

Figure 5: *Effect of particle size on dry mass loss for PLGA-capped particles.*

Figure 6 shows that PLGA-capped particles showed a slower mass loss than those of PLGA-COOH for all particle sizes. Moreover, it can be also seen that particles based on PLGA-COOH were fully degraded within 60-100 days whereas for particles based on PLGA-capped an insoluble residue was present at the end of the experimental period (180 days).

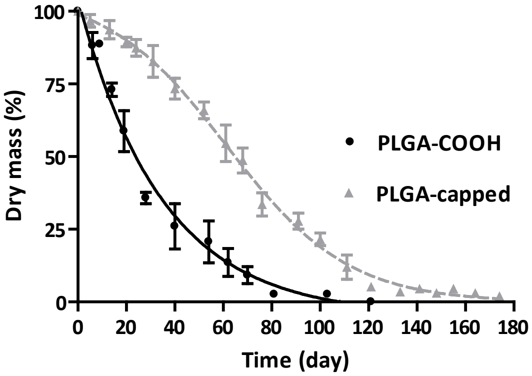

Figure 6: *Effect of capping group on particles' dry mass loss (size: 0.3 µm).*

Figure 7 demonstrates that the polymer hydrolysis kinetics is biphasic with an initial rapid decrease in molecular weight, followed by a slow and gradual further decrease. It is observed that the first degradation rate increases with increasing particle size, in line with literature [23, 38, 42]. Figure 8 shows a faster decrease in molecular weight of PLGA-COOH than PLGA-capped for particles of 0.3 µm; a similar trend was also observed for the particle of 1 and 20 µm. The second degradation phase is more or less independent of the particle size and polymer type and followed similar kinetics with a constant rate. The BSA loaded and placebo particles had similar degradation and dry mass loss patterns (Fig. 9).

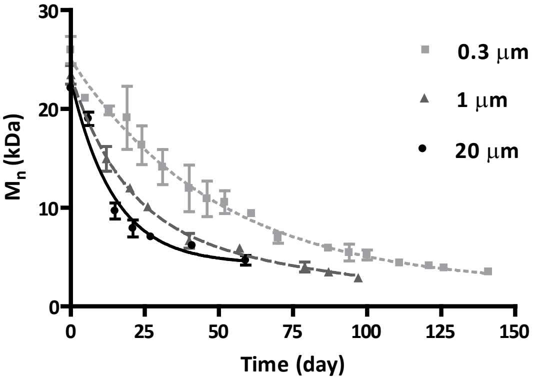

Figure 7: *Effect of size on particles' M_n decrease (PLGA-capped).*

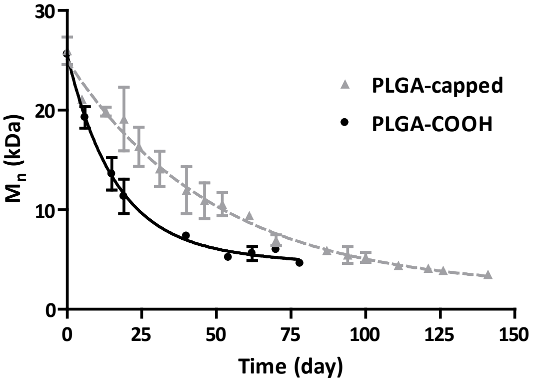

Figure 8: *Effect of capping group on M_n decrease (size: 0.3* µm*).*

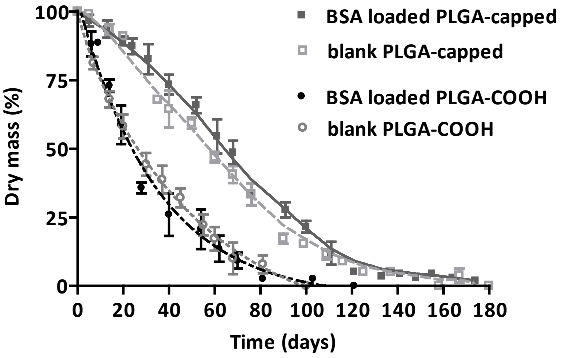

Figure 9: *Effect of BSA on particle degradation*

^{1}H-NMR analysis on the insoluble residues, isolated at different time points, demonstrated enrichment of lactic content and consequently a decrease of glycolic content in time for both PLGA-COOH and PLGA-capped. Furthermore, an increase in lauryl peak intensity (1.2 ppm) from 2 % to 7,4 % (w/w) in 120 days was found (Figs. 10 and 11). DSC data of freshly prepared particles showed a lower T_g for PLGA-capped than for the PLGA-COOH particles (45 versus 49°C, Fig. 12). This figure shows a significant decrease of T_g from 45 to 36 °C in 110 days for the residues of PLGA-capped, however for PLGA-COOH a slight increase in T_g of around 2 °C in 60 days was observed.

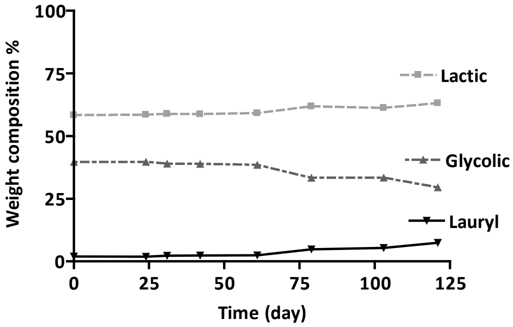

Figure 10: *Changes in polymer weight composition in time (PLGA-capped, size: 0.3 µm).*

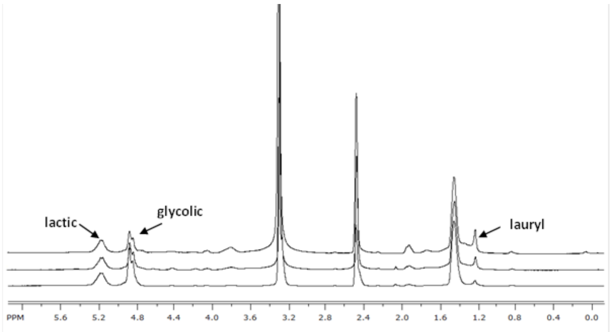

Figure 11: *^{1}H-NMR spectra of insoluble residues (in DMSO) isolated at day 0, 80 and 120 (from the bottom to the top) for particles based on PLGA-capped.*

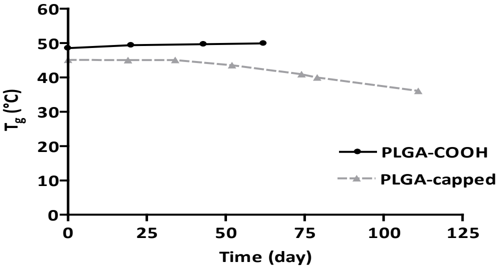

Figure 12: *Effect of the capping group on the T_g of the polymer in time.*

3.4. In vitro BSA release

The release profiles of BSA from PLGA particles of different sizes are shown in figures 13 and 14. PLGA-COOH particles, independent of their size, showed an initial burst around 10%. For particles of 0.3 µm, the burst was followed by a sustained release and reached complete release at ~60 days. In case of particles with 1 µm size, the release with nearly the same rate as the other two size particles started after a lag phase of around 50 days. On the other hand, particles of 1 and 20 µm based on PLGA-capped showed no initial burst release and after a lag phase of 15 (20 µm particles) and 40 days (1 µm particles) they showed continuous release over the next 100 and 60 days, respectively. The 0.3 µm PLGA-capped particles showed a small initial burst (around 5%) followed by an almost zero order release for ~110 days. All PLGA-capped particles exhibited an incomplete release ~70 % of the loading around day 110.

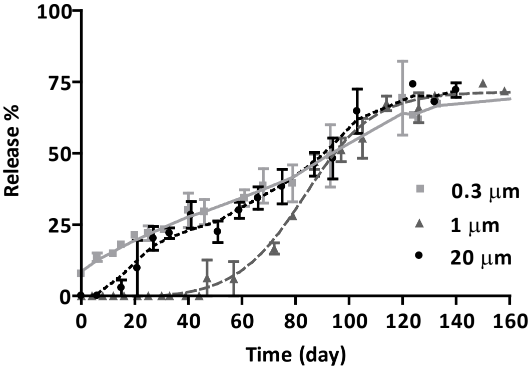

Figure 13: *Effect of particle size on BSA release (PLGA-capped)*

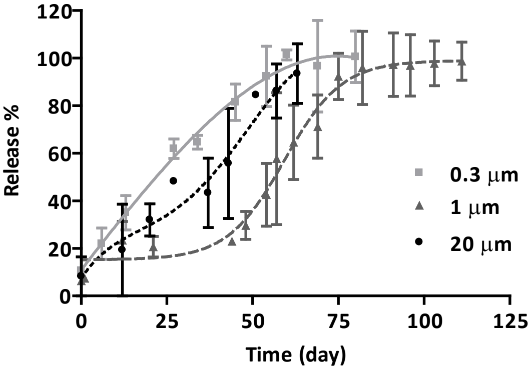

Figure 14: *Effect of particle size on BSA release (PLGA-COOH)*

4. Discussion

Nano- and microparticles based on PLGA-capped and PLGA-COOH with and without BSA loading were prepared by a double emulsion solvent evaporation technique. Our results in Table 2 show that dependent on the processing and formulation parameters, PLGA particles with different sizes (from ~0.3 µm to ~20 µm) were obtained. SEM analysis showed slight porosity for PLGA-COOH 20 µm particles whereas the other particles appeared to be nonporous. In line with our observation, other papers also reported higher porosity for microparticles based on PLGA-COOH compared to those of PLGA-capped polymer. It was argued that the orientation of the carboxylic end groups of the polymer towards the aqueous medium facilitates the absorption of water during the particle preparation procedure resulting in a porous structure [13, 43, 44]. Moreover, it can be also argued that due to higher T_g of PLGA-COOH (Fig. 12) rearrangement of polymer chains and thus pore closure is less likely to occur when compared to PLGA-capped particles with a lower T_g. In degrading polymeric matrices mass loss is the result of both the rate of hydrolysis of ester bonds and the rate of diffusion of water-soluble degradation products out of the degrading matrices [19]. Our results demonstrate that the rate of ester bond hydrolysis increases with increasing particle size, which means that formation of water-soluble degradation products in particles with larger size is faster than in particles of smaller sizes (Fig. 7). The slowest mass loss observed for 0.3 µm particles corresponds with their slowest rate of ester bond hydrolysis (slower drop in number average molecular weight, Fig. 7) and thus slower rate of formation of water soluble oligomers. A possible explanation for almost comparable weight loss for particles with 1 and 20 µm size would be the shorter pathway in smaller particles (1 µm) for transport of degradation products which might compensate for slower rate of polymer hydrolysis, resulting in similar relative erosion patterns for 1 and 20 µm particles (Figs. 4 and 5) [38]. Figure 6 shows that independent of size PLGA-capped particles showed a slower mass loss than those of PLGA-COOH. The slower degradation of particles based on PLGA-capped can be ascribed to the more hydrophobic nature of this polymer which results in a lower water-absorbing capacity of the particles. However, when the degradation proceeds the number of carboxylic end-groups and thus the hydrophilicity of the matrix increases such that after some time it starts to follow the same mass loss rate as uncapped PLGA matrix. In other words, in PLGA-capped particles the onset of the degradation is delayed. Figure 7 demonstrates that the polymer hydrolysis kinetics is biphasic. In the early phase of the degradation, the compact and dense structure of the particles leads to slow diffusion of acidic degradation products out of the polymer matrix and thus accumulation of acidic residues takes place leading to a drop in matrix pH that in turn accelerates ester bond hydrolysis [45-47]. However, smaller sized particles have a larger surface area, which provides a shorter pathway for acidic oligomers and monomers to escape [38] resulting in less acidification of the core and in a slower polymer hydrolysis. Taking particles of the same size but different types of polymer into account, a faster molecular weight decrease for PLGA-COOH particles was also found in the first phase (Fig. 8). Most likely higher water penetration into PLGA-COOH matrices due to their greater hydrophilicity results in faster ester bond hydrolysis and thus faster molecular weight decrease. The second degradation phase is more or less independent of the particle size and polymer type, and followed a more or less similar kinetic, suggesting that the degradation proceeds via the same mechanism(s). In this phase due to loss of mass in time, porous particles are formed, leading to faster penetration of water and buffer ions into the polymer matrix and also release of acidic degradation products from the porous degrading particles, resulting in neutralization of the carboxylic end groups and preventing matrix acidification [38]. Therefore, the occurrence of autocatalysis is less likely and polymer hydrolysis in the later stage of the degradation process proceeds by a combination of (mainly) random hydrolytic hydrolysis of the polymer back bone [48].and chain-end scission catalyzed by OH-end groups [49]. It should be also noted that decrease in molecular weight was observed for all formulations upon exposure to the degradation medium. This implies that in polyester based systems irrespective of using polymers with ester terminating or free carboxylic group, hydration happens faster than ester bond hydrolysis and therefore these systems are degraded via hydrolysis of ester bonds through the whole polymer matrix (bulk degradation) [50]. It has been reported that loaded drugs/compounds dispersed and/or dissolved in PLGA delivery systems influence the degradation kinetics of the polymer matrix [51, 52]. This phenomenon was especially observed in matrices loaded with a high concentration of acid/base drugs that were molecularly dispersed. Due to the buffering capacity of proteins [53], it cannot be ruled out that they affect (retard) the degradation kinetics of aliphatic polyesters. However, in the present study BSA loaded and placebo particles followed the same degradation and dry mass patterns (Fig. 9), which can be explained by its relative low content (loading 3-5 %) as well as lack of dissolution of BSA molecules in the polymer matrix. ^{1}H-NMR analysis on the insoluble residues, isolated at different time points, demonstrated enrichment of lactic content and consequently a decrease of glycolic content in time for both PLGA-COOH and PLGA-capped (Fig. 11). This demonstrates that the hydrolysis of the ester bonds preferentially occurs on the glycolic ester bonds due to lower steric hindrance [54]. Also, degradation production rich in glycolic acid likely have a better aqueous solubility and are therefore preferentially extracted from the degrading particles. Importantly, PLGA-capped particles showed a remarkable increase in lauryl peak content (peak at 1.2 ppm, Fig. 11) from 2 % to 7 % (w/w) in 100 days, which points to a low hydrolysis rate of the lauryl -lactic or -glycolic acid ester bond in combination with the low solubility of lauryl alcohol containing degradation products. DSC data (Fig. 12) showed a lower T_g for PLGA-capped than for the PLGA-COOH particles. Since both polymers have equal copolymer compositions and molecular weights, the slightly lower T_g for PLGA-capped implies that the lauryl end group acts as plasticizer. Figure 12 also shows a significant decrease of T_g from 45 to 36 °C in 110 days for the residues of PLGA-capped particles, however for PLGA-COOH a slight increase in T_g of around 2 °C in 60 days was observed. It is known that the T_g of PLGA increases with increasing lactic acid content and with an increase in their molecular weight [54, 55]. The slight increase in T_g found for PLGA-COOH during degradation can be attributed to a balance between the polymer M_n decrease and the lactic content increase, with a slight dominance of the latter effect. However, as this was not observed for PLGA-capped polymer it can be speculated that the increasing lauryl content influences the glass transition temperature of the polymer by its plasticizing effect. The release profiles of BSA from PLGA particles of different sizes are shown in figures 13 and 14. The initial burst observed for PLGA-COOH particles, independent of their size, is likely due to their slight porosity (SEM analysis, Fig. 3), which allows the protein close to the surface to diffuse out resulting in an initial burst [27, 56-58]. On the other hand, PLGA-capped based particles with 1 and 20 µm size showed no initial burst and protein release started with a constant rate only after a significant development of porous network (lag phase). The small initial burst (around 5%) and absence of a lag phase observed for PLGA-capped and uncapped 0.3 µm particles could be due to their smaller size and shorter diffusion distances resulting in a sustained release of the entrapped protein. It has been reported that the release of macromolecular drugs such as proteins and peptides from PLGA based systems is mainly by diffusion through the water-filled pores that are formed during degradation [6, 13, 27, 59]. Considering the same degradation pattern (pore formation) of 1 and 20 µm particles, independent of polymer type, in particles of larger size it should take longer for the protein to reach the surface through the water-filled pores. However, our results demonstrated that the 1 µm particles released the protein after a longer lag phase. It can be speculated that for 1 µm sized spheres due to higher density, perhaps by lower internal porosity, more removal of the degradation products is requiered to form enough space for large protein molecules to transport through [60]. Comparing PLGA-capped and PLGA-COOH particles of the same size, it was demonstrated that hydrophobic particles starts to decade with approximately the same rate as hydrophilic particles after an increase in carboxylic end groups upon ester bond hydrolysis during the degradation (Fig. 6). Therefore, it can be expected that after some time, the protein release kinetic of PLGA-capped particles becomes relatively similar to that of PLGA-COOH particles. However, results in figure 15 indicate that the rate of protein release from PLGA-capped particles is considerably slower through the whole degradation period and more importantly it does not reach its completion. This can be explained by two mechanisms: pore closure and interaction of the protein with lauryl end group.

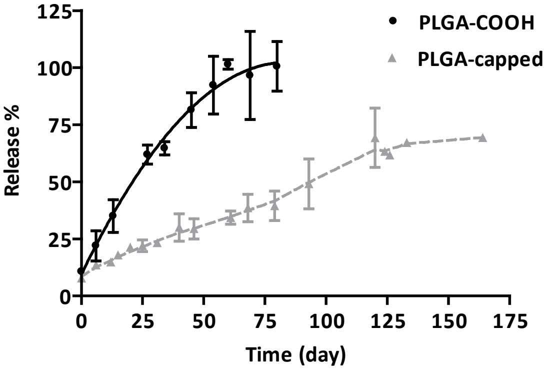

Figure 15: *Effect of capping group on BSA release (size: 0.3* μm*).*

Pore formation and pore closure are two important processes that control the release of the encapsulated macromolecular drugs in poly(D,L-lactide-co-glycolide)-based drug delivery systems [61]. It has previously been shown that the glass transition temperature of PLGA based systems in aqueous medium is around 10–15 °C and lower than in the dry state due the plasticizing effect of absorbed water [61, 62]. Furthermore, it has been also observed that addition of plasticizing agents to PLGA microspheres exposed to relative high humidity led to pore closure [63]. Our T_g findings (Fig. 12) demonstrates that the lauryl end group has a plasticizing effect. Therefore, it can be speculated that the release of BSA from PLGA-capped particles is controlled by a combination of pore formation and pore closure. This can reduce the rate of release compared to PLGA-COOH particles which is predominantly controlled by pore formation (particle erosion). Another important observation is the incomplete release (~70%) of BSA from

PLGA-capped particles while those based on the PLGA-COOH showed almost complete release. Figure 5 demonstrates that an insoluble residue was present at the end of the study (175 days) for BSA loaded PLGA-capped particles. The FTIR spectrum of this insoluble residue at day 175 (Fig. 16) shows that between 1500 and 1700 cm^{-1}, two peaks representative of BSA (amide I and amide Π, 1600-1700 and 1500-1600 cm^{-}1, respectively [64]) as well as peaks originating from PLGA (1760 cm $^{-1}$ [64]) are visible demonstrating that the residue is a mixture of insoluble protein and polymer degradation products rich in lauryl alcohol (NMR analysis, Fig. 11). The incomplete release of BSA from particles based on PLGA-capped is likely due to hydrophobic interactions between the aliphatic lauryl capping group and the protein. It is well known that albumin has several binding sites with high affinity for long hydrocarbon chain anions [65].

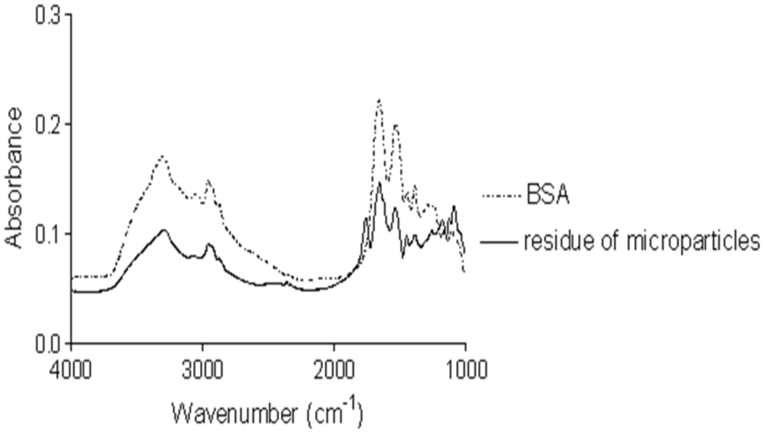

Figure 16: *FTIR Spectra of native BSA and the insoluble residue isolated after 175 days from degrading BSA loaded PLGA-capped 1* µm *particles.*

Conclusions

Different sized BSA-loaded nano- and microparticles based on capped and uncapped PLGA were prepared by using a double emulsion solvent evaporation method. It was demonstrated that the degradation behavior of particles is influenced by their size andpolymer properties. Small sized PLGA-capped particles showed slower degradation kinetics. It was also shown that protein release kinetics as well as polymer degradation kinetics can be highly affected by the capping group. Nearly zero-order and quantitative release was observed for nanoparticles from polymers with uncapped end groups. On the other hand, particles based on PLGA-capped degraded slower than those based on PLGA-COOH and as a consequence showed a slower release of BSA. Importantly, BSA was not quantitatively released from PLGA-capped particles likely because of its interaction with the lauryl capping group. Since many proteins have hydrophobic domains and pockets, similar interactions can be expected with therapeutic proteins [66, 67]. Therefore, PLGA-COOH is preferred for the design of protein formulations.

References

1. Wurm FM. Production of recombinant protein therapeutics in cultivated mammalian cells. *Nat Biotechnol*. 2004;22:1393-1398.

2. Andersen DC, Krummen L. Recombinant protein expression for therapeutic applications. *Curr Opin Biotechnol*. 2002;13:117-123.

3. Brown LR. Commercial challenges of protein drug delivery. *Expert Opin Drug Deliv*. 2005;2:29-42.

4. Jevsevar S, Kunstelj M, Porekar VG. PEGylation of therapeutic proteins. *Biotechnol J*. 2010;5:113-128.

5. Frokjaer S, Otzen DE. Protein drug stability: a formulation challenge. *Nat Rev Drug Discov*. 2005;4:298-306.

6. Cohen S, Yoshioka T, Lucarelli M, Hwang LH, Langer R. Controlled delivery systems for proteins based on poly(lactic/glycolic acid) microspheres. *Pharm Res*. 1991;8:713-720.

7. Shive MS, Anderson JM. Biodegradation and biocompatibility of PLA and PLGA microspheres. *Adv Drug Deliv Rev*. 1997;28:5-24.

8. Kim HK, Chung HJ, Park TG. Biodegradable polymeric microspheres with “open/closed” pores for sustained release of human growth hormone. *J Control Release*. 2006;112:167-174.

9. He J, Feng M, Zhou X, et al. Stabilization and encapsulation of recombinant humanerythropoietin into PLGA microspheres using human serum albumin as a stabilizer. *Int J Pharm*. 2011;416:69-76.

10. Golub JS, Kim YT, Duvall CL, et al. Sustained VEGF delivery via PLGA nanoparticles promotes vascular growth. *Am J Physiol Heart Circ Physiol*. 2010;298:H1959-65.

11. Geng Y, Yuan W, Wu F, Chen J, He M, Jin T. Formulating erythropoietin-loaded sustained-release PLGA microspheres without protein aggregation. *J Control Release*. 2008;130:259-265.

12. Aubert-Pouessel A, Venier-Julienne MC, Clavreul A, et al. In vitro study of GDNF release from biodegradable PLGA microspheres. *J Control Release*. 2004;95:463-475.

13. Fredenberg S, Wahlgren M, Reslow M, Axelsson A. The mechanisms of drug release in poly(lactic-co-glycolic acid)-based drug delivery systems—A review. *Int J Pharm*. 2011;415:34-52.

14. Yang YY, Chia HH, Chung TS. Effect of preparation temperature on the characteristics and release profiles of PLGA microspheres containing protein fabricated by double-emulsion solvent extraction/evaporation method. *J Control Release*. 2000;69:81-96.

15. Ye M, Kim S, Park K. Issues in long-term protein delivery using biodegradable microparticles. *J Control*

Release. 2010;146:241-260.

16. Sinha VR, Trehan A. Biodegradable microspheres for protein delivery. *J Control Release*. 2003;90:261-280.

17. Giteau A, Venier-Julienne MC, Aubert-Pouessel A, Benoit JP. How to achieve sustained and complete protein release from PLGA-based microparticles? *Int J Pharm*. 2008;350:14-26.

18. Kenley RA, Lee MO, Mahoney TR, Sanders LM. Poly(lactide-co-glycolide) decomposition kinetics in vivo and in vitro. *Macromolecules*. 1987;20:2398-2403.

19. Park TG. Degradation of poly (D, L-lactic acid) microspheres: effect of molecular weight. *J Control Release*. 1994;30:161–173.

20. Makino K, Arakawa M, Kondo T. Preparation and in vitro degradation properties of polylactide microcapsules. *Chem Pharm Bull (Tokyo)*. 1985;33:1195-1201.

21. Siepmann J, Faisant N, Akiki J, Richard J, Benoit JP. Effect of the size of biodegradable microparticles on drug release: experiment and theory. *J Control Release*. 2004;96:123-134.

22. Vert M, Schwach G, Engel R, Coudane J. Something new in the field of PLA/GA bioresorbable polymers? *J Control Release*. 1998;53:85-92.

23. Grizzi I, Garreau H, Li S, Vert M. Hydrolytic degradation of devices based on poly(DL-lactic acid) size-dependence. *Biomaterials*. 1995;16:305-311.

24. Belbella A, Vauthier C, Fessi H, Devissaguet J, Puisieux F. In vitro degradation of nanospheres from poly(D,L-lactides) of different molecular weights and polydispersities. *Int J Pharm*. 1996;129:95-102.

25. Spenlehauer G, Vert M, Benoit JP, Boddaert A. In vitro and in vivo degradation of poly(D,L lactide/glycolide) type microspheres made by solvent evaporation method. *Biomaterials*. 1989;10:557-563.

26. Zweers ML, Engbers GH, Grijpma DW, Feijen J. In vitro degradation of nanoparticles prepared from polymers based on DL-lactide, glycolide and poly(ethylene oxide). *J Control Release*. 2004;100:347-356.

27. Alexis F. Factors affecting the degradation and drug-release mechanism of poly(lactic acid) and poly[(lactic acid)-*co*-(glycolic acid)] *Polymer International*. 2005;54:36-46.

28. Gasper MM, Blanco D, Cruz ME, Alonso MJ. Formulation of L-asparaginase-loaded poly(lactide-co-glycolide) nanoparticles: influence of polymer properties on enzyme loading, activity and in vitro release. *J Control Release*. 1998;52:53-62.

29. Zambaux MF, Bonneaux F, Gref R, et al. Influence of experimental parameters on the characteristics of poly(lactic acid) nanoparticles prepared by a double emulsion method. *J Control Release*. 1998;50:31-40.

30. Tracy MA, Ward KL, Firouzabadian L, et al. Factors affecting the degradation rate of poly(lactide-co-glycolide) microspheres in vivo and in vitro. *Biomaterials*. 1999;20:1057-1062.

31. Frank A, Rath SK, Venkatraman SS. Controlled release from bioerodible polymers: effect of drug type and polymer composition. *J Control Release*. 2005;102:333-344.

32. Li L, Schwendeman SP. Mapping neutral microclimate pH in PLGA microspheres. *J Control Release*. 2005;101:163-173.

33. Zolnik BS, Burgess DJ. Effect of acidic pH on PLGA microsphere degradation and release. *J Control Release*. 2007;122:338-344.

34. Mehta RC, Thanoo BC, Deluca PP. Peptide containing microspheres from low molecular weight and hydrophilic poly(d,l-lactide-co-glycolide). *J Controlled Release*. 1996;41:249-257.

35. Blanco M, Alonso M. Development and characterization of protein-loaded poly(lactide-co-glycolide) nanospheres. *Eur J Pharm Biopharm*. 1997;43:287-294.

36. Makadia HK, Siegel SJ. Poly Lactic-co-Glycolic Acid (PLGA) as Biodegradable Controlled Drug Delivery Carrier. *Polymers (Basel)*. 2011;3:1377-1397.

37. Panyam J, Dali MM, Sahoo SK, et al. Polymer degradation and in vitro release of a model protein from poly(D,L-lactide-co-glycolide) nano- and microparticles. *J Control Release*. 2003;92:173-187.

38. Dunne M, Corrigan I, Ramtoola Z. Influence of particle size and dissolution conditions on the degradation properties of polylactide-co-glycolide particles. *Biomaterials*. 2000;21:1659-1668.

39. Sah H. A new strategy to determine the actual protein content of poly(lactide-co-glycolide) microspheres. *J Pharm Sci*. 1997;86:1315-1318.

40. Ghassemi AH, van Steenbergen MJ, Talsma H, et al. Preparation and characterization of protein loaded microspheres based on a hydroxylated aliphatic polyester, poly(lactic-co-hydroxymethyl glycolic acid). *J Control Release*. 2009;138:57-63.

41. Susi H, Byler DM. Protein structure by Fourier transform infrared spectroscopy: second derivative spectra. *Biochem Biophys Res Commun*. 1983;115:391-397.

42. Lamprecht A, Ubrich N, Hombreiro Perez M, Lehr C, Hoffman M, Maincent P. Biodegradable monodispersed nanoparticles prepared by pressure homogenization-emulsification. *Int J Pharm*. 1999;184:97-105.

43. Buske J, Konig C, Bassarab S, Lamprecht A, Muhlau S, Wagner KG. Influence of PEG in PEG-PLGA microspheres on particle properties and protein release. *Eur J Pharm Biopharm*. 2012;81:57-63.

44. Fredenberg S, Wahlgren M, Reslow M, Axelsson A. Pore formation and pore closure in poly(D,L-lactide-co-glycolide) films. *J Control Release*. 2011;150:142-149.

45. Lu L, Garcia CA, Mikos AG. In vitro degradation of thin poly(DL-lactic-co-glycolic acid) films. *J Biomed Mater Res*. 1999;46:236-244.

46. Vert M, Mauduit J, Li S. Biodegradation of PLA/GA polymers: increasing complexity. *Biomaterials*. 1994;15:1209-1213.

47. Ford Versypt AN, Pack DW, Braatz RD. Mathematical modeling of drug delivery from autocatalytically degradable PLGA microspheres--a review. *J Control Release*. 2013;165:29-37.

48. Li S. Hydrolytic degradation characteristics of aliphatic polyesters derived from lactic and glycolic acids. *J Biomed Mater Res*. 1999;48:342-353.

49. de Jong SJ, Arias ER, Rijkers DTS, van Nostrum CF, Kettenes-van den Bosch JJ, Hennink WE. New insights into the hydrolytic degradation of poly(lactic acid): participation of the alcohol terminus. *Polymer*. 2001;42:2795-2802.

50. Gopferich A. Mechanisms of polymer degradation and erosion. *Biomaterials*. 1996;17:103-114.

51. Klose D, Siepmann F, Elkharraz K, Siepmann J. PLGA-based drug delivery systems: importance of the type of drug and device geometry. *Int J Pharm*. 2008;354:95-103.

52. Siegel SJ, Kahn JB, Metzger K, Winey KI, Werner K, Dan N. Effect of drug type on the degradation rate of PLGA matrices. *Eur J Pharm Biopharm*. 2006;64:287-293.

53. Curvale RA. Buffer capacity of bovine serum albumin(BSA). The Journal of the Argentine Chemical Society. 2009;97:174-180.

54. Dinarvand R, Sepehri N, Manoochehri S, Rouhani H, Atyabi F. Polylactide-co-glycolide nanoparticles for controlled delivery of anticancer agents. *Int J Nanomedicine*. 2011;6:877-895.

55. JAMSHIDI K, HYON S, IKADA Y. Thermal Characterization of Polylactides. *Polymer*. 1988;29:2229-2234.

56. Wang J, Wang BM, Schwendeman SP. Characterization of the initial burst release of a model peptide from poly(D,L-lactide-co-glycolide) microspheres. *J Control Release*. 2002;82:289-307.

57. Yeo Y, Park K. Control of encapsulation efficiency and initial burst in polymeric microparticle systems. *Arch Pharm Res*. 2004;27:1-12.

58. van de Weert M, van ‘t Hof1 R, van der Weerd J, et al. Lysozyme distribution and conformation in a biodegradable polymer matrix as determined by FTIR techniques. *J Control Release*. 2000;68:31-40.

59. Huang X, Brazel CS. On the importance and mechanisms of burst release in matrix-controlled drug delivery systems. *J Control Release*. 2001;73:121-136.

60. Stevanovic M, Uskokovic D. Poly(lactide-co-glycolide)-based Micro and Nanoparticles for the Controlled Drug Delivery of Vitamins. *Current Nanoscience*. 2009;5.

61. Faisant N, Siepmann J, Benoit JP. PLGA-based microparticles: elucidation of mechanisms and a new, simple mathematical model quantifying drug release. *Eur J Pharm Sci*. 2002;15:355-366.

62. Blasi P, D'Souza SS, Selmin F, DeLuca PP. Plasticizing effect of water on poly(lactide-co-glycolide). *J Control Release*. 2005;108:1-9.

63. Bouissou C, Rouse JJ, Price R, van der Walle CF. The influence of surfactant on PLGA microsphere glass transition and water sorption: remodeling the surface morphology to attenuate the burst release. *Pharm Res*. 2006;23:1295-1305.

64. Porjazoska A, Goracinova K, Mladenovska K, et al. Poly(lactide-co-glycolide) microparticles as systems for controlled release of proteins -- preparation and characterization. *Acta Pharm*. 2004;54:215-229.

65. Spector AA. Fatty acid binding to plasma albumin. *J Lipid Res*. 1975;16:165-179.

66. Wang W. Instability, stabilization, and formulation of liquid protein pharmaceuticals. *Int J Pharm*. 1999;185:129-188.

67. Manning MC, Chou DK, Murphy BM, Payne RW, Katayama DS. Stability of protein pharmaceuticals: an update. *Pharm Res*. 2010;27:544-575.

3

Mechanistic Studies on the Degradation and Protein Release Characteristics of Poly(Lactic-co-Glycolic-co-Hydroxymethyl Glycolic Acid) Nanospheres

Neda Samadi
Cornelus F. van Nostrum
Tina Vermonden
Maryam Amidi
Wim E. Hennink

Department of Pharmaceutics, Utrecht Institute for Pharmaceutical Sciences, Utrecht University, Utrecht, The Netherlands

Biomacromolecules. 14(4):1044-53 (2013)

Abstract

The purpose of this study was to get mechanistic insights into the effect of different formulation parameters on the degradation and release behavior of protein-loaded nanoparticulate carrier systems based on an aliphatic polyester with pendant hydroxyl groups, poly(lactic-co-glycolic-co-hydroxymethyl glycolic acid) (PLGHMGA). Bovine serum albumin (BSA) was used as a model protein. BSA loaded PLGHMGA nanospheres of 400-700 nm were prepared using a solvent evaporation method using PLGHMGA of different molecular weights and different compositions. Also, the concentration of PLGHMGA in the organic phase was varied. The nanospheres showed a continuous mass loss accompanied by continuous decrease in number average molecular weight, which indicates that the degradation of the nanospheres is by bulk degradation with a rapid release of water-soluble low molecular weight fragments. Based on NMR analysis, it is concluded that intramolecular transesterification precedes extensive hydrolysis of the polymer and degradation of the nanospheres. BSA-loaded freeze-dried nanospheres showed a significant burst release of 40-50% of the BSA loading. In contrast, non-freeze-dried samples showed a small burst of around 10-20%, indicating that freeze-drying induced pore formation. Non-lyophilized nanospheres prepared from PLGHMGA with 64/18/18 lactic/glycolic/hydroxymethyl glycolic acid (L/G/HMG) ratio showed a relatively fast release of BSA for the next 30 days. Nanospheres prepared from a more hydrophobic PLGHMGA (74/13/13, L/G/HMG) showed a two phase release. Circular dichroism analysis showed that the secondary structure of the released protein was preserved. This study shows a correlation between release behavior and particle erosion rate, which can be modulated by the copolymer composition.

1. Introduction

Biomacromolecular therapeutics such as proteins, antigens and nucleic acids are an emerging class of drugs, which are presently used in the clinic or under (pre)clinical evaluation for the treatment of chronic and life threatening diseases [1-3]. Many of these biopharmaceuticals have to be delivered in the cytosol or cellular organelles to exert their aimed biological activity [4-8]. Because these molecules are large and hydrophilic, they do not pass cellular membranes by passive diffusion and consequently do not reach their intracellular site of action. Further, biopharmaceuticals are rapidly degraded by enzymes present in blood and extracellular fluids and/or are rapidly eliminated from the circulation [9, 10]. Carrier systems such as liposomes, polymeric and lipidic nanoparticles have been studied intensively to increase the physicochemical stability of biopharmaceuticals, target specific tissues and promote cellular association and internalization [9, 11-14]. Aliphatic polyesters such as poly(D,L-lactic-co-glycolic acid) (PLGA) are an important class of carrier systems for biopharmaceuticals because of their good biocompatibility, biodegradability and commercial availability [15-20]. However, there are some drawbacks associated with the use of PLGA for the development of protein formulations. During degradation of PLGA, acidic degradation products (monomers and oligomers) are formed, which accumulate in the polymer matrix and cause a drop in pH in the degrading particles that in turn induces protein acylation, denaturation and degradation [10, 21-23]. Therefore, the release of entrapped proteins from PLGA is incomplete and release profiles are difficult to tailor [10, 24]. Many efforts have been made to overcome the drawbacks of aliphatic polyester-based protein delivery systems, *e.g.* entrapment of PEGylated or precipitated proteins [25, 26] or addition of excipients like urea or basic inorganic salts such as sodium bicarbonate, magnesium hydroxide or calcium carbonate to the formulation [27, 28] to prevent acidification of the degrading matrix [29, 30]**.** We recently reported on poly(D,L-lactic-co-hydroxymethyl glycolic acid) (PLHMGA), an aliphatic polyester with pendant hydroxyl groups of which the hydrophilicity and degradation can be tailored by the copolymer composition [31]. Microspheres based on this aliphatic polyester with encapsulated proteins or a peptide showed tailorable release rates between 20 and 60 days, which was mainly governed by the kinetics of degradation/erosion of the microspheres [27, 32, 33]. It was further shown that these microspheres had better protein-compatibility [32] and were not susceptible to acidification during degradation [34]. These highly advantageous properties warrant further investigation of PLGHMGA poly(lactic-co-glycolic-co-hydroxymethyl glycolic acid: copolymers containing hydrophilic HMG units but also containing the glycolic acid units) for preparation of nanospheres that are potentially suitable for intracellular delivery of proteins. Protein-loaded nanoparticles with a size of 0.3-1 µm are suitable for vaccine delivery to target dendritic (and other antigen presenting cells) [35]. For the intracellular delivery of therapeutic proteins, particles with smaller sizes are preferred. However, it is noticed that for e.g. cancer therapy PEGylated particles (i.v. administered) are frequently used because of their stealth behavior and exploitation of the EPR effect. In our ongoing studies we found that just as for PLGA, PEGylation results in smaller particles [36].

For PLGA it has been shown that nano- and micro-particles have different degradation kinetics. The observed slower degradation of nanoparticles is ascribed to the lack of autocatalysis by COOH end group of formed polymer degradation fragments [37-39], and therefore the objective of this study was to get mechanistic insight into the degradation and release behavior of a model protein, bovine serum albumin (BSA), from nanospheres based on PLGHMGA. Nanospheres were prepared by a double w/o/w emulsion solvent evaporation method. The protein release and nanoparticle degradation were examined for different polymer parameters such as composition, molecular weight as well as the concentration of the polymer in the organic phase used for the preparation of the particles.

2. Materials and methods

2.1. Materials

O-Benzyl-L-serine was purchased from Senn Chemicals AG (Dielsdorf, Switzerland). Bovine serum albumin (BSA) was obtained from Sigma Chemical Company (St Louis, USA). D,L-lactide was obtained from Purac, The Netherlands. *N,N*-dimethylformamide (DMF), peptide grade dichloromethane (DCM), methanol, ethyl acetate, chloroform and tetrahydrofurane (THF) were purchased from Biosolve (Valkenswaard, The Netherlands). Benzyl alcohol was obtained from Merck (Darmstadt, Germany). Toluene (Acros, Geel, Belgium) was distilled from P_2O_5 and stored over 3Å molecular sieves under an argon atmosphere. *N,N*-Dimethylaminopyridine (DMAP) and sodium azide (NaN_3, 99%) were obtained from Fluka (Zwijndrecht, The Netherlands). Disodium hydrogen phosphate dihydrate ($Na_2HPO_4.2H_2O$) and sodium dihydrogen phosphate monohydrate ($NaH_2PO_4.H_2O$) were purchased from Merck (Darmstadt, Germany). Polyvinyl alcohol (PVAL; MW 30,000–70,000; 88% hydrolyzed) and tin (II) 2-ethylhexanoate (SnOct2) were from Sigma-Aldrich (St. Louis, USA). BCA reagent was from Interchim, USA. Pd/C (Palladium, 10 wt% on activated carbon, Degussa type E101 NE/W) was purchased from Aldrich, Zwijndrecht, The Netherlands. Unless otherwise stated, all chemicals were used as received.

2.2. Synthesis of copolymers of 3S-benzyloxymethyl-[1,4]-dioxane-2,5-dione with D,L-lactide

3*S*-benzyloxymethyl-[1,4]-dioxane-2,5-dione (or benzyloxymethyl glycolide, BMG) monomer was synthesized according to Leemhuis et al. [31]. BMG was subsequently copolymerized in the melt with D,L-lactide at two monomer ratios (25/75 and 35/65 mol/mol%) and at two monomer to initiator molar ratios (M/I) of 100/1 and 300/1 to obtain polymers with different compositions and molecular weights. Benzyl alcohol (BnOH) and stannous octoate ($SnOct_2$) were used as initiator and catalyst, respectively (Fig. 1) [31]. Briefly, as a typical example, a mixture of D,L-lactide (3.8 g) and BMG (2.1 g) was loaded into a schlenk tube followed by the addition of stannous octoate in dry toluene (24 mg, 72 µl from a 338 mg/ml stock solution in toluene) and an appropriate amount of initiator (benzyl alcohol, e.g. 13 mg, 37 µl from a 351 mg/ml stock solution in toluene; to obtain M/I ratio of 300/1). The protected copolymer, poly(D,L-lactic-co-glycolic-co-benzyloxymethyl glycolic acid) (PLGBMGA), was dissolved in 600 ml distilled and dry THF and 4 g Pd/C was added. After stirring at room temperature under a hydrogen atmosphere for 16 hours to remove the protecting benzyl group, the catalyst was removed by using Hyflo filter and THF was evaporated under vacuum. After removal of the benzyl groups, the units composing the co-polymer include lactic acid (L) originating from D,L, lactide as well as equimolar amounts of glycolic acid (G) and hydroxymethyl glycolic acid (HMG), both originating from BMG. From here on, the different copolymers will be denoted as PLGHMGA x/y/z, where x, y and z are the % of the monomers L, G and HMG in the copolymer as determined by ^{1}H NMR according to the following formulas:

$I_{HMG} = [(I_{3.8})/2 + (I_{4.2\text{-}4.5})/3]$

$I_{G} = (I_{4.7\text{-}5.0})/2$

$I_{L} = [I_{5.2\text{-}5.4} - (I_{3.8})/2]$

$\%HMG = I_{HMG} / (I_{HMG} + I_{G} + I_{L}) \times 100$

where I_{HMG}, I_{G} and I_{L} are the peak integrals per one proton of each monomer unit, and I_{number} are the integrals obtained from the NMR spectra at the indicated peak shifts (ppm).

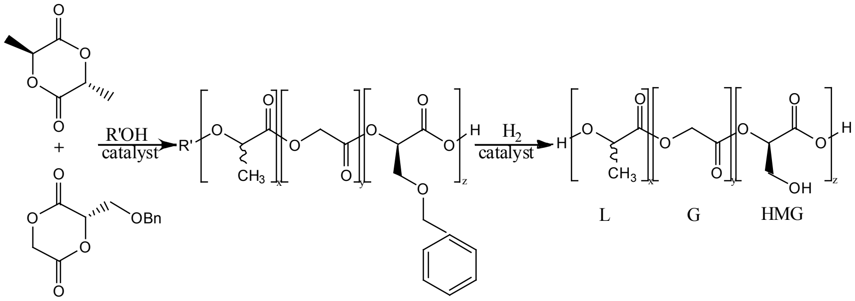

Figure 1: *Synthesis of hydrophilic aliphatic polyesters with pendant hydroxyl groups based on lactic acid, glycolic acid and hydroxymethyl glycolic acid, poly(lactic-co-glycolic-co-hydroxymethyl glycolic acid).*

2.3. Polymer characterization

^{1}H NMR analysis of the polymers dissolved in $CDCl_3$ was performed using a Gemini-300 MHz spectrometer at 298 K. The molecular weights of the obtained polymers were determined using GPC (Waters Alliance system), with a Waters 2695 separating module and a Waters 2414 refractive index detector. Two pl-gel 5 µm Mixed-D columns fitted with a guard column (Polymer Labs, MW range 0.2–400 kDa) were used and calibration was done using polystyrene standards with narrow molecular weight distributions. THF was used as the mobile phase (1 ml/min) [32]. The thermal properties of the different polymers were measured using differential scanning calorimetry (TA instrument, Q2000). Approximately 5 mg polymer was loaded into aluminum pans, and after heating from room temperature to 120 °C, with a heating rate of 5 °C/min, the sample was cooled down to -50 °C. Thereafter, the sample was heated to 120 °C with temperature modulation at ±1 °C and a ramping rate of 2 °C/min. The second cycle was used to determine the glass transition temperature (T_g) of the synthesized polymers.

2.4. Preparation of PLGHMGA nanospheres

PLGHMGA nanospheres were prepared by a double emulsion solvent evaporation technique based on literature procedures for PLGA nanospheres [40]. Briefly, a solution of BSA in reverse osmosis water (300 µl, 50 mg/ml) was emulsified in dichloromethane (DCM) containing PLGHMGA (3ml, 5-15% w/v) in an ice-bath using an ultra turrax (IKA® T10 basic ULTRA-TURRAX®, Germany) for 1 min at the highest speed (30000 rpm) to form a water-in-oil (w/o) emulsion. Then, this w/o emulsion was emulsified into an external aqueous phase containing polyvinyl alcohol (30 ml PVAL, 5% w/v in NaCl 0.9% (w/v), filtered through 0.2 µm Millipore filter) in an ice-bath using the ultra turrax for 2 min at 30000 rpm, which resulted in a water-in-oil-in-water (w/o/w) emulsion. DCM was subsequently evaporated at room temperature under reduced pressure for 30 minutes followed by N_2 flow for 15 minutes. After addition of 60 ml reverse osmosis water the formed nanospheres were recovered by ultracentrifugation (7000 X g for 30 min at 4 ° C, J-26XP, Beckman Colter, Avanti ®) and washed twice with 45 ml reverse osmosis water. For release studies, the washed particles were either directly suspended in release medium or first lyophilized and then resuspended in release medium with 4-6 mg/ml particle concentration. The washed particles were resuspended in deionized water, aliquoted and freeze dried at -50 °C and at 0.5 mbar in a Chris Alpha 1-2 freeze-drier (Osterode am Harz, Germany) for 12 hrs.

2.5. Characterization of the nanospheres

Nanospheres were suspended in distilled deionized water (RI=1.332 and viscosity 0.8898 cP) and the average size and size distribution of the nanospheres were determined by dynamic light scattering (DLS; Zetasizer 4000, Malvern Instruments, Malvern, UK) at 25 °C at an angle of 90°, taking the average of three measurements. The morphology of the nanospheres was studied by scanning electron microscopy (FEI, XL30SFEG). Nanospheres were glued on 12 mm diameter aluminum sample holder using conductive carbon paint (Agar scientific Ltd., England)

and coated with palladium under vacuum using an ion coater. DSC analysis on both BSA loaded and placebo particles was done by loading approximately 1 mg of the freeze-dried nanospheres into an aluminum pan. Thermograms were recorded using the same heating/cooling/heating protocol as described in Section 2.3 for PLGHMGA/PLGBMGA.

2.6. Protein loading efficiency and loading % of the nanospheres

Protein loading of the nanospheres was determined by dissolving about 10 mg of freeze-dried nanospheres in 1 ml DMSO. After particle dissolution, 5 ml of a 0.05 M NaOH solution containing 0.5% (w/v) SDS (sodium dodecyl sulfate) was added, essentially as described by Hongkee *et al.* [41]. The resulting solution was then analyzed for protein content by a BCA protein assay. BSA loading efficiency (LE) is defined as the amount of protein entrapped divided by the nominal protein loading X 100%. The protein loading % is expressed as the encapsulated amount of BSA divided by the dry weight of the nanospheres X 100%.

2.7. In vitro release studies

For in vitro release studies, after harvesting and washing the nanospheres, non-freeze-dried particles were resuspended in 40 ml of release buffer (PBS pH 7.4, containing 0.049 M NaH_2PO_4, 0.099 M Na_2HPO_4, 0.006 M NaCl and 0.05% (w/w) NaN_3). While stirring to keep the suspension homogenized, 20 ml of the nanoparticle suspension was divided into 400-µl aliquots in eppendorf tubes and were incubated at 37°C under 40 rpm rotation. The remaining suspension (20 ml) was washed once with 45 ml reverse osmosis water and centrifuged at 7000 X g for 30 minutes and then freeze-dried to determine the particle mass and loading efficiency. Thus, each eppendorf tube contained a known amount (4-6 mg/ml) nanospheres. At different time points, two tubes were taken and nanospheres were collected after centrifugation at 13000 X g for 15 min and the pH of supernatants was determined. The amount of BSA released in the supernatants was measured by UPLC (Acquity UPLC®) equipped with a BEH 300 C18 1.7 µm column. A gradient elution method was used with mobile phase A (95% H_2O, 5% ACN and 0.1% TFA) and mobile phase B (100% ACN and 0.1% TFA). The eluent linearly changed from 60:40 (A:B) to 1:100 (A:B) over 6 min and set back to 60:40 (A:B) in 4 min, with a flow rate of 0.250 ml/min. The injection volume was 7.5 µl, and UV absorbance was measured at 280 nm. BSA standards (10-300 µg/ml) were used for calibration. The amount of protein released is reported relative to the calculated amount of protein that was present in the known amount of nanospheres, based on the loading efficiency.

BSA release from freeze-dried BSA-loaded nanospheres was also carried out under the same condition with 5 mg/ml of particles in the same buffer. The released BSA from particles made of both high and low MW polymer was analyzed by far-UV CD spectroscopy (250–200 nm) at ambient temperature in a quartz cell (path length 0.05 cm) with a dual-beam DSM 1000 CD spectrophotometer (On- Line Instruments System, Bogart, GA, USA). Five scans of each sample were averaged. Figures were fitted by using Boltzman sigmoidal model of GraphPad software.

2.8. In vitro degradation of PLGHMGA nanospheres

Non-freeze-dried nanospheres dispersed (4-6 mg/ml) in 1 ml PBS buffer (0.049 M NaH_2PO_4, 0.099 M Na_2HPO_4, 0.006 M NaCl and 0.05% (w/w) NaN_3) were transferred into eppendorf tubes. The samples were incubated at 37 °C while gently shaken. At different time points, three tubes were taken and the nanospheres were collected after centrifugation at 13000 X g for 15 min and washed with 1 ml reverse osmosis water. After freeze-drying, the remaining weight of the samples was measured. NMR, DSC and GPC were used to analyze the remaining insoluble residues.

3. Results

3.1. Synthesis and characterization of poly(lactic-co-glycolic–co-hydroxymethyl glycolic acid) (PLGHMGA) differing in copolymer composition and molecular weight

Benzyl protected hydroxymethyl glycolide (BMG) and D,L-lactide (L) were copolymerized using a melt polymerization technique at 130 °C. The polymers were obtained in high yields (>90%). The results of copolymer composition and molecular weight determinations are presented in Table 1. NMR analysis showed that the copolymer compositions were close to the monomer feed ratios. This is common for polymers obtained in high yields [31]. The DSC thermograms showed that the different PLGBMGAs were completely amorphous with T_g's between 30 and 40 °C. Complete removal of the protecting benzyl groups by catalytic hydrogenation was confirmed by ^{1}H NMR analysis. The peak assignments are reported in Figure 2 and the % of each monomer in the copolymers are shown in Table 1.

Table 1: *Characteristics of protected (PLGBMGA) and deprotected (PLGHMGA) copolymers.*

Composition x:y [a]			(protected) Theoretical [c]	(protected) Measured [d]		(deprotected) Theoretical [c]	(deprotected) Measured [d]		T_g °C	
Feed ratio	Copolymer ratio [b]	M/I (mol)	M_n (kg/mol)	M_n(kg/mol)	M_w(kg/mol)	M_n(kg/mol)	M_n(kg/mol)	M_w(kg/mol)	protected polymer	deprotected polymer
35:65	37:63	100	17.6	12	27	14	12	21	33	54
35:65	36:64	300	54	27	57	43	24	44	42	57
25:75	26:74	100	17	12	23	14	13	21	33	53
25:75	26:74	300	50	40	85	43	43	80	37	57

[a] *x:y denotes the ratio of BMG/D,L-Lactide*

[b] *Determined by 1H-NMR*

[c] *The theoretical Mn is calculated from the [monomer]/[initiator] molar ratio*

[d] *Determined by GPC*

The deprotected copolymers poly(lactic-co-glycolic–co-hydroxymethyl glycolic acid) (PLGHMGA) were obtained in high yields (>80%) and the T_g's of ~55 °C were slightly higher than those of the protected copolymers, which is in agreement with previous findings [42]. Also, removal of the protecting benzyl groups was not associated with chain scission. Table 1 also shows that, as anticipated, the molecular weight of the polymer increased with increasing the molar ratio of monomers to initiator.

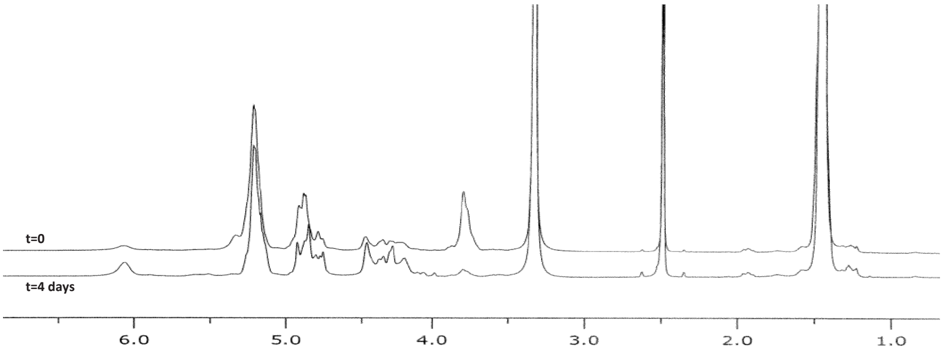

Figure 2: *^{1}H NMR spectrum of PLGHMGA 64/18/18 (L/G/HMG) in DMSO at day 0 (top) and after 4 days of degradation (bottom).*

δ = 1.3-1.5 (m, 3H, $-CH_3$), 2.5 (s, CH_3, DMSO), 3.3 (s, H_2O), 3.7-3.9 (m, 2H, CH-CH_2-OH), 4.2-4.5 (m, 3H, -O-$\underline{CH_2}$-$\underline{CH}$-OH of transesterified polymer), 4.7-5 (m, 2H, O-$\underline{CH_2}$-C(O)O), 5.2-5.4 (m, 2H, -$\underline{CH}$-CH_3 of lactic + 1H, $\underline{CH}$-CH_2-OH of HMG)

3.2. Preparation and characterization of nanospheres

BSA-loaded PLGHMGA nanospheres were prepared using a double emulsion solvent evaporation method. The obtained nanospheres appeared non-porous and had spherical geometries independent of polymer concentration, molecular weight and composition, as shown by a typical scanning electron micrograph (Fig. 3).

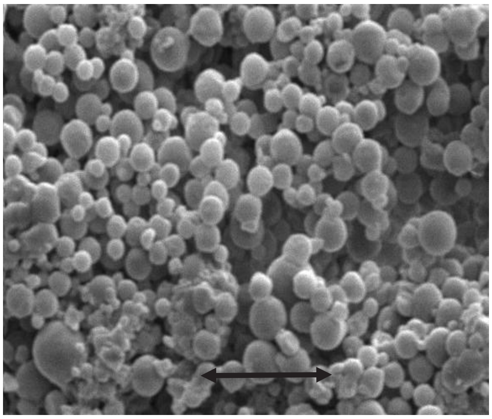

Figure 3: *SEM analysis of nanospheres of PLGHMGA 74/13/13 (L/G/HMG), 43 kg/mol (scale bar represents 5 µm).*

Nanospheres were prepared using solutions of PLGHMGA 64/18/18 in DCM with different concentrations. The results shown in Table 2 demonstrate that the size of the nanospheres increased with increasing polymer concentration (from 5% to 15% w/w), i.e. from 398 to 457 nm and from 418 to 613 nm for nanospheres made of low and high molecular weight polymers, respectively. The larger particle size for the copolymer of higher molecular weight was also observed for particles made of PLGHMGA 74/13/13, i.e. 671nm as compared to 483 nm for the corresponding low molecular weight copolymer. When the polymer concentration in the organic phase was at least 10% w/w, the BSA-loading efficiency was quite high (67-76%), with the highest values observed for particles prepared with polymers of higher molecular weight.

Table 2: *Characteristics of BSA-loaded nanospheres (2<n<5 depending on the batch) prepared using PLGHMGA copolymers with different copolymer compositions and molecular weights.*

Composition x:y:z[a]	**M_n (kg/mol)**	**Polymer concentration in DCM (%w/v)**	**Z-average diameter(nm)**	**L %** [b]	**LE** [c] **(%)**	**Yield (%)**
64/18/18	12	5	398±18	3.27±0.17	23.5±0.5	70±3
		10	421±6	4.83±0.49	67.5±3.0	72±6
		15	457±18	2.19±0.02	51.5±1.5	79±1
64/18/18	24	5	418±19	3.87±0.02	29.5±1.5	75±6
		10	466±32	4.80±0.25	76.3±2.6	80±3
		15	613±13	2.87±0.02	71.5±4.5	83±6
74/13/13	13	10	483±31	--	--	60±6
74/13/13	43	10	671±13	4.36±0.78	68.8±13.8	79±7

[a] *x:y:z denotes the ratio of L/G/HMG*

[b] *L% (loading %) expressed as encapsulated amount of protein divided by the total dry weight of the nanospheres.*

[c] *LE (Loading Efficiency) is expressed as the amount of entrapped protein divided by the initial amount of protein used for encapsulation*

3.3. Release of BSA from PLGHMGA nanospheres

Figure 4 shows the release of BSA from lyophilized and non-lyophilized nanospheres of PLGHMGA 64/18/18 of low and high molecular weights. The lyophilized nanospheres made of the low and high molecular weight polymer showed a burst release of around 50 and 40%, respectively. Due to this high burst, the release study of the freeze-dried particles was aborted and we only continued with the release of non-freeze-dried particles. Non-lyophilized nanospheres made of low molecular weight polymer showed a burst release of BSA of around 25% followed by an almost zero-order release of the protein during 60 days. The burst release was reduced to around 10% for nanospheres prepared of PLGHMGA with higher molecular weight and BSA was subsequently released with the same kinetics as that from the nanospheres of the low molecular weight polymer. Importantly, within the experimental error the non-freeze-dried particles released their complete protein contents in about 60 days.

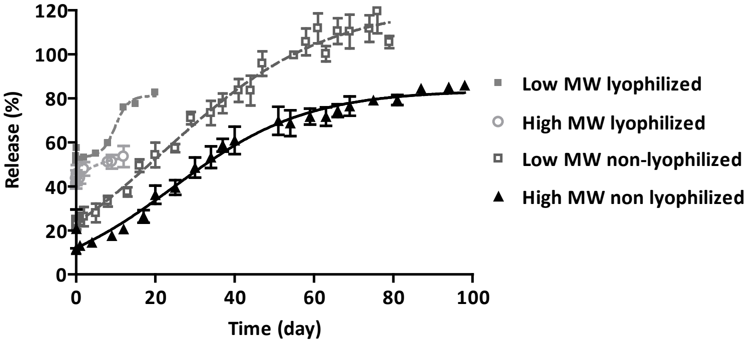

Figure 4: *BSA release from lyophilized (n=1 or 2) and non-lyophilized (n=4) nanospheres made of PLGHMGA 64/18/18 (L/G/HMG) of different molecular weights (Low = 12 kg/mol and High = 24 kg/mol).*

The release of BSA from non-lyophilized nanospheres based on PLGHMGA 64/18/18 prepared with solutions of this polymer in DCM of different concentrations are presented in Figure 5. This figure shows that the different nanospheres showed almost the same release patterns: a small burst of 20-25% followed by a sustained release for 60-80 days. Figure 6 shows that nanospheres made of PLGHMGA with a lower content of HMG (13%) showed a low burst release (6%). After a lag phase of ~40 days, these particles showed a relatively fast release over the next 20 days. Further, the far-UV CD spectrum of the released BSA reveals that the extent of α-helical secondary structure of the protein matches that of native BSA (Fig. 7). This finding demonstrates that the released protein retained its structural integrity**.**

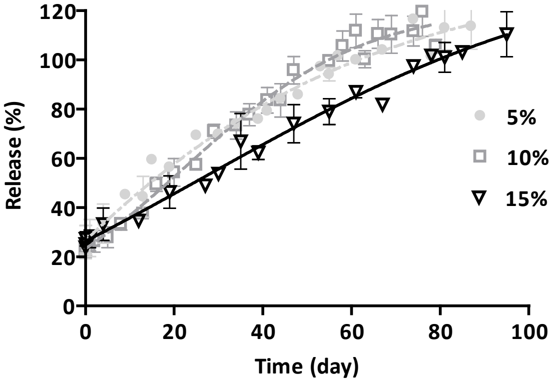

Figure 5: *BSA release from nanospheres of PLGHMGA 64/18/18 (L/G/HMG) 12 kg/mol, prepared by using different polymer concentrations (w/w %) in the organic phase (n=2).*

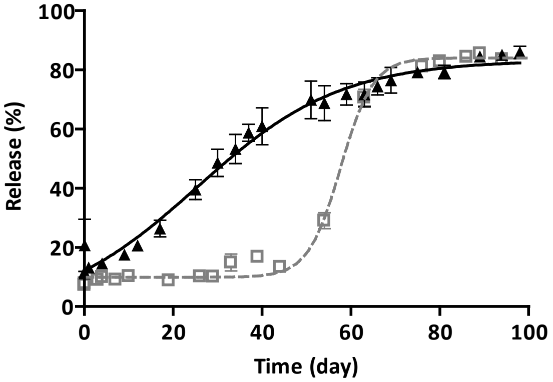

Figure 6: *BSA release from PLGHMGA nanospheres made of different PLGHMGA; (▲) 64/18/18 (L/G/HMG), 24 kg/mol (n=4) (☐) 74/13/13 (L/G/HMG), 43 kg/mol (n=2).*

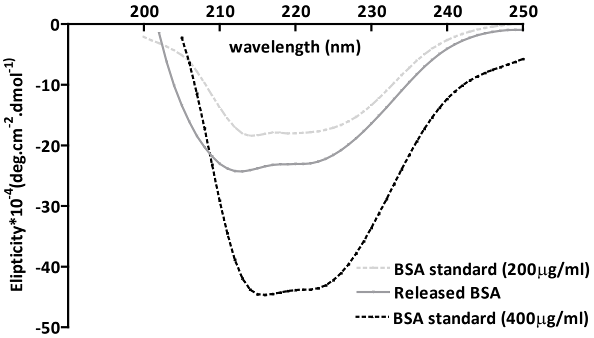

Figure 7: *Circular Dichroism spectra of native and released BSA in very last days of release.*

3.4. In vitro degradation and erosion of PLGHMGA nanospheres

Nanospheres of PLGHMGA of different molecular weights and copolymer compositions incubated at physiological conditions (PBS buffer pH 7.4, 37°C) showed a continuous weight loss in time for more than 100 days (Fig. 8a, 9a, 10a and 11a) and a decrease in number average molecular weights (Fig. 8b, 9b, 10b and 11b). It should be mentioned that no significant pH drop of the release medium was observed and the measured pH after complete particle degradation was 6.5±0.5. Dry-mass loss of PLGHMGA with the same copolymer compositions but different initial molecular weights showed similar patterns (8a and 9a). PLGHMGA 64/18/18 of high molecular weight showed a substantial decrease (50%) of the number average molecular weight during the first 4 days, whereas the M_n of the low molecular weight polymer showed a small decrease of around 20% (Fig. 8b). During the next 8 days, the molecular weights of both polymer samples reached the same value of 8 kg/mol and continued to follow the same degradation profile. A similar trend was observed for PLGHMGA 74/13/13 (Fig. 9b). The effect of copolymer composition of PLGHMGA on the degradation kinetic of nanospheres is shown in figure 10 (for the high molecular weight polymers) and 11 (for the low molecular weight polymers). The kinetics of the changes in M_n for nanospheres made of PLGHMGA 64/18/18 and 74/13/13 were similar. However, mass loss of nanospheres made of PLGHMGA 74/13/13 was slower than that of the 64/18/18 spheres (Fig. 10a and 11a).

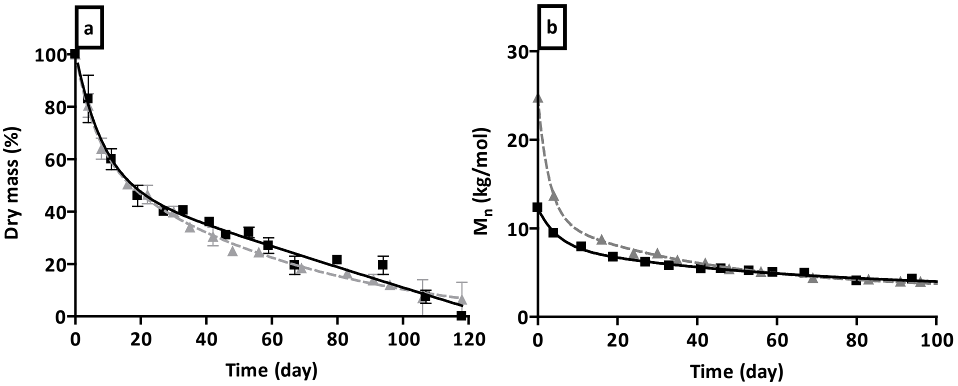

Figure 8: (a) *Relative mass (n=2) and (b) number average molecular weight (M_n) of PLGHMGA 64/18/18 (L/G/HMG) nanospheres during degradation in PBS buffer at 37 °C; starting molecular weights were (■) 12 kg/mol, (▲) 24 kg/mol.*

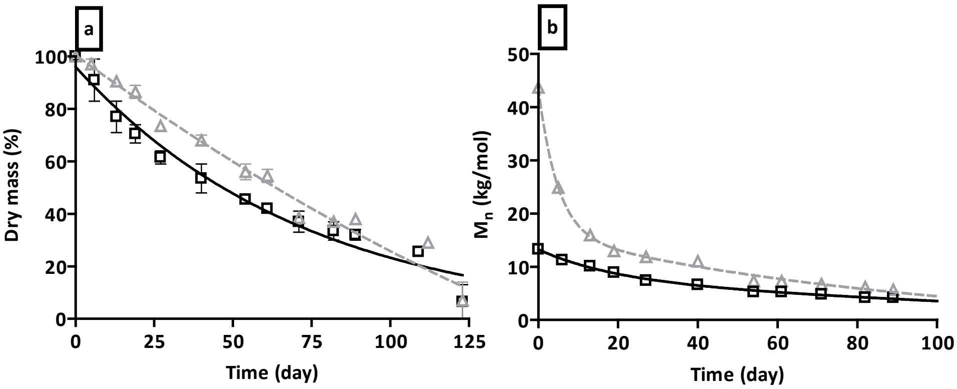

Figure 9: *(a) Relative mass (n=2) and (b) number average molecular weight (M_n) of PLGHMGA 74/13/13 (L/G/HMG) nanospheres during degradation in PBS buffer and 37 °C; starting molecular weights were (□) 13 kg/mol, (△) 43 kg/mol.*

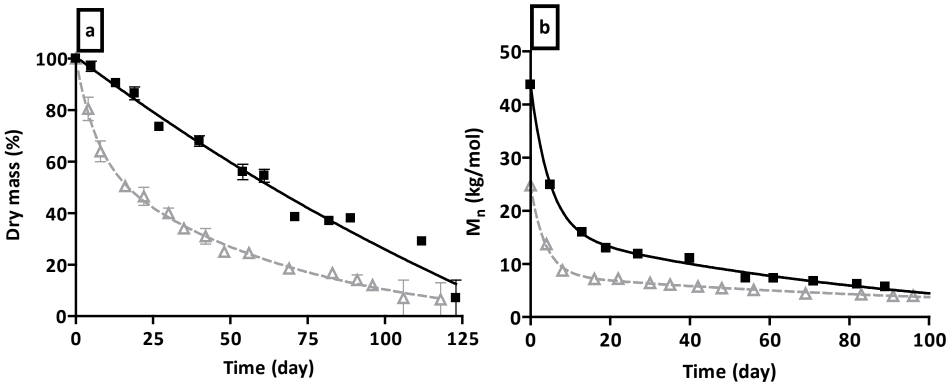

Figure 10: *a) Relative mass (n=2) and (b) number average molecular weight (M_n) of PLGHMGA nanospheres made of different PLGHMGA; a): (△) 64/18/18 (L/G/HMG), 24 kg/mol (■) 74/13/13 (L/G/HMG), 43 kg/mol; as a function of time.*

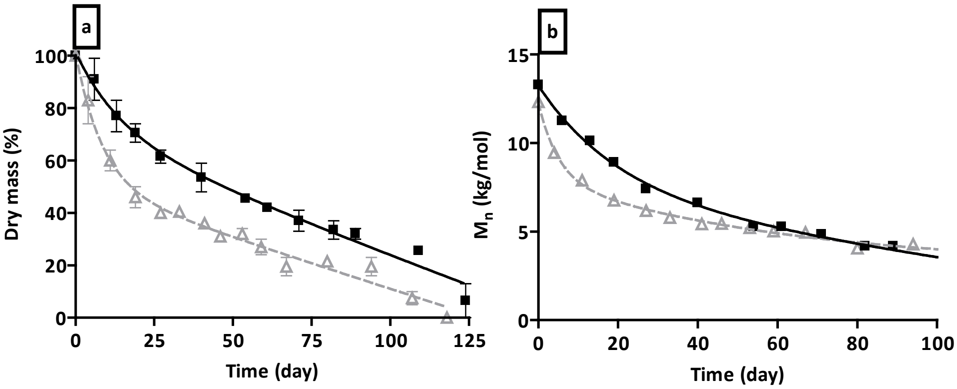

Figure 11: *(a) Relative mass (n=2) and (b) number average molecular weight (M_n) of PLGHMGA nanospheres made of different copolymer composition as a function of time; (△) 64/18/18, 12 kg/mol, (■) 74/13/13, 13 kg/mol.*

The changes in copolymer compositions of degrading nanospheres made of different PLGHMGAs were measured by ^{1}H NMR spectroscopy. The ^{1}H NMR spectrum of nanoparticles' residues showed a dramatic decrease of the peak at 3.8 ppm (attributed the CH_2 of the HMG unit [31]) during the first 4 days, with a concomitant increase of the peaks integral between 4.0 and 4.5 ppm relative to the integral of the lactide CH group at 5.2 ppm (Fig. 2). As it will be explained in the Discussion section, this is most likely due to intramolecular transesterification. Nevertheless, taking the peaks between 4.0 and 4.5 ppm into account, a gradual decrease from 18% to 11% of hydrophilic (HMG) and glycolic acid units in the remaining co-polymer occurred in time (Table 3). Differential scanning calorimetry was used to investigate the effect of changes in copolymer composition and molecular weight on polymer characteristics during degradation. Table 3 shows that the glass transition temperature (T_g) of PLGHMGA nanospheres remained constant during degradation. Glass transition analysis also showed the same value for both BSA-loaded and placebo particles.

Table 3: *Change in copolymer composition and glass transition temperature of nanospheres made of PLGHMGA 68/16/16 (L/G/HMG) (24 kg/mol) during degradation.*

Day	Copolymer composition			T_g °C
	HMG	Glycolic acid	Lactic acid	
0	18	18	64	57
4	15	19	65	54
8	15	16	69	54
11	13	15	71	54
19	13	14	73	54
94	11	11	78	54

4. Discussion

Formulation and processing parameters such as polymer concentration, composition and molecular weight can influence porosity, loading efficiency and size of drug loaded particles, which are known as the most important particle properties that affect the characteristics of the drug delivery system. In the present study, it is shown that increasing the polymer concentration and molecular weight led to an increase of the particle size (Table 2). Likely, a higher viscosity of the oil phase due to the higher polymer concentration results in larger emulsified droplets and consequently in the formation of larger nanospheres, as also observed for PLGA nanospheres [43]. BSA was entrapped with a high efficiency (upto 76%) in the nanospheres (Table 2). A higher entrapment was observed for nanospheres prepared with a higher polymer concentration (from 5 to 10-15%) (Table 2), as also observed for protein-loaded PLGA nanospheres [43, 44]. Likely, a higher viscosity of the organic phase reduces the partitioning of the protein into the external aqueous phase, resulting in an increase in protein entrapment efficiency. Moreover, a higher polymer concentration also results in a faster solidification of the polymer during the solvent evaporation process, which in turn will retard diffusion of the protein into the continuous phase [45]. However, this effect was not observed by increasing from 10 to 15% polymer concentration. Freeze-dried nanospheres showed a high burst release (40-50% of the loaded protein), whereas for non-freeze-dried nanospheres a low burst of 10-20% was observed (Fig. 4). A burst is generally attributed to rapid diffusion of the protein through existing pores in polymer matrix [46, 47]and also to protein present in interior pores and cracks of large sizes (cracks), and it can therefore be concluded that freeze-drying causes formation of pores [48] freeze drying was done under conditions that are normally used for the freeze-drying of polymeric (e.g. PLGA) particles. These conditions obviously result in the formation of pores [49, 50, 51]. By using lyoprotectants in combination with more sophisticated lyophilizators the formation of pores can likely be minimized or prevented [51, 52]. Likely, the formed nanospheres contain water originating from the primary w/o emulsion that is sublimated during the freeze-drying process resulting in a porous structure. It should be noted that SEM analysis of the particles did not reveal the presence of pores, meaning that the pores are smaller than the resolution of the image (around 50 nm) but are most likely bigger than the hydrodynamic diameter of BSA, which is approximately 7 nm. Particle size is an important factor that can influence the release profile of an entrapped drug. Smaller particles have a larger surface area, which might result in a (high) burst release and a shorter period of sustained release for drugs that are molecularly dissolved [39, 53]. However, the release pattern of proteins that are not molecularly dispersed in a polymer matrix mainly depends, except the initial burst, which is substantially due to diffusion of protein through pre-existing pores, on the erosion of the particles. The same T_g observed for BSA loaded and placebo particles suggests that the protein is not molecularly dissolved in the polymer matrix and is in line with expectations given the physico-chemical characteristics of the protein and polymers used in this study. Initial porosity can be influenced by different parameters such as polymer molecular weight and concentration in the oil phase used to prepare the particles. The results shown in figure 5 demonstrate that the size of particles ranging from 350-700 nm and prepared with DCM solutions of different polymer concentration has an effect on release. However, as compared to copolymer composition, this effect is minor. Similar BSA release kinetics were observed for nanospheres made of PLGHMGA 64/18/18 of different molecular weights (Fig. 4), which can be explained by the similar nanosphere erosion/degradation properties (Fig. 8). The slower release kinetics observed for nanospheres made of PLGHMGA 74/13/13 (Fig. 6) follows the slower polymer erosion/mass loss pattern (Fig. 10a and 11a) and suggests that erosion plays a major role for the release of BSA. It has been reported that the release of BSA from PLGA and matrices of related polymers mainly occurs by diffusion through water-filled pores of which the formation in turn is dependent on the kinetics of particle erosion [55]. In addition to this, it can be expected that an increasing number of hydroxyl pendent groups will result in an increase in water uptake of the particles and increase in permeability of the matrices for low molecular weight water-soluble (hydrophilic) compounds. Our finding also illustrates that desired drug release patterns can be effectively tailored by varying the density of pendant hydroxyl groups. Erosion (mass loss) is influenced by both the rate of ester bond hydrolysis and the rate of diffusion of formed water-soluble degradation products out of the polymer matrix [54], which also depends on morphological changes of the particles, particularly pore formation, and the solubility of formed oligomers in the surrounding medium. Intuitively, it can be expected that it would take longer for high molecular weight polymers to reach the minimum threshold molecular weight for dissolution thus they have slower erosion. However, our results (Fig. 8) show erosion rates that are independent of initial molecular weight. This can be explained by the faster decay in molecular weight of the high molecular weight polymers: figure 8b shows that M_n of the relatively high molecular weight polymer showed an initial faster decrease than that of the low molecular weight polymer, reaching the same value at day 8, which explains the almost same erosion profile of the nanosphere formulations made of low and high molecular weight PLGHMGA. The influence of initial molecular weight on the rate of decrease of M_n can be explained as follows. Assume we have two polymer chains with low molecular weight and one polymer chain with twice the molecular weight, meaning that the total number of ester bonds is equal. When all ester bonds have equal susceptibility for hydrolysis and when, let's say, two ester bonds are cleaved, then for the one chain this will give a 3 times reduction in average molecular weight, but with the two LMW chains this will give only 2 times reduction in average molecular weight (on average only one ester bond is split in each chain). In other words, for HMW chains the relative molecular weight drop is faster. This is also shown in figure 12, where the drop in average molecular weight is plotted against the total number of hydrolysed ester bonds in this theoretical model. Note that the model (Fig. 12) shows qualitatively a remarkable resemblance with the measured profiles of the M_n decrease in figures 8b and 9b.

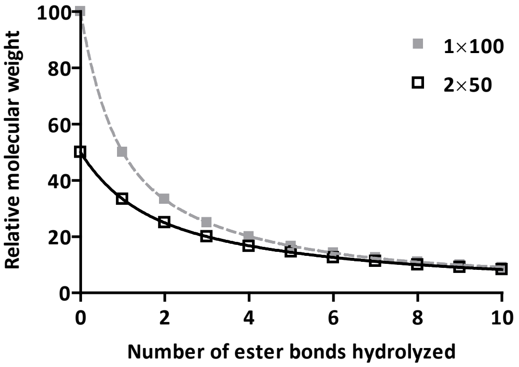

Figure 12: *Theoretical model calculation showing the change in relative M_n upon hydrolysis of one polymer chain of high molecular weight (1×100) and two polymer chains with half initial molecular weight (2×50).*

The nanospheres showed a continuous mass loss as well as a continuous decrease in molecular weight of the polymer (Figures 8, 9, 10 and 11). Mass loss coinciding with a drop in molecular weight implies that ester bond hydrolysis is followed by diffusion of water-soluble degradation products out of the polymer matrix, which indicates that the degradation mechanism is bulk degradation [56]. It has been shown that small polymeric particles can homogenously absorb water resulting in an equal rate of hydrolysis throughout of polymer matrix [56]. The rather constant PDI (M_w/M_n) of the degrading polymers of around 1.8 supports a homogenous polymer degradation [56]. Also the T_g of the polymers remained constant during nanoparticle degradation. Factors that influence T_g of polymers are polymer structure, molecular weight and presence of water and plasticizers. The constant T_g of the nanospheres during degradation can be attributed to the relatively constant copolymer composition and also fast diffusion of low molecular weight degradation products from the polymer matrix that might act as a plasticizer. A close analysis of the residual water-insoluble nanospheres by ^1H NMR revealed a decrease of the CH_2 peak of the HMG unit at 3.8 ppm relative to the lactide CH peak at 5.2 ppm, which might intuitively suggest that the HMG units are preferentially removed from the polymer during hydrolysis [57, 58]. However, also a relative increase of the peaks between 4.0 and 4.5 ppm in the NMR spectrum at day 4 as compared to the starting polymer was observed (Fig. 2). It is proposed that the origin of this peak shift to an intramolecular transesterification as depicted in figure 13 [59]. Nucleophilic attack of the hydroxyl group at the nearby carbonyl group generates a five-membered ring intermediate, which can either turn back to the original structure or result in transesterification and therefore change in copolymer molecular structure to a thermodynamically more stable ester (Fig. 13). This process causes a shift of the proton peaks at 3.8 ppm (CH_2) and 5.2 ppm (CH, coinciding with CH of lactide) for the HMG units in the original structure [60] to 4.0-4.5 ppm for the transesterified product (hydrogens at position 1 and 2 see figure 13) [61].

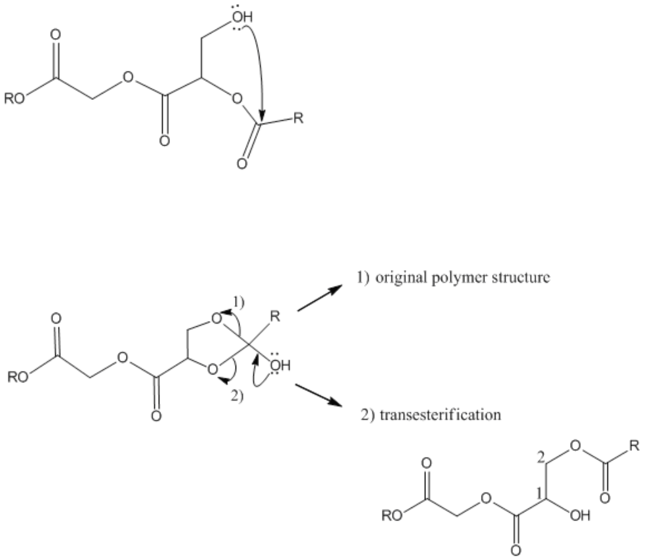

Figure 13: *Suggested transesterification mechanism in a PLGHMGA chain. The peaks between 4.0 and 4.5 ppm in the NMR spectrum (Fig. 2) can be assigned to the hydrogens at position 1 and 2.*

Besides this transesterification, ^{1}H NMR analysis of degrading samples shows a gradual decrease in both HMG (either in its native conformation or as transesterified units) and glycolic content in the copolymer from 18% to 11% (Table 3). Indeed, it has been argued that HMG ester bonds in PLGHMGA are more susceptible to hydrolysis [57] and results in a relatively fast release of HMG units from the degrading polymer matrix (Table 3). PLGHMGA 74/13/13 is more hydrophobic than 64/18/18 PLGHMGA and a slower hydrolysis as well as slower dry mass loss of the former polymer is expected due to its lower water-absorbing capacity (Fig. 10 and 11) [57]. As mentioned in the Introduction section, we previously reported on release of BSA from microspheres of similar copolymers containing similar amounts of hydrophilic HMG units but lacking the glycolic acid units (PLHMGA instead of PLGHMGA). With respect to these previous findings, the nanospheres presented in the present work showed slower degradation and release kinetic compared to microspheres. A recent study with PLHMGA microspheres showed almost no drop of micro environmental pH during the entire degradation time, suggesting that acid-induced autocatalytic hydrolysis did not occur [34]. Because the degradation and release is slower for the nanospheres presented here, it is anticipated that such autocatalysis did not either happen for the nanospheres. In fact, intuitively one would expect faster degradation and release for the nanospheres as compared to PLHMGA microspheres for two reasons. First, the nanospheres are prepared from a more hydrophilic copolymer (because of the glycolic acid units), and second the nanoparticles have a larger surface area than microspheres, which might enhance hydration and degradation. However, as faster degradation/release was not observed, it can be speculated that higher density of nanospheres, perhaps by lower porosity, might compensate for their larger surface area, causing lower water absorption and slower degradation. Indeed, it is known that beside polymer structure and degradation condition, hydration and rate of degradation depends on particle characteristics such as particle porosity and density [62]. Another parameter is the surface-associated PVAL. The amount of PVAL used for preparation of nanoparticles was much higher (5%) than that of microparticles (1%). It has been shown by others that surface associated PVAL in nanoparticles can form a barrier to penetration of water into and out of nanospheres leading to a slow degradation [63].

5. Conclusions

BSA-loaded nanospheres based on PLGHMGA of different copolymer compositions and molecular weights were prepared by using a double emulsion solvent evaporation method. Our study provides mechanistic insight into the particle degradation and its influence on protein release. It is demonstrated that the particles showed a gradual mass loss in time with faster erosion for those prepared from a more hydrophilic PLGHMGA. It was also shown that there is a good correlation between release of BSA and dry mass loss/particle erosion. Therefore, PLGHMGA nanoparticles are promising systems for controlled release of pharmaceutical proteins.

References

1. Vermonden, T.; Censi, R.; Hennink, W. E. Hydrogels for protein delivery. *Chem. Rev.* 2012*;112*: 2853-2888.

2. Jorgenson, L.; Nielson, H. M. *Delivery Technologies for Biopharmaceuticals: Peptides, Proteins, Nucleic Acids and Vaccines* John Wiley & Sons Ltd: UK, 2009.

3. Frokjaer, S.; Otzen, D. E. Protein drug stability: a formulation challenge. *Nat. Rev. Drug Discov.* 2005;*4*:298-306.

4. Woodhams, J.; Lou, P. J.; Selbo, P. K.; Mosse, A.; Oukrif, D.; MacRobert, A.; Novelli, M.; Peng, Q.; Berg, K.; Bown, S. G. Intracellular re-localisation by photochemical internalisation enhances the cytotoxic effect of gelonin--quantitative studies in normal rat liver. *J. Control. Release*. 2010*;142:*347-353.

5. Stayton, P. S.; El-Sayed, M. E.; Murthy, N.; Bulmus, V.; Lackey, C.; Cheung, C.; Hoffman, A. S. 'Smart' delivery systems for biomolecular therapeutics. *Orthod. Craniofac. Res.* 200; *8:*219-225.

6. Fattal, E.; Couvreur, P.; Dubernet, C. "Smart" delivery of antisense oligonucleotides by anionic pH-sensitive liposomes. *Adv. Drug Deliv. Rev.* 2004*;56*:931-946.

7. El-Sayed, M. E.; Hoffman, A. S.; Stayton, P. S. Smart polymeric carriers for enhanced intracellular delivery of therapeutic macromolecules. *Expert Opin. Biol. Ther.* 2005;*5:*23-32.

8. Bale, S. S.; Kwon, S. J.; Shah, D. A.; Banerjee, A.; Dordick, J. S.; Kane, R. S. Nanoparticle-mediated cytoplasmic delivery of proteins to target cellular machinery. *ACS Nano.* 2010;*4*:1493-1500.

9. Torchilin, V. P. Targeted pharmaceutical nanocarriers for cancer therapy and imaging. *AAPS J.* 2007;*9*:E128-47.

10. van de Weert, M.; Hennink, W. E.; Jiskoot, W. Protein instability in poly(lactic-co-glycolic acid) microparticles. *Pharm. Res.* 2000*;17:*1159-1167.

11. Hughes, G. A. Nanostructure-mediated drug delivery. *Nanomedicine.* 2005;*1:*22-30.

12. Holzer, M.; Vogel, V.; Mantele, W.; Schwartz, D.; Haase, W.; Langer, K. Physico-chemical characterisation of PLGA nanoparticles after freeze-drying and storage. *Eur. J. Pharm. Biopharm.* 2009;*72:*428-437.

13. Benfer, M.; Kissel, T. Cellular uptake mechanism and knockdown activity of siRNA-loaded biodegradable DEAPA-PVA-g-PLGA nanoparticles. *Eur. J. Pharm. Biopharm.* 2012;*80*:247-256.

14. Cheng, R.; Feng, F.; Meng, F.; Deng, C.; Feijen, J.; Zhong, Z. Glutathione-responsive nano-vehicles as a promising platform for targeted intracellular drug and gene delivery. *J. Control. Release.* 2011 *152:*2-12.

15. Danhier, F.; Ansorena, E.; Silva, J. M.; Coco, R.; Le Breton, A.; Preat, V. PLGA-based nanoparticles: An overview of biomedical applications. *J. Control. Release* 2012*;161*:505-522.

16. Mundargi, R. C.; Babu, V. R.; Rangaswamy, V.; Patel, P.; Aminabhavi, T. M. Nano/micro technologies for delivering macromolecular therapeutics using poly(D,L-lactide-co-glycolide) and its derivatives. *J. Control. Release.*2008*;125*:193-209.

17. Shive, M. S.; Anderson, J. M. Biodegradation and biocompatibility of PLA and PLGA microspheres. *Adv. Drug Deliv. Rev.* 1997*;28*:5-24.

18. Joung, Y. K.; Son, S.; Jang, J. Y.; Kwon, M. H.; Park, K. D. Sustained cytoplasmic delivery and anti-viral effect of PLGA nanoparticles carrying a nucleic acid-hydrolyzing monoclonal antibody. *Pharm. Res.* 2012*;29*:932-942.

19. Cun, D.; Jensen, D. K.; Maltesen, M. J.; Bunker, M.; Whiteside, P.; Scurr, D.; Foged, C.; Nielsen, H. M. High loading efficiency and sustained release of siRNA encapsulated in PLGA nanoparticles: quality by design optimization and characterization. *Eur. J. Pharm. Biopharm.* 2011*;77*:26-35.

20. Panyam, J.; Labhasetwar, V. Biodegradable nanoparticles for drug and gene delivery to cells and tissue. *Adv. Drug Deliv. Rev.* 2003*;55*:329-347.

21. Ding, A. G.; Schwendeman, S. P. Acidic microclimate pH distribution in PLGA microspheres monitored by confocal laser scanning microscopy. *Pharm. Res.* 2008*;25*:2041-2052.

22. Bilati, U.; Allemann, E.; Doelker, E. Strategic approaches for overcoming peptide and protein instability within biodegradable nano- and microparticles. *Eur. J. Pharm. Biopharm.* 2005*;59*:375-388.

23. Liu, Y.; Schwendeman, S. P. Mapping microclimate pH distribution inside protein-encapsulated PLGA microspheres using confocal laser scanning microscopy. *Mol. Pharm.* 2012*;9*:1342-1350.

24. Ye, M.; Kim, S.; Park, K. Issues in long-term protein delivery using biodegradable microparticles. *J. Control. Release.* 2010*;146*:241-260.

25. Giteau, A.; Venier-Julienne, M. C.; Marchal, S.; Courthaudon, J. L.; Sergent, M.; Montero-Menei, C.; Verdier, J. M.; Benoit, J. P. Reversible protein precipitation to ensure stability during encapsulation within PLGA microspheres. *Eur. J. Pharm. Biopharm.* 2008*;70*:127-136.

26. Jevsevar, S.; Kunstelj, M.; Porekar, V. G. PEGylation of therapeutic proteins. *Biotechnol. J.* 2010*;5:*113-128.

27. Giteau, A.; Venier-Julienne, M. C.; Aubert-Pouessel, A.; Benoit, J. P. How to achieve sustained and complete protein release from PLGA-based microparticles? *Int. J. Pharm.* 2008*;350:*14-26.

28. Diwan, M.; Park, T. G. PEGylation enhances protein stability during encapsulation in PLGA microspheres. *J. Control. Release.* 2001*;73*:233-244.

29. Shenderova, A.; Burke, T. G.; Schwendeman, S. P. The acidic microclimate in poly(lactide-co-glycolide) microspheres stabilizes camptothecins. *Pharm. Res.* **1999***, 16*, 241-248.

30. Schwendeman, S. P. Recent advances in the stabilization of proteins encapsulated in injectable PLGA delivery systems. *Crit. Rev. Ther. Drug Carrier Syst.* 2002*;19*:73-98.

31. Leemhuis, M.; vanNostrum, C. F.; Kruijtzer, J. A. W.; Zhong, Z. Y.; tenBreteler, M. R.; Dijkstra, P. J.; Feijen, J.; Hennink, W. E. Functionalized poly (alpha-hydroxy acid)s via ring-opening polymerization: toward hydrophilic polyesters with pendant hydroxyl groups. *Macromolecules.* 2006*;39*:3500–3508.

32. Ghassemi, A. H.; van Steenbergen, M. J.; Talsma, H.; van Nostrum, C. F.; Jiskoot, W.; Crommelin, D. J.; Hennink, W. E. Preparation and characterization of protein loaded microspheres based on a hydroxylated aliphatic polyester, poly(lactic-co-hydroxymethyl glycolic acid). *J. Control. Release.* 2009*;138*:57-63.

33. Ghassemi, A. H.; van Steenbergen, M. J.; Talsma, H.; van Nostrum, C. F.; Crommelin, D. J.; Hennink, W. E. Hydrophilic polyester microspheres: effect of molecular weight and copolymer composition on release of BSA. *Pharm. Res.* 2010*;27*:2008-2017.

34. Liu, Y.; Ghassemi, A. H.; Hennink, W. E.; Schwendeman, S. P. The microclimate pH in poly(d,l-lactide-co-hydroxymethyl glycolide) microspheres during biodegradation. *Biomaterials.* 2012*;33*:7584-7593.

35. Joshi, V. B.; Geary, S. M.; Salem, A. K. Biodegradable particles as vaccine delivery systems: size matters. *AAPS J.* 2013;*15*:85-94.

36. Zweers, M. L.; Engbers, G. H.; Grijpma, D. W.; Feijen, J. In vitro degradation of nanoparticles prepared from polymers based on DL-lactide, glycolide and poly(ethylene oxide). *J. Control. Release* 2004*;100*:347-356.

37. Klose, D.; Siepmann, F.; Elkharraz, K.; Siepmann, J. PLGA-based drug delivery systems: importance of the type of drug and device geometry. *Int. J. Pharm.* 2008*;354*:95-103.

38. Ogawa, Y.; Yamamoto, M.; Okada, H.; Yashiki, T.; Shimamoto, T. A new technique to efficiently entrap leuprolide acetate into microcapsules of polylactic acid or copoly(lactic/glycolic) acid. *Chem. Pharm. Bull. (Tokyo)* 1988*;36*:1095-1103.

39. Singh, R.; Lillard, J. W.,Jr Nanoparticle-based targeted drug delivery. *Exp. Mol. Pathol.* 2009*;86:*215-223.

40. Zambaux, M. F.; Bonneaux, F.; Gref, R.; Maincent, P.; Dellacherie, E.; Alonso, M. J.; Labrude, P.; Vigneron, C. Influence of experimental parameters on the characteristics of poly(lactic acid) nanoparticles prepared by a double emulsion method. *J. Control. Release.* 1998*;50*:31-40.

41. Sah, H. A new strategy to determine the actual protein content of poly(lactide-co-glycolide) microspheres. *J. Pharm. Sci.* 1997*;86*:1315-1318.

42. Seyednejad, H.; Ghassemi, A. H.; van Nostrum, C. F.; Vermonden, T.; Hennink, W. E. Functional aliphatic polyesters for biomedical and pharmaceutical applications. *J. Control. Release.* 2011*;152:*168-176.

43. Lamprecht, A.; Ubrich, N.; Hombreiro Perez, M.; Lehr, C.; Hoffman, M.; Maincent, P. Biodegradable monodispersed nanoparticles prepared by pressure homogenization-emulsification. *Int. J. Pharm.* 1999*;184*:97-105.

44. Ravi Kumar, M. N.; Bakowsky, U.; Lehr, C. M. Preparation and characterization of cationic PLGA nanospheres as DNA carriers. *Biomaterials.* 2004*;25*:1771-1777.

45. Rafati, H.; Coombes, A. G. A.; Adler, J.; Holland, J.; Davis, S. S. Protein-loaded poly (DLlactide-co-glycolide) microparticles for oral administration: formulation, structural and release characteristics. *J. Control. Release.* 1997*;43:*89–102.

46. Huang, X.; Brazel, C. S. On the importance and mechanisms of burst release in matrix-controlled drug delivery systems. *J. Control. Release.* 2001*;73*:121-136.

47. van de Weert, M.; van 't Hof1, R.; van der Weerd, J.; Heeren, R. M.; Posthuma, G.; Hennink, W. E.; Crommelin, D. J. Lysozyme distribution and conformation in a biodegradable polymer matrix as determined by FTIR techniques. *J. Control. Release.* 2000*;68*:31-40.

48. Yeo, Y.; Park, K. Characterization of reservoir-type microcapsules made by the solvent exchange method. *Aaps Pharmscitech* **2004***,5*:52.

49. van Noort, J. M.; Bsibsi, M.; Nacken, P. J.; Gerritsen, W. H.; Amor, S.; Holtman, I. R.; Boddeke, E.; van Ark, I.; Leusink-Muis, T.; Folkerts, G.; Hennink, W. E.; Amidi, M. Activation of an immune-regulatory macrophage response and inhibition of lung inflammation in a mouse model of COPD using heat-shock protein alpha B-crystallin-loaded PLGA microparticles. *Biomaterials.* 2013*;34*:831-840.

50. Allison, S. D. Analysis of initial burst in PLGA microparticles. *Expert Opin. Drug Deliv.* 2008*;5*:615-628.

51. Abdelwahed, W.; Degobert, G.; Stainmesse, S.; Fessi, H. Freeze-drying of nanoparticles: formulation, process and storage considerations. *Adv. Drug Deliv. Rev.* 2006*;58*:1688-1713.

52. Bozdag, S.; Dillen, K.; Vandervoort, J.; Ludwig, A. The effect of freeze-drying with different cryoprotectants and gamma-irradiation sterilization on the characteristics of ciprofloxacin HCl-loaded poly(D,L-lactide-glycolide) nanoparticles. *J. Pharm. Pharmacol.* 2005*;57*:699-707.

53. D'Aurizio, E.; van Nostrum, C. F.; van Steenbergen, M. J.; Sozio, P.; Siepmann, F.; Siepmann, J.; Hennink, W. E.; Di Stefano, A. Preparation and characterization of poly(lactic-co-glycolic acid) microspheres loaded with a labile antiparkinson prodrug. *Int. J. Pharm.* 2011*;409*:289-296.

54. Gopferich, A. Mechanisms of polymer degradation and erosion. *Biomaterials.* 1996*;17*:103-114.

55. Fredenberg, S.; Wahlgren, M.; Reslow, M.; Axelsson, A. The mechanisms of drug release in poly(lactic-co-glycolic acid)-based drug delivery systems—A review. *Int. J. Pharm.* 2011*;415*:34-52.

56. Zweers, M. L.; Engbers, G. H.; Grijpma, D. W.; Feijen, J. In vitro degradation of nanoparticles prepared from polymers based on DL-lactide, glycolide and poly(ethylene oxide). *J. Control. Release* 2004*;100*:347-356.

57. Leemhuis, M.; Kruijtzer, J. A.; Nostrum, C. F.; Hennink, W. E. In vitro hydrolytic degradation of hydroxyl-functionalized poly(alpha-hydroxy acid)s. *Biomacromolecules.* 2007*;8*:2943-2949.

58. Schmitt, E. A.; Flanagan, D. R.; Linhardt, R. J. Importance of distinct water environments in the hydrolysis of poly(dllactide-co-glycolide). *Macromolecules.* 1994*;27*:743– 748.

59. de Jong, S. J.; Arias, E. R.; Rijkers, D. T. S.; van Nostrum, C. F.; Kettenes-van den Bosch, J. J.; Hennink, W. E. New insights into the hydrolytic degradation of poly(lactic acid): participation of the alcohol terminus. *Polymer.* 2001*;42*:2795-2802.

60. Valcavi, U.; Aveta, R.; Brandt, A.; Corsi, G. B.; Pascucci, G.; Solinas, F. Analogues of phospholipids: Synthesis and biological evaluation of a series of 3-phosphocholine glyceric acid derivatives. *Eur. J. Med. Chem.* 1990*;25*:327-332.

61. Rosseto, R.; Bibak, N.; Hajdu, J. A new approach to the synthesis of lysophospholipids: Preparation of lysophosphatidic acid and lysophosphatidylcholine from p-nitrophenyl glycerate. *Tetrahedron Lett.* 2004*;45*:7371-7373.

62. Stevanovic, M.; Uskokovic, D. Poly(lactide-co-glycolide)-based Micro and Nanoparticles for the Controlled Drug Delivery of Vitamins. *Current Nanoscience.* 2009*;5*.

63. Panyam, J.; Dali, M. M.; Sahoo, S. K.; Ma, W.; Chakravarthi, S. S.; Amidon, G. L.; Levy, R. J.; Labhasetwar, V. Polymer degradation and in vitro release of a model protein from poly(D,L-lactide-co-glycolide) nano- and microparticles. *J. Control. Release.* 2003*;92*:173-187.

4

Nanoparticles Based on a Hydrophilic Polyester with a Sheddable PEG Coating for Protein Delivery

Neda Samadi
Mies. J. van Steenbergen
Joep. B. vanden Dikkenberg
Tina. Vermonden
Cornelus F. van Nostrum
Maryam. Amidi,
Wim. E. Hennink

[1] *Department of Pharmaceutics, Utrecht Institute for Pharmaceutical Sciences, Utrecht University, Utrecht, The Netherlands*

Accepted for publication in Pharmaceutical Research

Abstract

The purpose of this study was to investigate the effect of polyethylene glycol (PEG) in nanoparticles based on blends of hydroxylated aliphatic polyester, poly(D,L-lactic-co-glycolic-co-hydroxymethyl glycolic acid) (PLGHMGA) and PEG-PLGHMGA block copolymers on their degradation and release behavior. Protein-loaded nanoparticles were prepared with blends of varying ratios of PEG-PLGHMGA (molecular weight of PEG 2000 and 5000 Da) and PLGHMGA, by a double emulsion method with or without using poly(vinyl alcohol) (PVA) as surfactant. Bovine serum albumin and lysozyme were used as model proteins.

PEGylated particles prepared without PVA had a zeta potential ranging from ~-3 to ~-35 mV and size ranging from ~200 to ~600 nm that were significantly dependent on the content and type of PEG-block copolymer. The encapsulation efficiency of the two proteins however was very low (<30%) and the particles rapidly released their content in a few days. In contrast, all formulations prepared with PVA showed almost similar particle properties (size: ~250nm, zeta potential: ~ -1 mV), while loading efficiency for both model proteins was rather high (80-90%). Unexpectedly, independent of the type of formulation, the nanoparticles had nearly the same release and degradation characteristics. NMR analysis showed almost a complete removal of PEG in 5 days which explains these marginal differences.

In conclusion Protein release and particle degradation are not substantially influenced by the content of PEG, likely because of the fast shedding of the PEG blocks. These PEG shedding particles are interesting system for intracellular delivery of drugs.

1. Introduction

Biodegradable nanoparticles based on aliphatic polyesters are presently under investigation as injectable colloidal systems for the targeted (intracellular) delivery of classical drugs as well as biotherapeutics [1-3]. It is well known that to improve the biodistribution of nanoparticles, e.g. tumor accumulation, their surface properties should be modified to give them a stealth character. One of the most commonly used strategies to increase the circulation half-life of i.v. injected nanoparticles is to cover the surface with a hydrophilic, flexible and non-ionic polymer, such as poly(ethylene glycol) (PEG) [4-6]**.** The PEG coating, however, may obstruct the entry of nanoparticles into the target cells [7]. But even when the nanoparticles are endocytosed, the PEG layer may adversely affect endosomal escape [8]. The therapeutic efficacy of sterically stabilized nanoparticles can be enhanced by means of PEG shedding after arrival of the nanoparticles at the target site. Different approaches have been used for the design of PEG sheddable nanoparticles such as shedding by degradation of the coating material itself [9]; shedding by cleavage of a chemical bond between the stabilizing polymer and its anchor [7] and shedding by spontaneous extraction of stealth polymer from the nanoparticles [10]. The shedding kinetics should however be optimized: when the stealth coating is shed too fast, the circulation kinetics will be negatively affected whereas a too slow shedding will hamper cellular uptake.

In addition to providing a protective hydrophilic layer, some other characteristics of the nanoparticles such as particle surface charge and geometry, drug loading and release behavior of encapsulated compounds are affected by PEG [11-13]. It should be mentioned that PEG is not only present at the particle surface but might also be present in the bulk of the particles. The hydrophilic nature of PEG results in a greater water absorbing capacity of the matrix, thereby increasing the hydrolysis kinetics of the polymers and thus degradation rate of the particles [14-16]. The release of encapsulated biomacromolecules such as proteins or peptides from PLGA micro and nanoparticles is essentially governed by matrix degradation/erosion [17-20]. It has been also reported that polymer-protein interactions and the nature of such interactions (ionic, hydrophobic/hydrophilic) are also determinative factors for both loading and release of the therapeutic agent [21-23]. We have recently reported on protein loaded 10-15 µm microparticles and nanoparticles of 400-600 nm in diameter, based on an aliphatic polyester with pendant hydroxyl groups (poly(D,L-lactic-co-glycolic-co-hydroxymethyl glycolic acid), PLGHMGA), that were prepared using an emulsion solvent evaporation technique with PVA as a surfactant.

It was demonstrated that release patterns of bovine serum albumin as a model protein and octreotide as model peptide was modulated by varying the density of pendant hydroxyl groups [24-27]. However, for i.v. administration and intracellular delivery of therapeutic proteins, stealth particles with smaller size (<400 nm) are preferred [28].

Therefore, in the present study we explored the preparation of PEGylated nanoparticles, based on the same polyester, and studied the effect of PEG content and molecular weight on particle properties (size, charge), particle degradation and release behavior. Nanoparticles were prepared from blends of PLGHMGA with two different PEG-PLGHMGA block copolymers varying in molecular weight of the PEG block, by a double emulsion solvent evaporation method. The effect of blend composition, i.e. the type and amount of PEG-PLGHMGA block copolymer, on nanoparticles properties, degradation and protein release was investigated. BSA and lysozyme, proteins with different molecular weights and isoelectric points, were chosen as model proteins.

2. Materials and methods

2.1. Materials

O-Benzyl-L-serine was purchased from Senn Chemicals AG (Switzerland). Bovine serum albumin (BSA), poly(vinyl alcohol) (PVA; MW 30,000–70,000; 88% hydrolyzed), tin(II) 2-ethylhexanoate (SnOct2) and poly(ethylene glycol) monomethyl ether (MePEG) with molecular weights of 5000 and 2000 were obtained from Sigma Chemical Company (USA). Hen egg-white lysozyme was purchased from Fluka (Belgium). D,L-lactide was obtained from Purac, The Netherlands. *N,N*-dimethylformamide (DMF), peptide grade dichloromethane (DCM), methanol, ethyl acetate, chloroform and tetrahydrofuran (THF) were purchased from Biosolve (The Netherlands). Benzyl alcohol, disodium hydrogen phosphate (Na_2HPO_4) and sodium dihydrogen phosphate (NaH_2PO_4) were obtained from Merck (Germany). Toluene from Acros (Belgium) was stored over 3Å molecular sieves. *N,N*-Dimethylaminopyridine (DMAP) and sodium azide (NaN_3, 99%) were obtained from Fluka (The Netherlands). BCA reagent was from Interchim, USA. Pd/C (Palladium, 10 weight% on activated carbon, Degussa type E101 NE/W) was purchased from Aldrich (The Netherlands). Unless otherwise stated, all chemicals were used as received.

2.2. Synthesis of PEG-PLGHMGA and PLGHMGA copolymers

Random copolymers of benzyl protected hydroxymethyl glycolide (BMG) and D,L-lactide were synthesized by ring opening polymerization in the melt using benzyl alcohol (BnOH) as initiator and stannous octoate as catalyst, respectively, essentially as described previously [29]. Briefly, a mixture of D,L-lactide (1.5 g) and BMG (1.4 g) was loaded into a Schlenk tube followed by the addition of stannous octoate in dry toluene (11 mg, 32 µl from a 338 mg/ml stock solution in toluene) and 6 mg BnOH (M/I ratio of 300/1). After removal of toluene by applying vacuum, the Schlenk tube was closed and subsequently transferred into an oil bath of 130 °C. The melt polymerization proceeded overnight and after cooling to room temperature, the crude product was dissolved in chloroform, precipitated into an excess of methanol and vacuum dried overnight. The protecting benzyl groups were removed in a hydrogenation reaction using Pd/C as catalyst [29]. PEG-PLGHMGA block copolymers were synthesized with the same method as PLGHMGA using $MePEG_{2000}$ and $MePEG_{5000}$ as initiator. The amounts of MePEG used in polymerization were 109 mg for $MePEG_{2000}$ and 283 mg for $MePEG_{5000}$ (corresponding with M/I ratio of 300/1). The synthesized polymers are denoted as PLGHMGA for the copolymers of

D,L-lactic acid, hydroxymethyl glycolic acid (HMG) and glycolic acid and PEG-PLGHMGA for the block copolymers of MePEG and PLGHMGA.

2.3. Polymer characterization

^{1}H NMR analysis of the polymers dissolved in DMSO was performed using a Gemini-300 MHz spectrometer at 298 K. The composition of the PEG-PLGHMGA copolymers as well as their molecular weight and PEG content were determined by ^{1}H NMR, using the following equations:

The molar % of composing units (lactic acid (%L), glycolic acid (%G) and hydroxymethyl glycolic acid (%HMG)) was determined according to the following formulas:

$I_{HMG} = [(I_{3.8})/2 + (I_{4.2\text{-}4.5})/3]$

$I_G = (I_{4.7\text{-}5.0})/2$

$I_L = [I_{5.2\text{-}5.4} - (I_{3.8})/2]$

$\%L = I_L / (I_{HMG} + I_G + I_L) \times 100$

$\%G = I_G / (I_{HMG} + I_G + I_L) \times 100$

$\%HMG = I_{HMG} / (I_{HMG} + I_G + I_L) \times 100$

where I_{HMG}, I_G and I_L are the peak integrals per one proton of each monomer unit, and I_{number} are the integrals obtained from the NMR spectra at the indicated peak shifts (ppm).

Molecular weight of the diblock copolymers: (I_{HMG}/I_{PEG} X MW HMG unit) + (I_L/I_{PEG} X MW L unit) + (I_G/I_{PEG} X MW G unit) + PEG molecular weight (2000 or 5000),

where I_{PEG} is the peak integrals per one proton of PEG;

%PEG: PEG molecular weight/ calculated diblock molecular weight × 100%;

The relative molecular weights and molecular weight distributions of the obtained polymers were determined using GPC (Waters Alliance system), with a Waters 2695 separating module and a Waters 2414 refractive index detector. Two PL-gel 5 µm Mixed-D columns fitted with a guard column (Polymer Labs, MW range 0.2–400 kDa) were used and calibration was done using polystyrene standards with narrow molecular weight distributions. THF was used as the mobile phase and the elution rate was 1 ml/min. The thermal properties of the different polymers were measured using differential scanning calorimetry (TA instrument, Q2000). Approximately 5 mg polymer sample was loaded into an aluminum pan, and after heating from room temperature to 120 °C, with a heating rate of 10 °C/min, the sample was cooled down to -50 °C. Thereafter, the sample was heated to 120 °C with temperature modulation at ±1 °C and a ramping rate of 2 °C/min. The second cycle was used to determine the glass transition temperature (T_g) of the synthesized polymers.

2.4. Nanoparticle preparation

Nanoparticles were prepared by a double emulsion solvent evaporation technique [30]. Briefly, a solution of protein (BSA or lysozyme) in reverse osmosis water (300 µl, 50 mg/ml) was emulsified in 3 ml dichloromethane (DCM) containing PEG-PLGHMGA or different blends of PEG-PLGHMGA and PLGHMGA (total polymer concentration was 5% w/v) in an ice-bath using an ultrasonic homogenizer (LABSONIC P, B.Braun Biotech) for 1 min at 40% amplitude. The w/o emulsion thus formed was then emulsified into an external aqueous phase (30 ml) with or without surfactant [(poly(vinyl alcohol) (5% w/v) in NaCl (0.9% w/v)), filtered through 0.2 µm Millipore filter)] in an ice-bath using the same ultrasonic homogenizer for 2 min at 60% amplitude to form a water-in-oil-in-water (w/o/w) emulsion. Next, DCM was evaporated at room temperature under reduced pressure for 1 hour. The obtained nanoparticles were collected by ultracentrifugation (20000Íg for 20 min, J-26XP, Beckman Colter, Avanti ®) and washed twice with 45 ml of 0.9% NaCl in water. Finally, the particles were suspended in a certain volume of sodium phosphate buffer (NaCl 6 mM, Na_2HPO_4 99 mM, NaH_2PO_4 49 mM, NaN_3 4 mM, pH 7.4) to obtain a dispersion of 4-6 mg particles for release and degradation studies. Empty (placebo) nanoparticles were prepared in the same way, but using water without protein as the internal aqueous phase.

2.5. Characterization of the nanoparticles

Nanoparticles were suspended in distilled deionized water and their average size and size distribution were measured using Dynamic Light Scattering (DLS; Zetasizer 4000, Malvern Instruments, Malvern, UK) at 25 °C at an angle of 90° (Z-average). The zeta-potential of the nanoparticles, suspended in 10 mM sodium phosphate buffer (NaCl 0.4 mM, Na_2HPO_4 6.6 mM, NaH_2PO4 3 mM, pH: 7.4), was determined by laser Doppler electrophoresis using a

Zetasizer Nano-Z (Malvern Instruments Ltd.). The morphology of the nanoparticles was studied by Transmission Electron Microscopy (TEM, Tecnai 10, Philips, 100kV). The samples for TEM visualization were prepared according to the following procedure: 25 µl of nanoparticle suspension was pipetted onto parafilm, and a formvar/carbon-coated copper grid was placed on top of the sample droplet for 2 minutes to adsorb particles on the grid. Excess liquid was removed by filter paper. Subsequently, the grid was negatively stained by placing them on top of a 20 µl droplet of 2% uranyl acetate in demineralized water on parafilm for 2 minutes. Excess liquid was removed by filter paper and the grid was dried for 5 minutes at room temperature before the measurement.

2.6. In vitro release of proteins

The obtained particles (described in section 2.4) were suspended in sodium phosphate buffer (composition given in section 2.4) and samples of 1 ml of the homogeneous particle suspension were aliquoted into 1.5 ml eppendorf tubes. Two aliquots were washed twice with reverse osmosis water (centrifuged for 20 minutes at 20000 X g; Hermle Z233MK-2 centrifuge) and the obtained pellets were freeze-dried and used to determine the protein loading efficiency and particle concentration of the dispersion. The washed particles were resuspended in deionized water, aliquoted and freeze dried at -50 °C and at 0.5 mbar in a Chris Alpha 1-2 freeze-drier (Osterode am Harz, Germany) for 12 hrs. The other eppendorf tubes were incubated at 37°C under mild agitation. At different time points, a tube was taken and the particles were centrifuged at 20000 X g for 20 min and the pH of supernatants was determined. The amount of protein in the supernatant was measured by UPLC (Acquity UPLC®) equipped with a BEH C18 1.7 µm column, using a linear elution gradient starting at 100% solvent A (95% H2O, 5% ACN and 0.1% Trifluoroacetic acid (TFA)) to 60% solvent A and 40% solvent B (100% ACN and 0.1% Trifluoroacetic acid (TFA)) over 6 minutes, followed by re-equilibration to 100% solvent A in 4 minutes. The flow rate was 0.25 ml/min, and typically 7.5 µl of sample was injected. Detection was performed by measuring the UV absorbance at 280 nm. Protein standard solutions (10-300 µg/ml) were used for calibration.

2.7. Protein loading efficiency and loading %

Protein loading of the nanoparticles was determined by a BCA protein assay, essentially as described by Hongkee et al. [31]. Briefly, about 10 mg of freeze-dried nanoparticles was dissolved in 1 ml DMSO. Next, 5 ml of a 0.05 M NaOH solution containing 0.5% (w/v) SDS (sodium dodecyl sulfate) was added. After an overnight incubation at 37 °C a clear solution was obtained, which was analyzed for protein content. Protein loading efficiency (LE) is defined as the amount of protein entrapped divided by the nominal protein X 100%. The protein loading % (L%) is calculated as the encapsulated amount of protein divided by the dry weight of the loaded particles X 100%.

2.8. In vitro degradation of BSA-loaded nanoparticles

Samples of 1 ml of BSA-loaded particles suspension in sodium phosphate buffer at concentration of 4-6 mg/ml (section 2.4.) were transferred into eppendorf tubes. The samples were incubated at 37 °C while gently shaken. At different time points, one tube was taken and the particles were collected after centrifugation at 20000 X g for 20 minutes and washed twice with reverse osmosis water. After freeze-drying, the remaining weight of the samples was measured, and NMR and GPC (see section 2.3) were used to analyze the remaining insoluble residues.

3. Results and discussions

3.1 Synthesis and characterization of the synthesized polymers

Random copolymers of benzyl protected hydroxymethyl glycolide (BMG) and D,L-lactide, using BnOH or MePEG (molecular weight of 2000 or 5000 Da) as initiators and stannous octoate as catalyst, were synthesized by ring opening polymerization in the melt at 130 °C (Fig. 1). After removal of the protective benzyl groups by hydrogenation, the polymers (MePEG-PLGHMGA and PLGHMGA) were obtained in high yields (>70%). The copolymer compositions as well as number average molecular weights for the diblock copolymers were determined by 1H NMR.

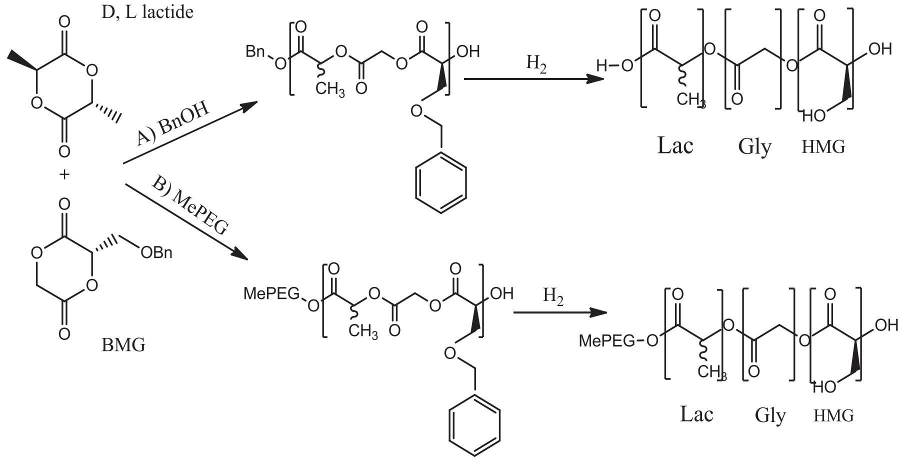

Figure 1: *Synthesis of hydrophilic aliphatic polyesters with pendant hydroxyl groups based on lactic acid, glycolic acid and hydroxymethyl glycolic acid: poly(lactic-co-glycolic-co-hydroxymethyl glycolic acid, PLGHMGA).* ***A)*** *PLGHMGA copolymer using Bn-OH as initiator* ***B)*** *PLGHMGA blockcopolymers with PEG using MePEG-OH as macroinitiator.*

Figure 2 shows a representative NMR spectrum of one of the synthesized PEG-PLGHMGA block copolymers which demonstrates complete removal of the protecting benzyl groups, in line with previous experiences [29]. The characteristics of the synthesized copolymers are given in Table 1 which demonstrates that the copolymer compositions are close to the monomer feed ratios. Further, the number average molecular weights of the diblock copolymers based on NMR are in good agreement with the theoretical molecular weights. DSC analysis showed that the synthesized polymers were fully amorphous (Fig. 3). PLGHMGA had a T_g at 58 °C, and PEG_{5000}-PLGHMGA and PEG_{2000}-PLGHMGA diblock copolymers showed T_g at 42 °C and 47 °C, respectively (see Table 1).

Table 1: *Characteristics of the polymers used in this study.*

Polymer	Composition x:y [a]		Molecular weight (Kg/mol)				PEG W%	Measured T_g (°C)
	Feed ratio	Polymer ratio (NMR)	GPC M_w	GPC M_n	NMR	Theoretical		
$MePEG_{2000}$-PLGBMGA	35:65	38:62	30	19	38	56	5.2	ND
$MePEG_{2000}$-PLGHMGA		31:69	26	16	42	45	4.7	47
$MePEG_{5000}$- PLGBMGA		31:69	23	15	44.5	59	11	ND
$MePEG_{5000}$- PLGHMGA		37:63	20	13	54.4	48	9	42
PLGBMGA		36:64	57	27	--	54	--	ND
PLGHMGA		36:64	44	24	--	43	--	58

[a] x:y *denotes the molar ratio of BMG/D,L-Lactide or HMG/D,L-lactide*

ND: *not determined*

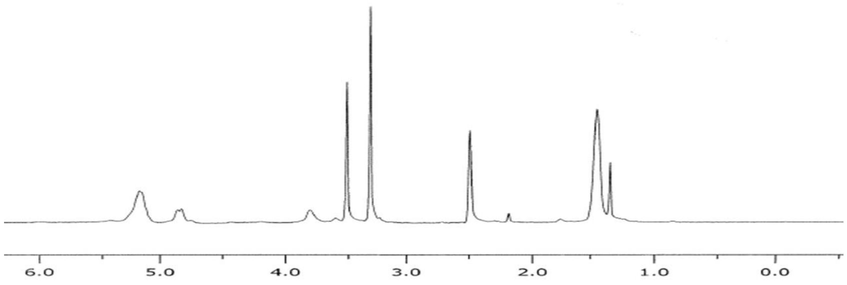

Figure 2: *^{1}H NMR spectrum of PEG_{5000}-PLGHMGA in deuterated DMSO.*

δ = 1.3-1.5 (m, 3H, -CH_3), 2.5 (s, CH_3, DMSO), 3.3 (s, H_2O), 3.5 (O-$\underline{CH_2}$-$\underline{CH_2}$ of MePEG), 3.7-3.9 (m, 2H, CH-$\underline{CH_2}$-OH), 4.7-5.0 (m, 2H, O-$\underline{CH_2}$-C(O)O), 5.2-5.4 (m, 2H, 1H (-$\underline{CH}$-CH_3 of lactic acid) plus 1H ($\underline{CH}$-CH_2-OH of HMG)).

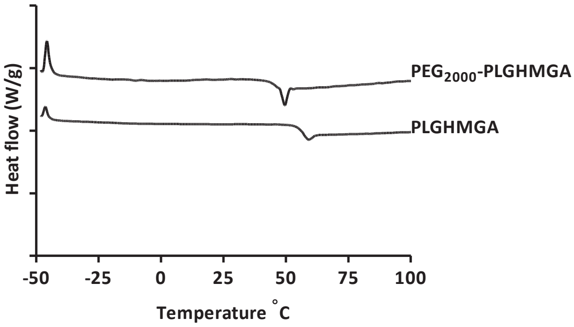

Figure 3: *DCS thermograms of PLGHMGA and PEG_{2000}-PLGHMGA*

Like the diblock copolymers, also the blends of PEG-PLGHMGA and PLGHMGA revealed only one T_g between that of the two components. In polymer blends, with increasing PEG-PLGHMGA weight fraction from 10% to 100%, a decrease of T_g from 58 to 47 °C was observed for PEG_{2000}-PLGHMGA blends and from 57 to 42 °C for PEG_{5000}-PLGHMGA blends. The observed single T_g's both for diblocks and polymer blends demonstrates miscibility of PEG and PLGHMGA blocks in the solid state. This is supported by calculating the theoretical T_g for polymer blends using the Fox equation: $1/T_g=W_{PLGHMGA}/T_{g\ PLGHMGA}+W_{diblock}/T_{g\ diblock}$ [32]. As illustrated in Figure 4, the observed linear decrease in experimental T_g values are indeed in good agreement with the values calculated by the Fox equation, demonstrating indeed full miscibility of PLGHMGA and PEG-PLGHMGA [33]. Based on DSC data it was previously shown that PEG is also (partially) miscible with structurally related polymers like PLA or PLGA [29].

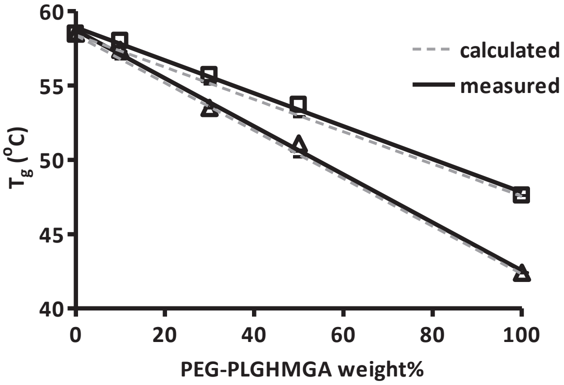

Figure 4: *Measured (DSC) and calculated T_g (Fox equation) of nanoparticles made of △) blends of PEG_{5000}-PLGHMGA and □) blends of PEG_{2000}-PLGHMGA.*

3.2. Preparation and characterization of placebo and protein-loaded nanoparticles without PVA

Nanoparticles with and without protein loading and based on different blends of PEG-PLGHMGA and PLGHMGA were prepared by a double emulsion solvent evaporation method (see Table 2). PEG-PLGHMGA is an amphiphilic polymer with surface-active properties. Therefore nanoparticles were prepared without using a surfactant (PVA) in the external water phase. It was confirmed by NMR that the diblock copolymer was quantitatively incorporated in the particles. Particles prepared without PEG-PLGHMGA diblock copolymers and with low content of PEG_{2000}-PLGHMGA (i.e. 10%) showed aggregation, whereas small particles were obtained for all formulations containing PEG_{5000} diblock copolymers. This implies higher shielding of the nanoparticles with PEG 5000 than with PEG 2000, suggesting that even at the lowest contents of diblock copolymer (10%) and thus very low PEG_{5000} contents (i.e. 0.9 %) a PEG corona most likely covers the surface, rendering sterically stabilized particles in aqueous medium. Figure 5 shows that with increasing PEG-PLGHMGA content the particle size as well as polydispersity of particles decreased. This effect is more pronounced for particles prepared using PEG_{2000}-PLGHMGA blends (size decrease from 636 to 213 nm) than for the blends that contained PEG_{5000}-PLGHMGA, which showed a decrease in particle size from 393 to 249 nm. This decrease in size can be explained as follows: the size of polymeric particles is dependent on the size of the droplets formed during the emulsification process. PEG-PLGHMGA, due to its amphiphilicity and surface active properties, likely locates at the interface of the emulsified droplets and water. As a result, the interfacial tension between the two immiscible phases decreases with increasing PEG content of the formulation resulting in smaller particles.

Table 2: *Characteristics of protein loaded nanoparticles formulated with PVA (n=2).*

Protein	PEG	PEG-PLGHMGA w%	Hydrodynamic diameter (nm)	PDI	L% (BCA)	LE%
BSA	2000	10	289 ± 7	0.10 ± 0.05	7.9 ± 0.0	79 ± 0
		30	263 ± 16	0.08 ± 0.03	7.0 ± 0.1	70 ± 1
		100	247 ± 1	0.08 ± 0.01	7.3 ± 0.0	73 ± 0
	5000	10	246 ± 5	0.06 ± 0.03	8.0 ± 0.4	79 ± 5
		30	238 ± 5	0.07 ± 0.06	7.9 ± 0.1	79 ± 2
Lysozyme	2000	10	268 ± 5	0.05 ± 0.01	10.0 ± 1.0	95 ± 5
		30	262 ± 2	0.06 ± 0.02	9.0 ± 1.0	92 ± 8

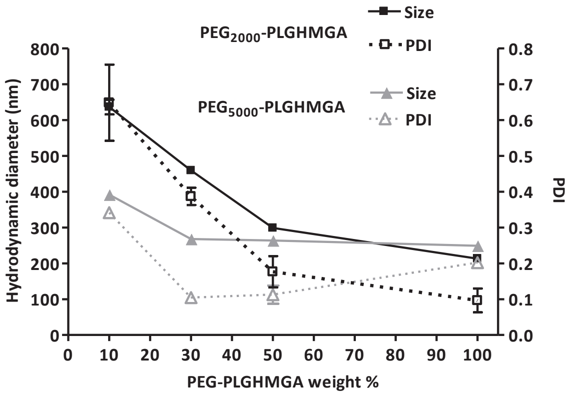

Figure 5: *Size and poly dispersity index of placebo nanoparticles based on blends of PEG-PLGHMGA formulated without PVA (n=3).*

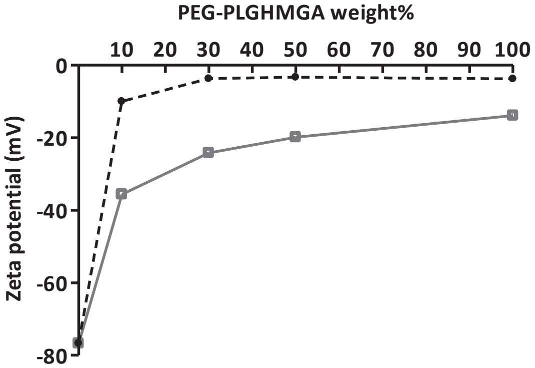

Figure 6: *Zeta-potential of placebo nanoparticles formulated without PVA as a function of the PEG-PLGHMGA weight%. ☐ : PEG$_{2000}$-PLGHMGA, ● : PEG$_{5000}$-PLGHMGA*

Zeta-potential values of placebo nanoparticles (Fig. 6) demonstrated a significant effect of PEG. As depicted in figure 6, the nanoparticles prepared using blends of PEG-PLGHMGA and PLGHMGA showed a decrease in zeta potential with increasing PEG content demonstrating shielding of the surface charge and points to, as expected, localization of PEG chains on the surface of the particles. This figure also shows that at similar block copolymer contents, nanoparticles containing PEG$_{5000}$-PLGHMGA showed significantly lower zeta potentials than particles containing PEG$_{2000}$-PLGHMGA (i.e. -3 versus -24 mV at 30% PEG-PLGHMGA content). In line with expectation, the surface charge masking effect of PEG is dependent on the thickness of the PEG corona, which increases with molecular weight [4]. The zeta potential of PLGHMGA nanoparticles before centrifugation was highly negative (-76 mV) which is in agreement with previous findings for PLGA particles [34]. The negative zeta-potential of PLGHMGA nanoparticles is due to the charged carboxylic end-groups of the polymer (see Fig. 1A) at pH 7. However, despite their high negative surface charge, PLGHMGA nanoparticles could not be redispersed after centrifugation. Colloids can be stabilized by either electrostatic repulsion or steric stabilization [35]. Since stable dispersions were only observed for PEGylated and not for bare PLGHMGA particles, it can be assumed that steric stabilization by PEG is the main contributing factor for the stability of the particle dispersions. For most of the blend particles prepared in this study, TEM analysis revealed non-porous, spherical particles with a smooth surface (see Fig. 7A for a typical example). Interestingly, a mixture of worm shape and spherical particles were found for the formulation based on only PEG$_{5000}$-PLGHMGA, that contained the highest amount of PEG of all formulations studied here (i.e. 9 w% of PEG; see Fig. 7B). The other particles that all had lower PEG content, including PEG_{2000}-PLGHMGA based particles with 4.7 w% of PEG (see Fig. 7C), gave spherical particles. It has been reported that amphiphilic diblock copolymers self-assemble in dilute aqueous solution into three basic morphologies: spherical micelles, worm-like micelles, and vesicles. The assembly of amphiphilic diblock copolymers into these differently shaped nanostructures depends on the weight fraction of the hydrophilic block [13, 36] as well as on the applied processing route (e.g., solvent exchange, film rehydration, pH switch, etc.) [37]. For PLA-PEG based particles it was previously observed that with a weight fraction of the PEG block less than ~50%, the hydrophilic corona imparts such curvature to the copolymer assembly that worm-like micelles are the predominant morphology [38]**.** Probably, when the PEG content becomes too low (i.e. <5%, as for most of our formulations), PEG will not be able to control the particle morphology, and regular round-shaped droplets will be formed during the emulsification process. A detailed influence of block length ratio’s on the particle morphology would need further investigation which is however beyond the scope of the present paper.

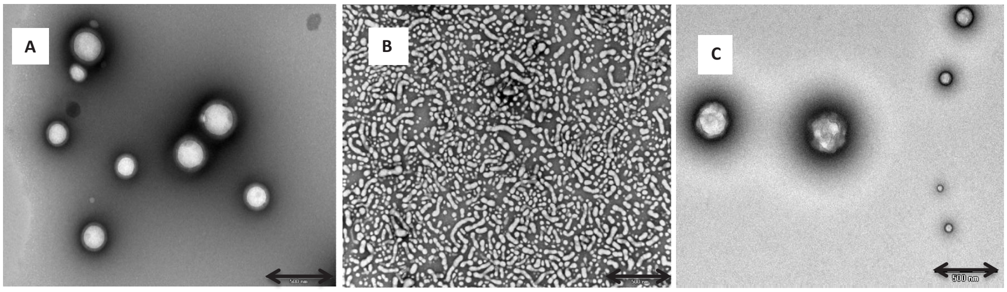

Figure 7: *TEM pictures of particles prepared from* ***A)*** *blend of 30%* PEG_{5000}*-PLGHMGA and PLGHMGA* ***B)*** *100%* PEG_{5000}*-PLGHMGA* ***C)*** *100%* PEG_{2000}*-PLGHMGA; (scale bar:500nm).*

For protein encapsulation (both lysozyme and BSA) it was observed that the formulations containing 50 and 100% PEG-PLGHMGA, showed no protein incorporation. This can be due to high hydrophilicity of the formulation resulting in high water penetration during particle preparation and thus migration of protein to external water phase. Therefore, in the further experiments lower contents of diblock polymer (i.e. 10 and 30%) were used. However, the particles that were prepared using formulations containing 10 and 30% of PEG-PLGHMGA, still showed low encapsulation efficiency (10-30%) and showed complete release of the loaded protein in one day (Figure. 8).

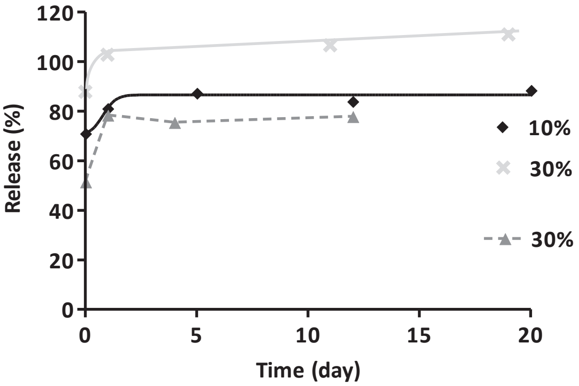

Figure 8: *BSA release from nanoparticles based on different blends prepared without PVA.* ▲*: PEG$_{2000}$-PLGHMGA and* ✕*,* ◆*: PEG$_{5000}$-PLGHMGA.*

3.3. Preparation and characterization of protein-loaded nanoparticles with PVA

In order to improve protein incorporation and release duration, nanoparticles were prepared using PVA (5% w/v) in the external water phase. PVA (the most common surfactant used in emulsion solvent evaporation method for the preparation of PLGA nano and microparticles) [30, 39] and other surfactants such as polysorbates have been used to stabilize PEG-PLGA nanoparticles [3, 40]. It has been shown that an increasing PVA concentration (and thus increasing viscosity of the external water phase) used for the preparation of BSA loaded PLGA NPs, resulted in a higher resistance for entrapped proteins to diffuse from the internal to the external water phase and therefore yielded particles with a higher protein loading. Probably more importantly, the presence of PVA at the interface of the organic and the aqueous phase acts as barrier for protein diffusion not only during particle formation but also during release from the solidified nanoparticles [41, 42]. The size of the particles prepared in the presence of PVA was around 240-280 nm and PDI was < 0.1, which were not profoundly influenced by the PEG content (Table 2). These results demonstrate that smaller sized particles with lower polydispersity were formed in the presence of PVA as compared to particles prepared without this surfactant. The zeta-potential of placebo and protein-loaded nanoparticles was around -1 mV for all formulations demonstrating excellent shielding of the surface charge by combination of PEG and PVA. This table also shows that BSA was efficiently encapsulated in the nanoparticles (~80%) and an even higher loading efficiency of 90-95% was obtained for lysozyme. It has been reported that protein-polymer ionic interactions contribute to the extent of protein incorporation in polymer matrices [43]. The relatively high molar ratio of carboxylic end groups to lysozyme (e.g. mol COOH/

mol lysozyme >5 in the formulation containing 30% PEG_{2000}-PLGHMGA) therefore likely explains the higher encapsulation efficiency of lysozyme. To further study the colloidal stability, placebo nanoparticles containing 30% PEG_{5000}-PLGHMGA formulated with and without PVA were dispersed in buffer of pH 7.4, incubated at 37 °C and particle size was measured at different time points. All formulations showed a gradual increase of both particle size and PDI indicating particle aggregation; however, this was more severely observed for formulations without PVA (Fig. 9). Besides, a decrease in zeta potential from -1 to -3 mV and from -3 to -40 mV at day 6 was observed for nanoparticles prepared with and without PVA, respectively, implying removal of the particle surface coating and exposure of carboxylic end groups. The low negative zeta potential of the nanoparticles suggests that the stability of these particles is likely due to their surface coverage by either PVA or combination of PEG and PVA providing steric stabilization. It has been shown previously that even after several washing steps PVA remains associated with PLGA particles [30, 42, 44-46]. However, during incubation PVA is slowly removed from the particle surface [47].

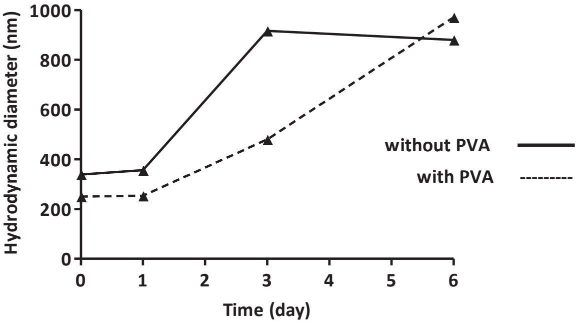

Figure 9: *Size of particles based on blend 30%* PEG_{5000}*-PLGHMGA during incubation at 37 °C and pH: 7.4.*

^{1}H NMR spectra of placebo and protein loaded particles with and without PVA (Fig. 10) demonstrated a significant decrease of the PEG content at day 5. Altogether, these results indicate that the observed particle aggregation is likely caused by removal of the PEG corona as well as PVA. The removal of PEG points to a preferential cleavage of the ester bond connecting PEG to the PLGHMGA block which is in agreement with previous observation on particles based on PEG-PLGA blockcopolymers [15,16]. A possible explanation is that the ester bonds that connect PEG and PLGHMGA are mainly located at the surface of the nanoparticles and consequently are more accessible for surrounding water molecules resulting in (fast) hydrolysis [43].

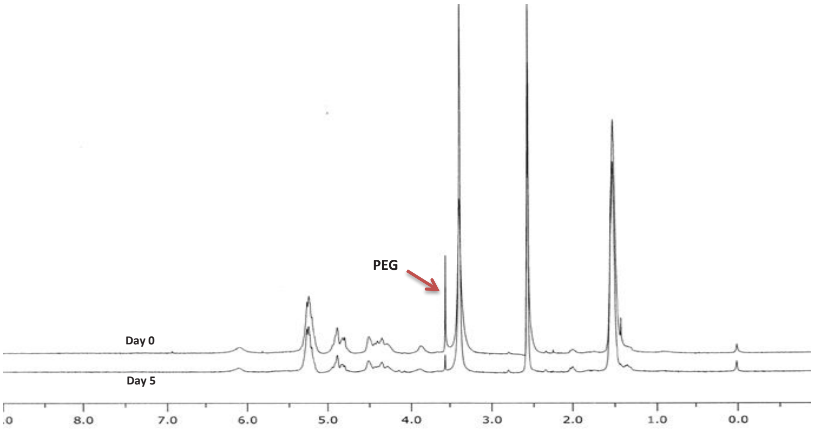

Figure 10: *^{1}H NMR spectra of nanoparticles made of a blend of PEG$_{5000}$-PLGHMGA (30%) and PLGHMGA (70%) at day 0 and after 5 days incubation at 37 °C and pH 7.4. The nanoparticle samples were dissolved in deuterated DMSO.*

3.4. In vitro degradation of the nanoparticles prepared with PVA

^{1}H NMR analysis of the degrading samples showed a shift of the proton peaks attributed to the HMG units at 3.8 ppm (CH_2) and 5.2 ppm (CH, coinciding with CH of lactide) in the original structure, to 4.2-4.5 ppm. This was previously explained by the occurrence of an intramolecular transesterification reaction [25]. Moreover, in line with our previous findings, a gradual decrease in both HMG and glycolic content in the copolymer was observed (Table 3). As pointed out in our previous paper [25] the HMG ester bonds in PLGHMGA are more susceptible to hydrolysis which subsequently results in a relatively fast release of HMG units from the degrading polymer matrices. As also indicated in the previous section, NMR analysis also revealed a substantial decrease in PEG content (e.g. ~10 mol% of its initial content remained at day 5). It is generally accepted that steric stabilization by PEG is not required for all steps in the drug targeting process. A PEG coating favors circulating kinetics but also hampers (target) cell/nanoparticle interactions and can therefore be an obstacle for internalization of the drug loaded nanoparticles [48]. In general, loss of the PEG coating after arrival of drug-loaded nanoparticles at their target site is desirable, allowing enhanced target cell binding and internalization. This is particularly of interest for drugs that do not pass cellular membranes passively [7]. PEG-PLGA and PEG-PLA nanoparticles have also been shown to shed PEG during incubation, which however, occurs in a couple of weeks [15, 16] which is not desirable for efficient delivery. The fact that our particles loose PEG at a much faster rate is a clear advantage for the design of delivery systems with prolonged circulation time and yet a sufficient interaction with target cells. The explanation for relatively faster shedding of PEG-PLGHMGA systems as compared to related ones (e.g. PEG-PLGA and PEG-PLA systems) can be due to greater hydrophilicity of the PLGHMGA matrix causing faster hydrolysis of the PEG-PLGHMGA ester bonds both at the surface and within the matrix. The BSA-loaded nanoparticles demonstrated a continuous weight loss accompanied by continuous decrease in number average molecular weight in time (Fig. 11A, 11B). Nanoparticles were fully degraded in 60 days and, in contrast to expectations, there were no significant differences between the degradation rates of different formulations. Nanoparticle degradation is initiated by water-uptake followed by hydrolysis of the ester bonds of the PLGHMGA block. So, it can be expected that more hydrophilic matrices (thus matrices with more PEG) initially swells to a greater extent than matrices of lower PEG content [49]. However, with the loss of PEG, which occurs in the early stage of degradation for all nanoparticle formulations, degradation of the matrix is dominated by hydrolysis of PLGHMGA resulting in degradation patterns that are hardly affected by the initial PEG content of the particles.

Table 3: *Change in copolymer composition of different BSA loaded nanoparticles during incubation in sodium phosphate buffer at 37 °C.*

Formulation	Day	Copolymer composition (%)		
		HMG	Glycolic acid	Lactic acid
PEG_{5000}-PLGHMGA: 30 w%	0	17	17	66
	5	15	15	70
	10	13	13	74
	16	11	11	78
	21	10	11	79
	31	11	9	80
PEG_{2000}-PLGHMGA: 30 w%	0	17	17	66
	5	13	13	74
	18	11	11	78
	23	13	10	77
PEG_{5000}-PLGHMGA: 10 w%	0	17	17	66
	10	12	12	76

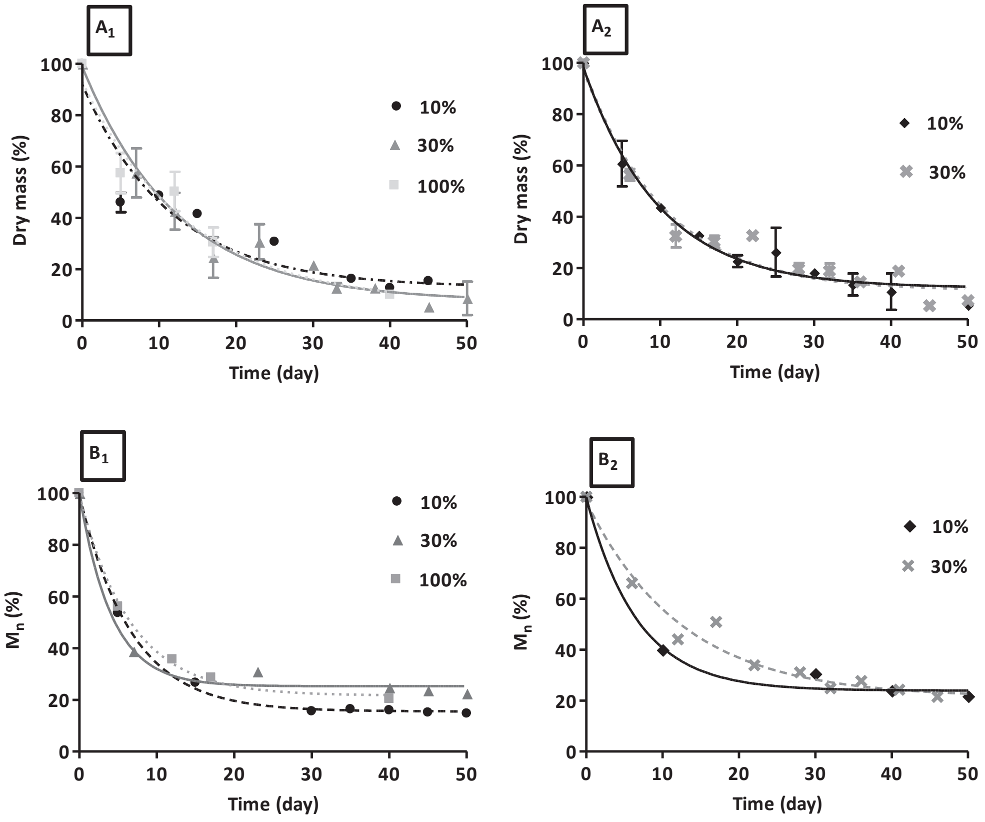

Figure 11: *$A_{1,2}$) Relative dry mass (n=2); $B_{1,2}$) number average molecular weight (M_n) % of BSA-loaded nanoparticles based on different blends: ●, ■, ▲: PEG_{2000}-PLGHMGA and ✕, ◆: PEG_{5000}-PLGHMGA.*

3.5. In-vitro protein release from nanoparticles prepared with PVA

The release profiles of BSA and lysozyme from different formulations are presented in figures 12A and 12B. For the different BSA-loaded particles based on blends of 10% and 30% of PEG-PLGHMGA, the release patterns consisted of an initial burst of the encapsulated protein (6-12%) followed by a continuous release reaching completion in 40 days. Nanoparticles of 100% PEG_{2000}-PLGHMGA, however, showed faster release and around 80% of BSA was released in 5 days. In an ongoing and previous studies, using the same method for particle preparation, we have demonstrated, using advanced spectroscopic techniques, that the structural integrity of the released proteins was preserved [25, 50, 51]. Since proteins do not dissolve in hydrophobic polymeric matrices and have a low (or absent) mobility in such matrices, their release from PLGA based systems and matrices of related polymers is mainly governed by diffusion through water-filled pores that are initially present or formed during degradation [52, 53]. Since the degradation rate of 100% PEG_{2000}-PLGHMGA nanoparticles was not significantly different from particles prepared from the blends, their fast protein release in early stage can be explained as follows. For the particles based on 100% PEG_{2000}-PLGHMGA, a considerable amount of PEG is present in the bulk, because of the good miscibility of PEG and PLGHMGA blocks (DSC analysis, Figure 4). This consequently results in strong hydration of the matrix allowing relatively fast diffusion and thus release of the protein, as also observed for the release of BSA from PEGylated PLGA particles [14]. Lysozyme-loaded nanoparticles showed a low burst of approximately 5% and over the next 35 days the protein was completely released. In line with the BSA release data, no significant difference in lysozyme release patterns for the different formulations was observed. Besides polymer degradation, protein-matrix interactions are also reported as an important controlling factor for protein release [22, 54]. Taking into account the different physicochemical characteristics of the two proteins in this study (BSA and lysozyme), different release patterns could be also expected. However, our results demonstrate nearly similar release rates for both proteins meaning that the release is mainly governed by particles' degradation and other factors have only a minor effect.

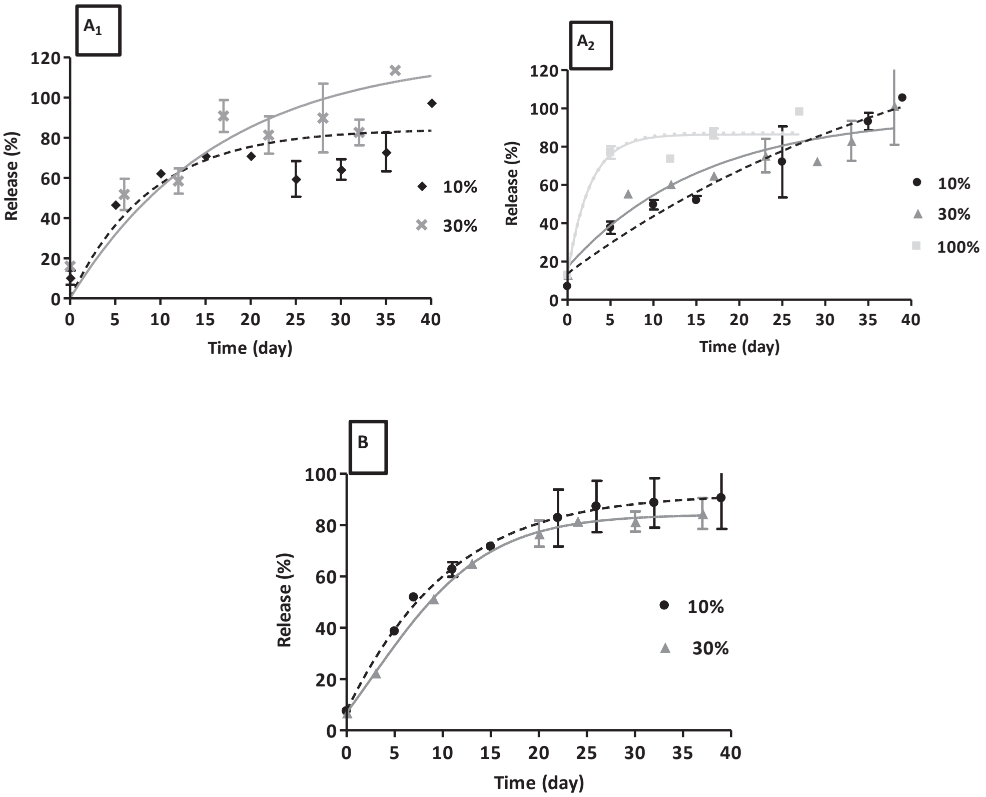

Figure 12: *A$_{1,2}$) BSA and B) lysozyme release from nanoparticles based on different blends (n=2).* ●, ■, ▲*: PEG$_{2000}$-PLGHMGA and* ✕, ◆*: PEG$_{5000}$-PLGHMGA.*

The percentage of the released protein is relative to the amount of protein encapsulated in the nanoparticles.

Conclusions

Nanoparticles based on blends of PEG-PLGHMGA and PLGHMGA were successfully prepared without using PVA as surfactant. Differences in particle size, morphology and surface charge were observed by changing the PEG-PLGHMGA content. High protein loading and sustained release was however only achieved when PVA was used in the external water phase. The different nanoparticles, independent of their composition, showed almost a similar protein release and degradation behavior demonstrating that the controlling factors of the degradation and protein release characteristics of the nanoparticles were determined by the relatively hydrophobic polyester core (PLGHMGA), whereas the initial PEG content had no major effect. The observed shedding of the PEG coating of the nanoparticles in around 5 days is attractive for the design of polymeric particulate nanocarriers. Such systems will likely remain sufficiently long in the circulation to accumulate in e.g. tumors at good levels. The PEG coating cleavage on the other hand is fast enough to allow cellular binding and internalization.

References

1. Danhier F, Ansorena E, Silva JM, Coco R, Le Breton A, Preat V. PLGA-based nanoparticles: An overview of biomedical applications. *J Control Release*. 2012;161:505-522.

2. Mundargi RC, Babu VR, Rangaswamy V, Patel P, Aminabhavi TM. Nano/micro technologies for delivering macromolecular therapeutics using poly(D,L-lactide-co-glycolide) and its derivatives. *J Control Release*. 2008;125:193-209.

3. Hrkach J, Von Hoff D, Mukkaram Ali M, et al. Preclinical development and clinical translation of a PSMA-targeted docetaxel nanoparticle with a differentiated pharmacological profile. *Sci Transl Med*. 2012;4:128ra39.

4. Gref R, Luck M, Quellec P, et al. 'Stealth' corona-core nanoparticles surface modified by polyethylene glycol (PEG): influences of the corona (PEG chain length and surface density) and of the core composition on phagocytic uptake and plasma protein adsorption. *Colloids Surf B Biointerfaces*. 2000;18:301-313.

5. Tobio M, Gref R, Sanchez A, Langer R, Alonso MJ. Stealth PLA-PEG nanoparticles as protein carriers for nasal administration. *Pharm Res*. 1998;15:270-275.

6. Quellec P, Gref R, Dellacherie E, Sommer F, Tran MD, Alonso MJ. Protein encapsulation within poly(ethylene glycol)-coated nanospheres. II. Controlled release properties. *J Biomed Mater Res*. 1999;47:388-395.

7. Romberg B, Hennink WE, Storm G. Sheddable coatings for long-circulating nanoparticles. *Pharm Res*. 2008;25:55-71.

8. Parr MJ, Masin D, Cullis PR, Bally MB. Accumulation of liposomal lipid and encapsulated doxorubicin in murine Lewis lung carcinoma: the lack of beneficial effects by coating liposomes with poly(ethylene glycol). *J Pharmacol Exp Ther*. 1997;280:1319-1327.

9. Lee Y, Koo H, Jin GW, et al. Poly(ethylene oxide sulfide): new poly(ethylene glycol) derivatives degradable in reductive conditions. *Biomacromolecules*. 2005;6:24-26.

10. Silvius JR, Zuckermann MJ. Interbilayer transfer of phospholipid-anchored macromolecules via monomer diffusion. *Biochemistry*. 1993;32:3153-3161.

11. Champion JA, Katare YK, Mitragotri S. Particle shape: a new design parameter for micro- and nanoscale drug delivery carriers. *J Control Release*. 2007;121:3-9.

12. Peracchia MT, Gref R, Minamitake Y, Domb A, Lotan N, Langer R. PEG-coated nanospheres from amphiphilic diblock and multiblock copolymers: Investigation of their drug encapsulation and release characteristics. *J Controlled Release*. 1997;46:223-231.

13. Dalhaimer P, Engler AJ, Parthasarathy R, Discher DE. Targeted worm micelles. *Biomacromolecules*.

2004;5:1714-1719.

14. Buske J, Konig C, Bassarab S, Lamprecht A, Muhlau S, Wagner KG. Influence of PEG in PEG-PLGA microspheres on particle properties and protein release. *Eur J Pharm Biopharm*. 2012;81:57-63.

15. Zweers ML, Engbers GH, Grijpma DW, Feijen J. In vitro degradation of nanoparticles prepared from polymers based on DL-lactide, glycolide and poly(ethylene oxide). *J Control Release*. 2004;100:347-356.

16. Avgoustakis K, Beletsi A, Panagi Z, Klepetsanis P, Karydas AG, Ithakissios DS. PLGA-mPEG nanoparticles of cisplatin: in vitro nanoparticle degradation, in vitro drug release and in vivo drug residence in blood properties. *J Control Release*. 2002;79:123-135.

17. Alexis F. Factors affecting the degradation and drug-release mechanism of poly(lactic acid) and poly[(lactic acid)-*co*-(glycolic acid)] *Polymer International*. 2005;54:36-46.

18. Fredenberg S, Wahlgren M, Reslow M, Axelsson A. The mechanisms of drug release in poly(lactic-co-glycolic acid)-based drug delivery systems—A review. *Int J Pharm*. 2011;415:34-52.

19. Giteau A, Venier-Julienne MC, Aubert-Pouessel A, Benoit JP. How to achieve sustained and complete protein release from PLGA-based microparticles? *Int J Pharm*. 2008;350:14-26.

20. Ye M, Kim S, Park K. Issues in long-term protein delivery using biodegradable microparticles. *J Control Release*. 2010;146:241-260.

21. Samadi N, Abbadessa A, Di Stefano A, et al. The effect of lauryl capping group on protein release and degradation of poly(d,l-lactic-co-glycolic acid) particles. *J Control Release*. 2013;172:436-443.

22. Park TG, Yong Lee H, Sung Nam Y. A new preparation method for protein loaded poly(D, L-lactic-co-glycolic acid) microspheres and protein release mechanism study. *J Control Release*. 1998;55:181-191.

23. Sophocleous AM, Desai KG, Mazzara JM, et al. The nature of peptide interactions with acid end-group PLGAs and facile aqueous-based microencapsulation of therapeutic peptides. *J Control Release*. 2013;172:662-670.

24. Ghassemi AH, van Steenbergen MJ, Talsma H, van Nostrum CF, Crommelin DJ, Hennink WE. Hydrophilic polyester microspheres: effect of molecular weight and copolymer composition on release of BSA. *Pharm Res*. 2010;27:2008-2017.

25. Samadi N, van Nostrum CF, Vermonden T, Amidi M, Hennink WE. Mechanistic studies on the degradation and protein release characteristics of poly(lactic-co-glycolic-co-hydroxymethyl glycolic acid) nanospheres. *Biomacromolecules*. 2013;14:1044-1053.

26. Liu Y, Ghassemi AH, Hennink WE, Schwendeman SP. No acid microclimate pH in poly (D,L –lactide –co-hydroxymethyl glycolide) micrsopheres during biodegrdation. *Biomaterials.* 2012.

27. Ghassemi AH, van Steenbergen MJ, Barendregt A, et al. Controlled release of octreotide and assessment of peptide acylation from poly(D,L-lactide-co-hydroxymethyl glycolide) compared to PLGA microspheres. *Pharm Res*. 2012;29:110-120.

28. Salmaso S, Caliceti P. Stealth properties to improve therapeutic efficacy of drug nanocarriers. *J Drug Deliv*. 2013;2013:374252.

29. Leemhuis M, vanNostrum CF, Kruijtzer JAW, et al. Functionalized poly (alpha-hydroxy acid)s via ring-opening polymerization: toward hydrophilic polyesters with pendant hydroxyl groups. *Macromolecules*. 2006;39:3500–3508.

30. Zambaux MF, Bonneaux F, Gref R, et al. Influence of experimental parameters on the characteristics of poly(lactic acid) nanoparticles prepared by a double emulsion method. *J Control Release*. 1998;50:31-40.

31. Sah H. A new strategy to determine the actual protein content of poly(lactide-co-glycolide) microspheres. *J Pharm Sci*. 1997;86:1315-1318.

32. Jackson JK, Hung T, Letchford K, Burt HM. The characterization of paclitaxel-loaded microspheres manufactured from blends of poly(lactic-co-glycolic acid) (PLGA) and low molecular weight diblock copolymers. *Int J Pharm*. 2007;342:6-17.

33. Beletsi A, Leontiadis L, Klepetsanis P, Ithakissios DS, Avgoustakis K. Effect of preparative variables on the properties of poly(dl-lactide-co-glycolide)-methoxypoly(ethyleneglycol) copolymers related to their application in controlled drug delivery. *Int J Pharm*. 1999;182:187-197.

34. Beletsi A, Panagi Z, Avgoustakis K. Biodistribution properties of nanoparticles based on mixtures of PLGA with PLGA-PEG diblock copolymers. *Int J Pharm*. 2005;298:233-241.

35. Ortega-Vinuesa JL, Martín-Rodríguez A, Hidalgo-Álvarez R. Colloidal Stability of Polymer Colloids with Different Interfacial Properties: Mechanisms. *J Colloid Interface Sci*. 1996;184:259-267.

36. Israelachvili JN, Mitchell DJ, Ninham BW. Theory of self-assembly of lipid bilayers and vesicles. *Biochim Biophys Acta*. 1977;470:185-201.

37. Blanazs A, Madsen J, Battaglia G, Ryan AJ, Armes SP. Mechanistic insights for block copolymer morphologies: how do worms form vesicles? *J Am Chem Soc*. 2011;133:16581-16587.

38. Geng Y, Discher DE. Hydrolytic degradation of poly(ethylene oxide)-block-polycaprolactone worm micelles. *J Am Chem Soc*. 2005;127:12780-12781.

39. Scholes PD, Coombes AG, Illum L, et al. Detection and determination of surface levels of poloxamer and PVA surfactant on biodegradable nanospheres using SSIMS and XPS. *J Control Release*. 1999;59:261-278.

40. Johnstone TC, Kulak N, Pridgen EM, Farokhzad OC, Langer R, Lippard SJ. Nanoparticle encapsulation of mitaplatin and the effect thereof on in vivo properties. *ACS Nano*. 2013;7:5675-5683.

41. Coombes AG, Yeh MK, Lavelle EC, Davis SS. The control of protein release from poly(DL-lactide co-glycolide) microparticles by variation of the external aqueous phase surfactant in the water-in oil-in water method. *J Control Release*. 1998;52:311-320.

42. Sahoo SK, Panyam J, Prabha S, Labhasetwar V. Residual polyvinyl alcohol associated with poly (D,L-lactide-co-glycolide) nanoparticles affects their physical properties and cellular uptake. *J Control Release*. 2002;82:105-114.

43. Paillard-Giteau A, Tran VT, Thomas O, et al. Effect of various additives and polymers on lysozyme release from PLGA microspheres prepared by an s/o/w emulsion technique. *Eur J Pharm Biopharm*. 2010;75:128-136.

44. Lee SC, Oh JT, Jang MH, Chung SI. Quantitative analysis of polyvinyl alcohol on the surface of poly(D, L-lactide-co-glycolide) microparticles prepared by solvent evaporation method: effect of particle size and PVA concentration. *J Control Release*. 1999;59:123-132.

45. Torche AM, Le Corre P, Albina E, Jestin A, Le Verge R. PLGA microspheres phagocytosis by pig alveolar macrophages: influence of poly(vinyl alcohol) concentration, nature of loaded-protein and copolymer nature. *J Drug Target*. 2000;7:343-354.

46. Zielhuis SW, Nijsen JF, Figueiredo R, et al. Surface characteristics of holmium-loaded poly(L-lactic acid) microspheres. *Biomaterials*. 2005;26:925-932.

47. Panyam J, Dali MM, Sahoo SK, et al. Polymer degradation and in vitro release of a model protein from poly(D,L-lactide-co-glycolide) nano- and microparticles. *J Control Release*. 2003;92:173-187.

48. Lammers T, Kiessling F, Hennink WE, Storm G. Drug targeting to tumors: principles, pitfalls and (pre-) clinical progress. *J Control Release*. 2012;161:175-187.

59. Clapper JD, Skeie JM, Mullins RF, Guymon CA. Development and characterization of photopolymerizable biodegradable materials from PEG–PLA–PEG block macromonomers. *Polymer*. 2007;48:6554-6564.

50. Ghassemi AH, van Steenbergen MJ, Talsma H, et al. Preparation and characterization of protein loaded microspheres based on a hydroxylated aliphatic polyester, poly(lactic-co-hydroxymethyl glycolic acid). *J Control Release*. 2009;138:57-63.

51. Samadi N, Kijanka MM, Oliveira S, Vermonden T, vanden Dikkenberg JB, vanNostrum CF. Nanobody-targeted and RNase-loaded nanoparticle based on a hydrophilic polyester aimed for cancer therapy. *In preparation*.

52. Huang X, Brazel CS. On the importance and mechanisms of burst release in matrix-controlled drug delivery systems. *J Control Release*. 2001;73:121-136.

53. van de Weert M, Hennink WE, Jiskoot W. Protein instability in poly(lactic-co-glycolic acid) microparticles. *Pharm Res*. 2000;17:1159-1167.

54. Blanco D, Alonso MJ. Protein encapsulation and release from poly(lactide-co-glycolide) microspheres: effect of the protein and polymer properties and of the co-encapsulation of surfactants. *Eur J Pharm Biopharm*. 1998;45:285-294.

5

Nanobody-Targeted and RNase-Loaded Nanoparticles Based on a Hydrophilic Polyester Aimed for Cancer Therapy

Neda Samadi [1]*
Marta M. Kijanka [2]*
Sabrina Oliveira [2]
Tina Vermonden [1]
Cornelus F. van Nostrum [1]
Maryam Amidi [1]
Paul M. P. van Bergen en Henegouwen [2]
W.E. Hennink [1]

[1] *Department of Pharmaceutics, Utrecht Institute for Pharmaceutical Sciences, Utrecht University, Utrecht, The Netherlands*

[2] *Cell Biology, Department of Biology, Faculty of Science, Utrecht University, Padualaan 8, 3584 CH Utrecht, The Netherlands*

*Authors contributed equally

Manuscript in preparation

Abstract

The aim of this study was to develop a nanomedicine based on a hydrophilic polyester (poly lactic-co-glycolic-co-hydroxymethyl glycolic acid; PLGHMGA) for targeted delivery of RNase A as a modality for cancer treatment. RNase-loaded pegylated PLGHMGA nanoparticles (NPs) of ~280 nm were prepared by a double emulsion solvent evaporation method. Encapsulated RNase was almost completely released within 12 days and it was shown that the enzymatic activity of the released protein was fully preserved. Ten % Maleimide-PEG-PLGA was added to the formulation to graft the Her2 targeted nanobody (11A4) at the surface of the NPs to render them specific for breast cancer cells. Alexa Fluor 532 labeled 11A4-decorated NPs showed substantially higher binding to and uptake by Her2 over-expressing cancer cells (Skbr3) than particles without nanobody. Interestingly, no binding of the nanobody-conjugated particles was observed onto Her2 negative cells (MDA-MB-231). The RNase-loaded 11A4-NPs exhibited a dose-dependent cytotoxicity with an IC_{50} of 5 µM, whereas free RNase was ineffective up to 100 µM. These results demonstrate that nanobody conjugated PLGHMGA NPs are promising carriers for targeted delivery of RNase.

1. Introduction

Ribonucleases (RNases) are small (10–28 kDa) basic proteins with a net positive charge under physiological conditions which can bind to negatively charged cell membranes, enter cells by endocytosis and translocate into the cytosol where they degrade RNA, when evading the ribonuclease inhibitor protein (RI) [1]. Therefore, these proteins have raised attention for use as anti-cancer therapeutics [2, 3]. However, because of the low molecular weight of these enzymes and as a consequence rapid renal filtration (half-life: < 5 minutes [4]) repetitive administration of high doses is required, which due to accumulation of these proteins in the kidneys is associated with renal toxicity [5-7]. Local administration in (the vicinity of) tumors decreases the side effects of these proteins, but the efficacy remains relatively poor due to insufficient cellular internalization. Importantly, It has been shown that when these proteins were introduced into the cytosol of cells using different strategies they become thousands of times more effective [8, 9]. Successful evasion from the RNase inhibitor (RI), a 50 kD protein present in the cytosol of mammalian cells, has also been mentioned to be essential for the accomplishment of the cell killing activity of RNase. The interaction between RI and RNases is among the strongest of known protein-protein complexes [10-12]. Ranpirnase (Onconase®, ONC) is the only ribonuclease that has been evaluated in phase III clinical trials for malignant mesothelioma in the U.S.A. and Europe [13, 14]. This enzyme can exert its cytotoxic effect to cancer cells at much lower concentrations as compared with other RNases [6, 14]. Although still debatable, different mechanisms have been proposed for the high potency of Onconase®, such as a greater cell association due to existence of specific receptors for Onconase® on mammalian cell surfaces, evasion from neutralization by RI, and cleavage of dsRNAs into small interfering RNAs (RNAi) which in turn can cause cell death [1, 5, 13, 15, 16]. Importantly, different studies have shown that if RNase A (RI sensitive) and Onconase® are conjugated to targeting ligands such as antibodies, and actively delivered into the cytosol of specific cancer cells, both enzymes exert similar cytotoxic efficacy [17, 18]. Efforts have been made to enhance the cytotoxic efficacy of RNases by amongst others linking these proteins to cell binding ligands to render them cell specific [19], combination therapy [18] and encapsulation of RNase into nanogels [20]. Several studies have shown that conjugation of RNases to tumor targeting antibodies or antibody fragments resulted in enhanced intracellular delivery and hence a substantial therapeutic potency [21-23]. In recent years, nanoparticulate carrier systems [24, 25] and particularly those based on biodegradable polyesters (e.g. PLGA and PLLA) have been investigated for (intracellular) delivery of therapeutic peptides and proteins [26-31]. The high drug loading capacity, high stability, and also physical protection of the loaded protein against degradation in the lysosomes, make them attractive candidates for intracellular delivery of proteins in general and thus also for ribonuclases. Moreover, long circulating targeted NPs can be obtained by surface modification of NPs with PEG, and targeting molecules such as antibodies, antibody fragments, peptides and nanobodies can render them cell specific [32]. Nanobodies are the variable domains of heavy chain only antibodies present in Camelidae and some sharks. They are promising targeting molecules because of their higher affinity than other antibody fragments derived from conventional antibodies [33-35]. The Her2 (or EGFR2; human epidermal growth factor receptor 2) receptor is overexpressed in aggressive types of breast cancer cells and has become in recent years an important target for therapy [36, 37]. Therefore, a Her2 specific nanobody (11A4) has been developed recently and we have demonstrated specific binding of 11A4 to the Her2 receptor in vitro and in vivo, in molecular optical imaging studies [38].

Recently, we have reported on particles of nano and micro meter size based on a hydrophilic polyester, (poly(D,L-lactic-co-glycolic-co-hydroxymethyl glycolic acid) (PLGHMGA)), which showed tailorable release patterns for model proteins and peptides [39-42] and relatively fast degradation and better protein compatibility due to lack of acidification during degradation [40-43]. We also investigated the protein release characteristics of pegylated nanoparticles prepared from blends of PEG-PLGHMGA and PLGHMGA [44]. In the present study, we evaluated the potential of these pegylated PLGHMGA nanoparticles for the intracellular delivery of RNase A. To actively target these to Her2 positive cells, we developed a method to conjugate the functional nanobody 11A4 mentioned above.

2. Materials and methods

2.1. Materials

Ribonuclease A (RNase A) and ribonucleic acid from baker's yeast (S. Cerevisiae) were purchased from Sigma-Aldrich (USA). D,L-lactide was obtained from Purac (The Netherlands). Peptide grade dichloromethane (DCM), chloroform, methanol, ethyl acetate, acetonitrile, diethyl-ether, tetrahydrofuran (THF), glacial acetic acid and toluene were purchased from Biosolve (The Netherlands). Disodium hydrogen phosphate (Na_2HPO_4), sodium dihydrogen phosphate (NaH_2PO_4), sodium azide (NaN_3, 99%), aldrithiol, poly(ethylene glycol) methyl ether (MePEG) with molecular weight of 2000, poly(vinyl alcohol) (PVA; MW 30,000–70,000; 88% hydrolyzed) and tin (II) 2-ethylhexanoate ($SnOct_2$) were products of Sigma-Aldrich (USA). BCA reagent was from Interchim (USA), and Pd/C (palladium, 10 wt% on activated carbon, Degussa type E101 NE/W) was purchased from Aldrich (The Netherlands). Alexa Fluor 532 (Alexa 532) was purchased from LI-COR Biosciences (USA). SH-PEG$_{2000}$-NH$_2$ was from creativePEGworks (USA). Maleimide-PEG$_{5000}$-PLGA (lactide/glycolide molar ratio 50:50, MW PLGA-PEG: 25kDa) was purchased from PolySciTech (USA). 4',6-Diamidino-2-phenylindole (DAPI) and PBS were purchased from Roche (The Netherlands) and Lonza Verviers (Belgium), respectively. The 11A4 nanobody was produced as described before [38]. Unless otherwise stated, all chemicals were used as received. The purity of the RNase was analyzed and confirmed by non-reducing SDS-PAGE according to a standard protocol (Fig. 1) [45].

Characterization of RNase by SDS-PAGE

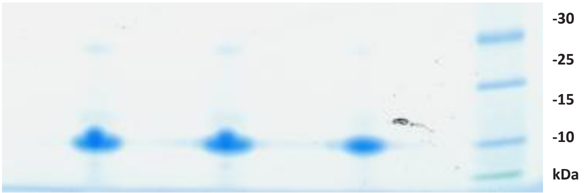

Figure 1 : *The RNase purity was established by SDS-Page analysis of the protein under non-reducing condition. An intensive band is visible around 15 kDa (13.7 kDa is the molecular weight of free RNase A).*

2.2. Synthesis of the 2-pyridyldithio-PEG-amine macroinitiator from aldrithiol-2 and thiol-PEG$_{2000}$-amine

The macroinitiator pyridyldithio-PEG-NH$_2$ was synthesized in a single step reaction from aldrithiol-2 and thiol-PEG$_{2000}$-amine (Scheme 1). In detail, a solution of thiol-PEG-amine (500 mg, 0.5 mmol) in methanol (10 ml) was added drop-wise to a solution of aldrithiol-2 (88 mg, 1 mmol) in methanol (10 ml) to which a catalytic amount (10 µl) of glacial acetic was added. The resulting reaction mixture was stirred at room temperature under an N$_2$ atmosphere for 5 h. Subsequently, methanol was evaporated under reduced pressure and the resulting crude product (yellow oil), was dissolved in chloroform and precipitated in diethyl ether two times. Finally, the obtained product, 2-pyridyldithio-PEG-amine, was obtained as white/greenish solid. The structure of the obtained product was confirmed by ^{1}H NMR analysis and the percentage of converted thiol end groups was calculated by dividing the peak area of one proton of pyridine to one proton of PEG$_{2000}$.

2.3. Synthesis of (methoxy or thiol)-PEG-PLGHMGA and PLGHMGA (co)polymers

Random and diblock copolymers of benzyl protected hydroxymethyl glycolide (BMG) and D,L-lactide were synthesized by ring opening polymerization in melt using benzyl alcohol (BnOH), MePEG$_{2000}$ or 2-pyridyldithio-PEG-amine as initiators and stannous octoate as catalyst, as described previously [39, 44, 46] The molar ratio of initiator/monomer was 1/300. The protecting benzyl and the pyridinethiol groups of the resulting 2-pyridyldithio-PEG-PLGBMGA were removed in a hydrogenation reaction using Pd/C as catalyst [46]. The synthesized polymers are denoted as PLGHMGA for the copolymer of D,L-lactic acid, hydroxymethyl glycolic acid (HMG) and glycolic acid, and PEG-PLGHMGA and thiol-PEG-PLGHMGA for the block copolymers of MePEG and thiol-PEG-amine with PLGHMGA, respectively.

^{1}H-NMR (DMSO, d^6): 1.3-1.5 (m, 3H, -CH$_3$), 2.5 (s, CH$_3$, DMSO), 3.3 (s, H$_2$O), 3.5 (PEG methylene units), 3.7-3.9 (m, 2H, CH-$\underline{CH_2}$-OH), 4.7-5 (m, 2H, O-$\underline{CH_2}$-C(O)O), 5.2-5.4 (m, 2H, -$\underline{CH}$-CH$_3$ of lactic + 1H, $\underline{CH}$-CH$_2$-OH of HMG)

2.4. Synthesis of Alexa 532-PEG-PLGHMGA

The synthesis of PLGHMGA labeled with Alexa 532 was performed as follows. Three mg (20 µM) dithiothreitol (DTT) was added to a solution of 50 mg thiol-PEG-PLGHMGA in 1 ml DCM while stirring at room temperature to reduce possible disulfide bonds. After 15 minutes, the polymer was precipitated in dry methanol, collected by filtration and dried under an N_2 atmosphere overnight. Next, the polymer was dissolved in 1 ml ACN and added to a solution of maleimide-functional Alexa 532 in PBS pH 7.4 (1 mg/ml, approximately 1 µmol polymer (-SH)/1 µmol Alexa 532 (maleimide)), also containing 25 mM EDTA under an N_2 atmosphere and vigorous stirring. The reaction was continued for 3 hours at room temperature. ACN was then evaporated under reduced pressure and the precipitated polymer in the remaining aqueous phase (PBS) was recovered after centrifugation. To remove unreacted Alexa 532, the polymer was dissolved in chloroform and precipitated in methanol.

2.5. Polymer characterization

The compositions of the copolymers were determined by ^{1}H NMR in DMSO using a Gemini-300 MHz spectrometer at 298 K. To investigate the removal of the 2-pyridinethiol group after hydrogenation of 2-pyridyldithio-PEG-PLGBMGA, the polymers before and after hydrogenation were treated with DTT in chloroform and precipitated in diethyl-ether (DEE). The absorbance of the resulting supernatant was measured at 343 nm using UV spectrophotometry to detect the release of 2-pyridinethiol. The molar composition (lactic acid (L), glycolic acid (G) and hydroxymethyl glycolic acid (HMG)) was determined as described before [39]. The molecular weights of the obtained polymers were determined using GPC (Waters Alliance system), with a Waters 2695 separating module and a Waters 2414 refractive index detector. Two PL-gel 5 µm Mixed-D columns fitted with a guard column (Polymer Labs, MW range 0.2–400 kDa) were used and calibration was done using polystyrene standards with narrow molecular weight distributions. THF was used as the mobile phase (1 ml/min). The Alexa 532 conjugated polymer was characterized using GPC with dual RI and fluorescence detection (excitation wave length 531 nm, emission wave length 554 nm).

2.6. NPs preparation

NPs were prepared by a double emulsion solvent evaporation technique as described in the literature [47-49]. PLGHMGA and the different diblock copolymers were dissolved in DCM to a final concentration of 5% w/v (150 mg/3 ml). For example, to prepare nanobody conjugated and Alexa 532 labelled NPs loaded with RNase, 1.5 mg of labelled diblock copolymer, 15 mg maleimide-PEG_{5000}-PLGA, 15 mg PEG_{2000}-PLGHMGA and 119 mg PLGHMGA were dissolved in 3 ml DCM (for the preparation of NPs without maleimide, 15 mg maleimide-PEG_{5000}-PLGA was replaced by PEG_{2000}-PLGHMGA). A solution of RNase in reverse osmosis water (300 µl, 150 mg/ml) was then emulsified in solution of 3 ml of polymer in DCM in an ice-bath using an ultrasonic homogenizer (LABSONIC P, B.Braun Biotech) for 1 min at 40% amplitude. Subsequently, the w/o emulsion was emulsified into an external aqueous phase (30 ml) containing poly(vinyl alcohol) 5% (w/v) in NaCl 0.9% (w/v), filtered through 0.2 µm Millipore filter), in an ice-bath using the same ultrasonic homogenizer for 2 min at 60% amplitude to form a water-in-oil-in-water (w/o/w) emulsion. DCM was subsequently evaporated at room temperature under reduced pressure for 1 hour. NPs were recovered by ultracentrifugation (20000 X g for 20 min, J-26XP, Beckman Colter, Avanti ®) and washed twice with 45 ml 0.9% NaCl.

2.7. Characterization of the NPs

NPs were suspended in distilled water and their average size and size distribution were measured using Dynamic Light Scattering (DLS; Zetasizer 4000, Malvern Instruments, Malvern, UK) at 25 °C at an angle of 90° (Z-average). The zeta-potential of the NPs, suspended in 10 mM sodium phosphate buffer (NaCl 0.4 mM, Na_2HPO_4 6.6 mM, NaH_2PO_4 3 mM, pH 7.4), was determined by laser Doppler electrophoresis using a Zetasizer Nano-Z (Malvern Instruments Ltd.). The morphology of the NPs was studied using Transmission Electron Microscopy (TEM, Tecnai 10, Philips, 100kV) according to the following procedure. Twenty five µl of nanoparticle suspension was placed onto parafilm, and formvar/carbon-coated copper grids were placed on top of the sample droplets for 2 minutes. Excess liquid was removed by filter paper and, subsequently, the grids were negatively stained by placing them on top of 20 µl droplets of 2% uranyl acetate in demineralized water on parafilm for 2 minutes. Excess liquid was removed by filter paper and the grids were dried for 5 minutes at room temperature before the measurement.

2.8. Conjugation of 11A4 nanobody to the nanoparticle surface

The 11A4 nanobody was produced and purified as described before [38]. The 11A4 protein has one additional cysteine group at the C-terminal region for site-directed conjugation. Prior to conjugation of the nanobody to maleimide functionalized NPs, the nanobody dissolved in PBS buffer (1 mg/ml) was reduced in 50 mM Tris-HCl pH 8.5 also containing 20 mM TCEP. The reduction step was done at room temperature for 15 min after which TCEP was removed from the nanobody sample by buffer exchange with 0.4 mM EDTA-PBS pH 7 using Zeba Spin Desalting Columns (ThermoScientific). Maleimide functionalized NPs were mixed with a solution of nanobody (molar ratio of 2 nanobodies to 1 maleimide) and incubated overnight at 4 °C while rotating head-over-head (15 rpm/min). Subsequently, the NPs were centrifuged for 15 min at 15000 X g at 4 °C and washed with PBS buffer twice to remove unconjugated nanobody. The obtained pellet of maleimide functionalized NPs conjugated to 11A4 nanobody was then resuspended in PBS. Conjugation of 11A4 nanobody to the nanoparticle surface was confirmed by dot blot using rabbit anti VHH protein G purified serum (homemade) and goat anti rabbit IR800 antibody for detection. The amount of unconjugated 11A4 present in the supernatant obtained after centrifugation was analyzed by gel electrophoresis and compared to standard nanobody solutions with known concentrations.

2.9. Protein loading%

To determine the remaining RNase loading after nanobody conjugation, we exposed non-conjugated RNase-loaded nanoparticles to the same conditions as we used for the nanobody-conjugation but in the absence of nanobody (i.e. incubation overnight in PBS/EDTA buffer at 4 ^{o}C and centrifugation and washing). Particles were freeze dried at -50 °C and at 0.5 mbar in a Chris Alpha 1-2 freeze-drier (Osterode am Harz, Germany) for 12 hrs. Protein loading was determined by dissolving about 10 mg of freeze-dried NPs in 1 ml DMSO. Next, 5 ml of a 0.05 M NaOH solution containing 0.5% (w/v) SDS (sodium dodecyl sulfate) was added, essentially as described by Hongkee *et al.* [50]. The resulting solution was then analyzed for protein content by a BCA protein assay. The protein loading % (L%) is expressed as the encapsulated amount of protein divided by the dry weight of the loaded particles X 100%.

2.10. In vitro release of RNase

For release, non-conjugated particles were suspended in a certain volume of sodium phosphate buffer (NaCl 6 mM, Na_2HPO_4 99 mM, NaH_2PO4 49 mM, NaN_3 4 mM, pH 7.4) to obtain a dispersion of ~2 mg particles/ml. Samples of 300 µl of the homogeneous particle suspension were aliquoted into 500 µl eppendorf tubes. Also, 2 ml of the particle suspension was taken and washed twice with reverse osmosis water (centrifuged for 20 minutes at 20000 X g; Hermle Z233MK-2 centrifuge) and the obtained pellets were freeze-dried and used to determine the exact particle concentration as well as protein loading. The particle suspensions in Eppendorf tubes were incubated at 37 °C under mild agitation. At different time points, a tube was taken and the particles were centrifuged at 20000 X g for 20 min. The amount of RNase released in the supernatant was measured by UPLC (Acquity UPLC®) equipped with a BEH300 C18 1.7 µm column. A gradient was run from the starting composition, ACN/H_2O, (5/95%) / 0.1% TFA, to ACN/H_2O, (60/40%) / 0.1% TFA in 6 min. The mobile phase was delivered to the column at a flow rate of 0.250 ml/min, the injection volume was 7.5 µl, and detection was by measuring the UV absorbance at 280 nm. RNase standard solutions (10-400 µg/ml) were used for calibration.

2.11. RNase bioactivity assay

The bioactivity of released RNase was determined by a method described by Kalnitsky et al. [51] based upon the release of acid-soluble oligonucleotides following the digestion of yeast RNA. In short, solutions with different concentrations of RNase (0-12 µg/ml) in 0.1 M sodium acetate buffer pH 5 were freshly prepared and incubated at 37 °C for 5-8 minutes. RNA was dissolved in the same buffer (concentration 10 mg/ml) and also incubated at 37 °C. Next 500 µl of the enzyme solution was added to 500 µl of the RNA solution and the tubes were incubated for 4 minutes at 37 °C. The enzymatic reaction was stopped by the addition of 500 µl of solution of uranyl acetate (0.75%)/perchloric acid (25%) in water and the tubes were transferred into an ice bath and cooled for 5 minutes. After centrifugation for 10 min at 15000 X g the supernatant was taken and diluted 30 times with reverse osmosis water and the absorbance at 260 nm was measured. Specific enzyme activity was calculated as follows: units/µg= A_{260} X 30/µg enzyme.

2.12. Cell line and cell culture condition

Two human breast cancer cell lines Skbr3 (ATCC® HTB-30™, Her2 overexpressing) and MDA-MB-231 (ATCC® CRM-HTB-26™, Her2 negative) were obtained from American Type Culture Collection (ATCC, LGC Standards GmbH, Wesel, Germany) and maintained in Dulbecco's Modified Eagle's Medium (DMEM, Gibco) with 7.5% (v/v) FBS, 100 IU/ml penicillin, 100 mg/ml streptomycin, and 2 mM L-glutamine at 37 °C in a humidified atmosphere containing 5% CO_2.

2.13. Cellular binding of NPs

Five hundred thousand Skbr3 cells (Her2 positive cells) or MDA-MB-231 cells (Her2 negative cells) were seeded on glass cover slips and cultured in DMEM overnight. The next day, the medium was removed and the cells were incubated with Alexa 532 labelled NPs (with or without nanobody conjugated) for only 1h at 4 °C in CO_2-independent medium (Gibco) to avoid internalization. After incubation, the cells were washed once with CO_2-independent medium, fixed with 4% paraformaldehyde (PFA) and the cell nuclei were stained with DAPI. Cell-bound NPs were visualized by fluorescence microscopy. Images were acquired using wide-field fluorescence (Olympus AX70) and confocal microscopy (Confocal Laser Scanning microscope Zeiss LSM5 Pascal).

2.14. Uptake and cytotoxicity of NPs

Five thousand Skbr3 cells (Her2 positive cells) or MDA-MB-231 cells (Her2 negative cells) were seeded into a 96 well plate in DMEM. After overnight culture, the medium was exchanged by medium containing the nanoparticle formulations (particle concentration: 0.375-12 mg/ml), free nanobody (1-1000 nM) or RNase (3 to 100 µM RNase). The cells were subsequently incubated for 72 hours without medium refreshment. Cells incubated with Alexa 532 labelled NPs were visualized with fluorescence microscopy using an EVOS microscope (Advanced Microscopy Group, AMG, Thermo Fischer Scientific) equipped with 10x objective (Plan Fluor, 10x, NA 0.3, air and working distance 8.3 mm) and a LED-based fluorescence light cube (Cat. no. 12-563-471, Westover Scientific Inc., AMG). Phase contrast images were also obtained to assess cell morphology. ImageJ software was used for quantification of the mean fluorescence intensity. Regions of interest (ROI) were drawn around 8 cells per picture as well as in an area without cells (background). After background subtraction, the average fluorescence intensity of each ROI was calculated. Cell viability was assessed after 72h using the AlamarBlue reagent, which is an indicator for living-cells’ reducing environment, according to the manufacturer›s instructions. The mean values of two independent experiments with triplicates are shown ± SD.

3. Results and discussions

3.1. Synthesis and characterization of PLGHMGA, MePEG-PLGHMGA and thio-PEG-PLGHMGA

2-Pyridinethiol was coupled to thiol-PEG$_{2000}$-NH$_2$ in methanol and the aimed product, 2-pyridyldithio-PEG$_{2000}$-NH$_2$, was obtained in a yield of ~60% (Scheme 1). Thiopyridine is used to protect functional thiol end groups during the ring opening polymerization [52]. In the NMR spectrum of the pyridyldithio-PEG$_{2000}$-NH$_2$ (Fig. 2) it appeared that the signals of methylene protons (at 2.3 and 2.6 ppm) next to functional thiol end group of the starting compound disappeared and shifted to 3.0-3.2 ppm corresponding to methylene protons next to pyridyldithio group. This indicates (almost) quantitative end group conversion. Random copolymers of benzyl protected hydroxymethyl glycolide (BMG) and D,L-lactide (L) (BMG/D,L-lactide: 35/65 mol%), using BnOH, MePEG or 2-pyridyldithio-PEG$_{2000}$-NH$_2$ as initiators, were synthesized by ring opening polymerization in melt at 130 °C (Scheme 2).

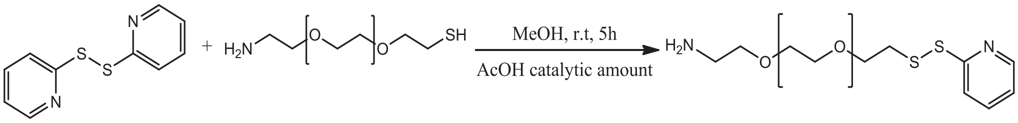
MeOH, r.t, 5h
AcOH catalytic amount
H2N
SH
S
N

Scheme 1: *Synthesis of the 2-pyridyldithio-PEG-NH$_2$ macroinitiator.*

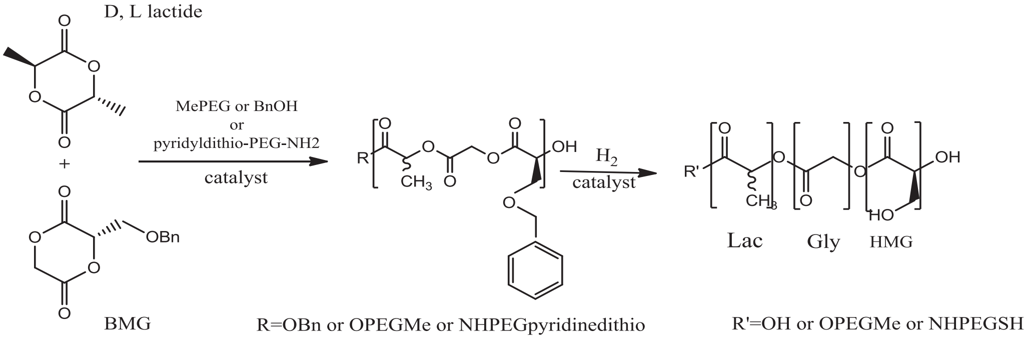
D, L lactide
BMG
OBn
MePEG or BnOH
or
pyridyldithio-PEG-NH2
catalyst
H2
catalyst
R
R'
CH3
OH
Lac
Gly
HMG
R=OBn or OPEGMe or NHPEGpyridinedithio
R'=OH or OPEGMe or NHPEGSH

Scheme 2: *Synthesis of hydrophilic aliphatic polyesters with pendant hydroxyl groups based on lactic acid, glycolic acid and hydroxymethylglycolic acid; poly(lactic-co-glycolic-co-hydroxymethylglycolic acid).*

After removal of the protective groups, the copolymers were obtained in high yields (>70%). The copolymer compositions as well as number average molecular weights for the diblock copolymers were determined by ^{1}H NMR spectroscopic analysis. The results presented in Table 1 demonstrate that the copolymer compositions were close to the monomer feed ratios. ^{1}H NMR analysis also demonstrates that complete removal of the protecting benzyl groups of

BMG units occurred after catalytic hydrogenation. Due to relative minor proportion of the number of pyridine protons to the number of polymer chain protons, the 2-pyridinethiol groups were not visible in the NMR spectra of the diblock 2-pyridyldithio-PEG-PLGBMGA. Therefore, successful removal of the 2-pyridinethiol group during the hydrogenation of this polymer was proven by releasing any covalently bound 2-pyridinethiol using DTT in chloroform before and after hydrogenation, and subsequent precipitation of the polymer in diethyl-ether. The thus obtained supernatant from 2-pyridyldithio-PEG-PLGBMGA (i.e. before hydrogenation) revealed a significant absorbance at 343 nm after treatment with DTT, confirming the presence of 2-pyridinethiol. However, the supernatant from the hydrogenated polymer showed no UV absorbance at 343 nm indicating that the 2-pyridinethiol group was indeed removed from the polymer during hydrogenation. The conjugation of Alexa 532 to the obtained sulfhydryl reactive end group of PEG-PLGHMGA copolymer was conducted via a simple click chemistry reaction by mixing dye and copolymer. The obtained polymer was characterized using GPC with dual RI and fluorescence detection. Appearance of the Alexa 532 fluorescence peak with the same retention time of the polymer in the RI signal indicates successful conjugation of the fluorophore to the thiol end group of PEG-PLGHMGA.

Table 1: *Characteristics of the polymers.*

Polymer	Composition x:y [a]		Molecular weight (kg/mol)			
	Feed ratio	Polymer ratio (NMR)	GPC M_n	GPC M_w	NMR	Theoretical M_n [b]
$MePEG_{2000}$-PLGBMGA	35:65	37:63	19	30	38	56
$MePEG_{2000}$-PLGHMGA		31:69	16	26	45	45
2-pyridyldithio-PEG-PLGBMGA		35:65	16	23	43	56
SH-PEG_{2000}- PLGHMGA		32:68	15	23	49	45
PLGBMGA		36:64	27	57	--	54
PLGHMGA		36:64	24	44	--	43

[a] *x:y denotes the molar ratio of BMG/D,L-Lactide or HMG/D,L-Lactide*

[b] *based on the initiator/monomer molar ratio of 1/300.*

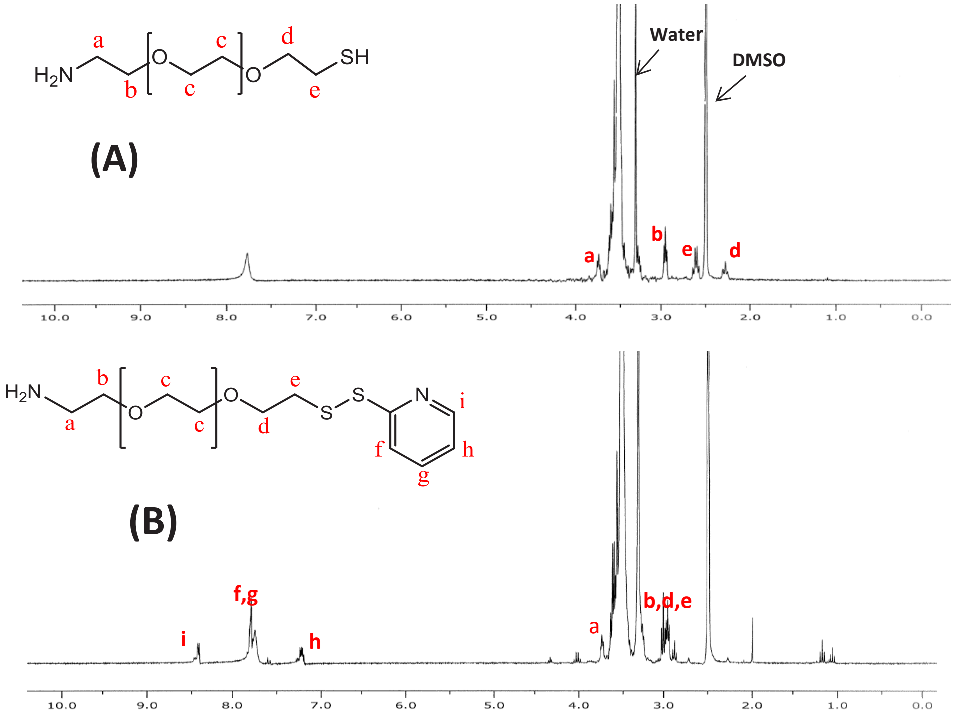

Figure 2: *^{1}H NMR spectrum in deuterated DMSO of 2-pyridyldithio-PEG-amine (used as macroinitiator for the synthesis of 2-pyridyldithio-PEG-PLGBMGA).*

^{1}H δ :

A) 2.5 (s, CH_3, DMSO), 2.9-3.1 (m, 6H, O-$\underline{CH_2}$-$\underline{CH_2}$-S and $\underline{CH_2}$-CH_2-NH_2), 3.3 (s, H_2O), 3.5 (PEG methylene units), 3.7 (m, 2H, O-CH_2-$\underline{CH_2}$-NH_2), 7.1-8.5 (m, 4H, pyridine ring), 7.8-8.0 (s, 2H, NH_2).

B) 2.3 (m, 2H, O-$\underline{CH_2}$-CH_2-SH), 2.5 (s, CH_3, DMSO), 2.6 (m, O-CH_2-$\underline{CH_2}$-SH), 3.0 (m, 2H, $\underline{CH_2}$-CH_2-NH_2), 3.3 (s, H2O), 3.5 (PEG methylene units), 3.7 (m, 2H, O-CH_2-$\underline{CH_2}$-NH_2), 7.8-8.0 (s, 2H, NH_2).

3.2. Preparation and characterization of RNase-loaded NPs

RNase-loaded NPs were prepared by a double emulsion solvent evaporation method [48, 49]. To obtain surface-functionalizable NPs, maleimide-PEG$_{5000}$-PLGA was added to the formulation. It has been previously shown that surface-functionalizable PLGA NPs were prepared by the addition of PEG-PLGA/PLA with a reactive group (e.g. maleimide) at the PEG terminal [53-55] using the same method as used in the present study. It should be noted that *in vivo* studies done by Gref et al. demonstrated that for optimal stealth behavior, the threshold w% content of PEG in NPs made of blends of different PEG diblock copolymers (e.g. PEG-PLGA and PEG-PLA) was

2-5% [56]. Since we used 10 w% of maleimide-PEG_{5000}-PLGA, we also added 10% of $MePEG_{2000}$-PLGHMGA to obtain particles with a total of ~2 w% PEG for optimal stealth behavior. We choose to use PEG_{2000} for the latter component (versus PEG_{5000} for the maleimide functional block copolymer) to favor the accessibility of the maleimide units on the surface of the NPs for reaction with the nanoboy [57]. It appeared that particles of around 280 nm and with a relatively low PDI (around 0.1) were obtained. RNase loading % (L%) after exposure of the NPs to the conditions of nanobody conjugation was around 3.5%. TEM analysis shows that spherical and non-porous NPs were formed (Fig. 3).

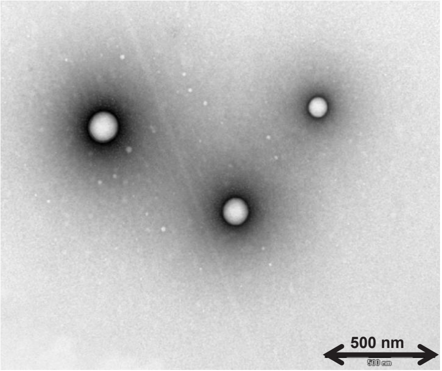

Figure 3: *TEM picture of non-conjugated NPs.*

3.3. Release of RNase from NPs

RNase-loaded NPs showed no initial burst and a sustained release of RNase reaching 80% at day 10 (Fig. 4). UPLC analysis of released RNase showed a single peak with the same retention time of native RNase, indicating that the primary structure of the released protein was retained [58, 59] (Fig. 5). Importantly, a digestion bioactivity assay showed that the enzymatic activity of released RNase was fully preserved, demonstrating that the structural integrity of the released protein was retained.

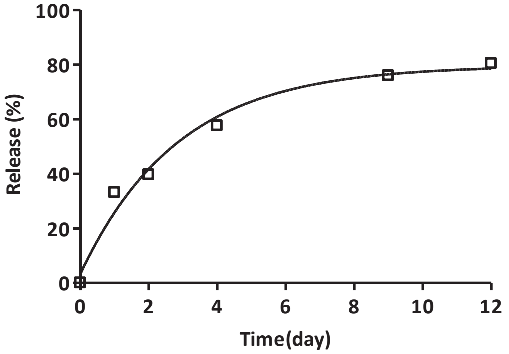

Figure 4: *Release of RNase from non-conjugated NPs (n=1). The percentage of the released protein is relative to the amount of protein encapsulated in the nanoparticles.*

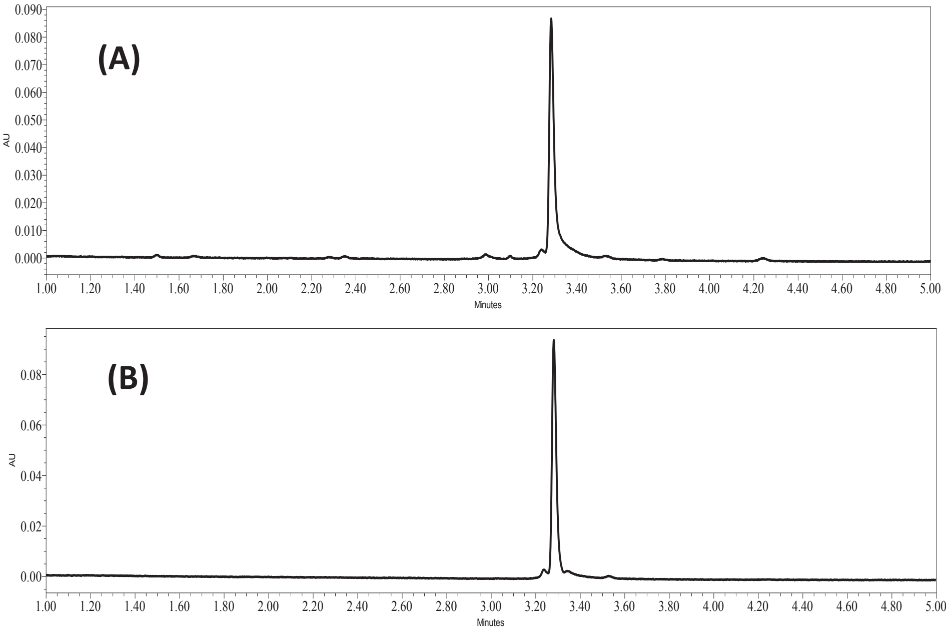

Figure 5: *UPLC chromatogram of A) RNase released from NPs and B) native RNase.*

3.4. Conjugation of 11A4 nanobody to the surface of NPs

The 11A4 nanobody was reduced using TCEP to make the C-terminal cysteine available for conjugation with the maleimide functionalities present at the terminal end of the PEG-chains exposed at the surface of the NPs. After incubation of the reduced nanobody with the nanoparticles, non-conjugated nanobody was removed by centrifugation. Dot blot analysis of the pelleted nanoparticles clearly showed the presence of nanobody (Fig. 6C); In addition, gel electrophoresis analysis of the unconjugated nanobody present in the supernatant also confirmed that 65% of the nanobody was conjugated. Dot blot analysis of particles lacking maleimide groups that were incubated with the nanobody showed after centrifugation no fluorescence demonstrating that the nanobody was not physically adsorbed on the surface of the NPs (Fig. 6D). The zeta potentials of NPs before and after nanobody conjugation were -1.3 and -0.7 mV, respectively. This small change can be explained by the slight positive charge of the nanobody at pH 7.4 (theoretical pI: 8.48, http://web.expasy.org/protparam/).

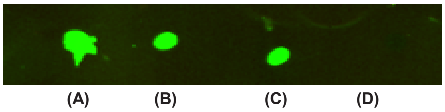

Figure 6: *Dot blot analysis of A) 11A4 nanobody B) 11A4 nanobody treated with DTT C) 11A4 nanobody conjugated NPs D) non-conjugated NPs.*

3.5. Cell binding of NPs

The ability of nanobody-conjugated NPs to bind to Her2-(over)expressing cells was investigated using Alexa 532-labelled NPs. Figure 7B shows that incubation of these NPs with Her2 positive Skbr3 cells at 4 °C resulted in a clear membrane staining, whereas very low fluorescence was detected after incubation of the same nanoparticles with Her2 negative MDA-MB-231 cells (Fig. 7A). This proves that the nanobody coupled to the surface of the NPs preserved its binding specificity for the receptor. The binding of non-conjugated NPs to Her2 positive cells was also tested and hardly any binding of these NPs was detected compared to binding of nanobody-conjugated NPs [Fig. 7C and 7D]. This low unspecific binding of the nanobody decorated NPs to cells lacking Her2 receptors and of the non-conjugated NPs to Her2 positive cells can likely be explained by the almost neutral zeta-potential of the NPs (see section 3.4). Overall, these results convincingly demonstrate that specific targeting of nanobody-decorated nanoparticles to Her2 positive cells occurs.

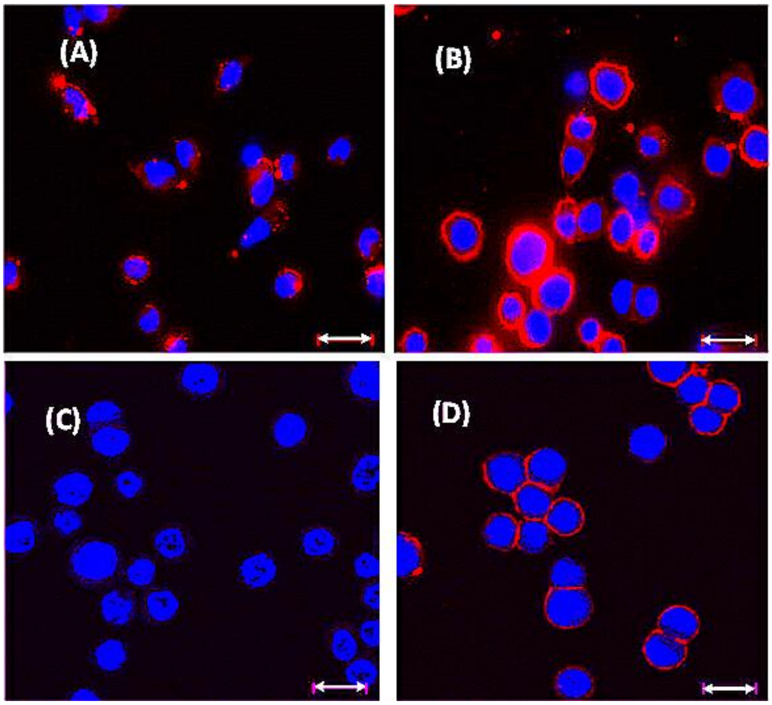

Figure 7: *Wide-field fluorescence microscopy pictures of nanobody-conjugated NPs incubated with* ***A)*** *MDA-MB-231 (Her2 negative) cells, and* ***B)*** *Skbr3 (Her2 over expressing) cells. Confocal microscopy pictures of Skbr3 cells incubated with* ***C)*** *non-conjugated NPs* ***D)*** *nanobody-conjugated NPs. Incubation was at 4 °C for 1h and scale bar= 20* µm*.*

3.6. Uptake and cytotoxic activity of NPs

Her2 positive Skbr3 cells were incubated with fluorescently labelled NPs with and without nanobody conjugation. Both conjugated as well as non-conjugated NPs were taken up by the cells (Fig. 8). Importantly, nanobody decorated NPs showed substantially higher uptake (about a factor 5). Figure 8 also shows that untreated cells were regularly shaped, with perfectly delineated borders, while cells treated with RNase loaded NPs had had irregular shapes and were smaller. These results indicate that cell viability was compromised upon incubation of RNase-loaded NPs with cells.

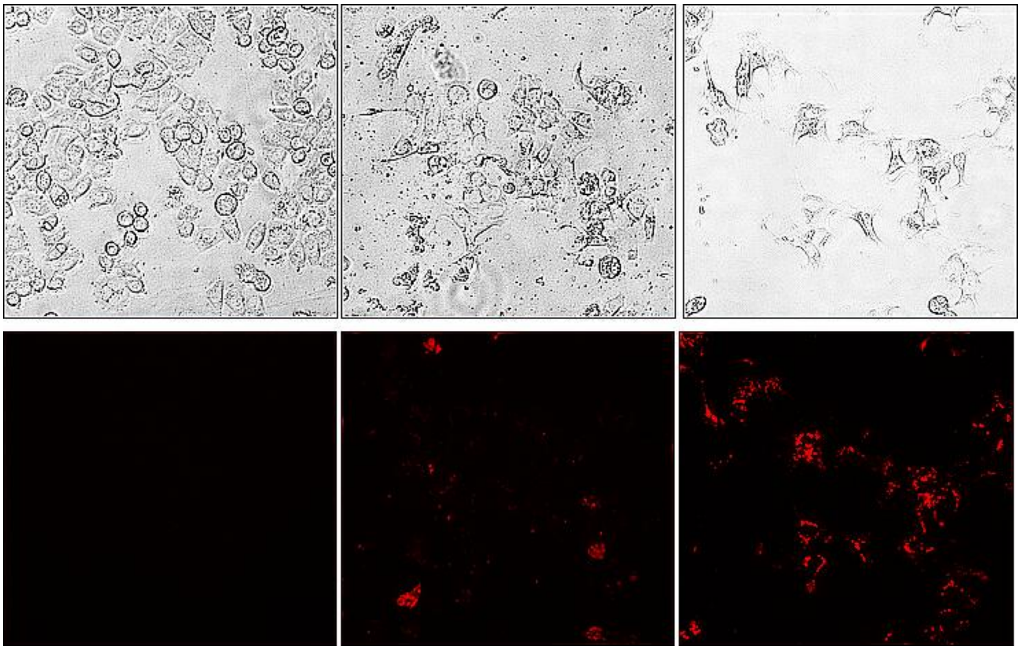

Figure 8: *Phase contrast images (top) and fluorescent images (bottom) obtained with an Evos inverted microscope* ***A)*** *non treated Skbr3 cells* ***B)*** *cells incubated with non-conjugated RNase-loaded and fluorescent labelled NPs (RNase: 28* µM**)** ***C)*** *cells incubated with 11A4 nanobody-conjugated RNase-loaded and fluorescent labelled NPs (RNase: 28* µM*).*

The cytotoxic effect of RNase-loaded and nanobody conjugated NPs was compared to that of free RNase, non-conjugated RNase-loaded NPs, and empty NPs (Fig. 9). The results show that both empty NPs (up to 12 mg/ml particle concentration, which is equivalent to highest concentration of RNase loaded NPs tested) and free RNase (up to a concentration of 100 µM) did not affect cell viability of Skbr3 cells whereas non-conjugated NPs showed toxicity which led to 75% cell death at the highest concentration of RNase tested (28 µM; IC_{50}: 15 µM, Fig. 10). The results show that both empty NPs (up to 12 mg/ml particle concentration, which is equivalent to highest concentration of RNase loaded NPs tested) and free RNase (up to a concentration of 100 µM) did not affect cell viability of Skrb3 cells whereas non-conjugated NPs showed toxicity which led to 75% cell death at the highest concentration of RNase tested (28 µM; IC_{50}: 15 µM, Fig. 4, during the incubation time of 3 days, non-conjugated RNase-loaded NPs showed 60% of RNase release. Assuming that the release happened to the same extent during the cytotoxicity test, it can be anticipated that the real IC_{50} values are even lower than reported above. To rule out the possibility of an effect of the 11A4 nanobody on cell viability, the free nanobody, at a much higher dose than that was present in the NP formulation, was incubated with the Her2 overexpressing as well as the Her2 negative cell lines. Our results demonstrated no reduction in cell viability.

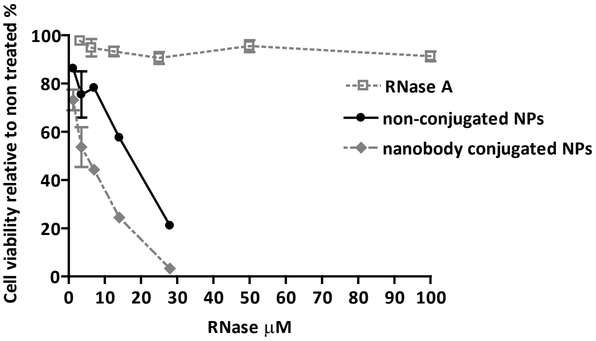

Figure 9: *Viability of Skbr3 cells upon 72 h incubation with RNase-loaded conjugated and non-conjugated NPs, RNase (non-treated cells set to 100%). Empty NPs up to concentration of 12 mg/ml did not affect the cell viability. This is the same concentration of nanoparticles at highest* μM *concentration of RNase.*

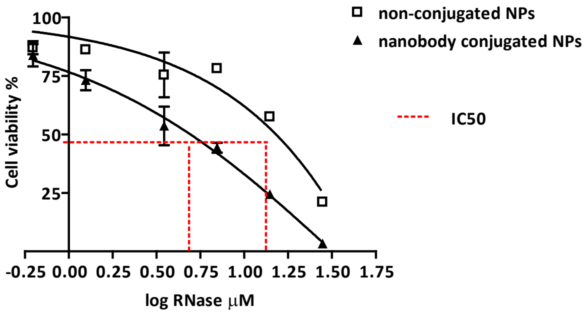

Figure 10: *IC_{50} values of RNase-loaded nanobody-conjugated and non-conjugated NPs.*

Early studies have demonstrated that most RNases do not exert considerable cytotoxic activities unless these proteins are internalized [9, 60]. The results of figure 9 which demonstrate that free RNase did not show cytostatic activity are likely because this protein is insufficiently taken up. Importantly, the observed high cytotoxic effect of nanobody conjugated NPs is therefore most likely due to their high cellular binding and internalization. It has to be remarked that RNase should be present in the cytoplasm to induce apoptotic cell death as a result of RNase-catalyzed degradation of cytosolic RNAs. Thus, the cytotoxic effect of the RNase-loaded NPs is due to either the release of RNase in the endosome which subsequently destabilizes these cellular compartments resulting in release of the enzyme into the cytosol, or due to destabilization of the endosomes by particles followed by release of the entrapped enzyme in the cytosol (or due to a combination of both). Enhanced and selective uptake of PLGA and other polymer-based NPs decorated with different AntiHer2 antibodies (e.g. Trastuzumab and herceptin) into different cell lines including Skbr3 has been reported previously by others [61-63]. It has been shown that actively internalized RNases are able to escape endosomal compartments (pre-lysosomal endosomes or lysosomes) and evade degradation by [17, 19]. Secondary endosomes and lysosomes are predominantly acidic (pH 4 to 5). At this pH, RNase (pI 9.6) has a strong positive charge and hence likely interacts with negatively charged membranes, leading to membrane destabilization and their subsequent release into the cytoplasm. Previous studies on the cellular processing of (non-conjugated) PLGA nanoparticles have shown that after uptake a main fraction of the nanoparticles recycle back to the outside of the cell, while a small fraction enters secondary endosomes and lysosomes and finally translocates into the cytoplasm via an essentially unknown mechanism [64]. Given the structural resemblance with PLGA, the same cellular fate can be also expected for PLGHMGA NPs. Furthermore it has been shown that the cellular uptake of PLGA NPs depends on their size and surface properties, but also on cell type, incubation time and particle concentration. However, it is important to emphasize that ligand-conjugated NPs have different intracellular trafficking pathways than non-conjugated NPs [65]. It should be mentioned that in our previous study almost complete removal of PEG (shedding) of PLGHMGA NPs occurred in five days due to preferential hydrolysis of the ester bond between the PEG and PLGHMGA block. The cellular binding of our NPs and their subsequent internalization occurs in 1-2 days at most (Fig. 8) which demonstrates that the shedding of the PEG layer does not occur to a great extent outside the cell. During further incubation, however, it is possible that the gradual PEG shedding results in enhanced endosomal/lysosomal escape of NPs.

Conclusions

PLGHMGA NPs loaded with RNase as a therapeutic protein were successfully prepared by a double emulsion solvent evaporation technique. The NPs showed 80% release of the loaded protein in 12 days and a fully preserved catalytic activity of the released RNase was confirmed by an enzymatic activity assay. A nanobody specific for the Her2 receptor was coupled via a terminal cysteine to maleimide groups present at the distal end of the PEG chains and exposed at the surface of the NPS. Alexa 532-labelled and nanobody-conjugated NPs showed greater binding and uptake by Her2 over-expressing cells compared to NPs devoid of nanobody, and no binding to Her2 negative cells, indicating that the Her2 nanobody on the surface of the NPs interacts with the Her2 receptor of the cells. Free RNase exhibited no cytotoxicity demonstrating inefficient uptake of this enzyme. In contrast, significant and dose-dependent cytotoxicity was observed for nanobody-conjugated RNase-loaded NPs. It can be concluded that targeted PLGHMGA nanoparticles are potential candidates to exploit therapeutic potential of RNases.

References

1. Youle RJ, Newton D, Wu YN, Gadina M, Rybak SM. Cytotoxic ribonucleases and chimeras in cancer therapy. *Crit Rev Ther Drug Carrier Syst*. 1993;10:1-28.

2. De Lorenzo C, D'Alessio G. From immunotoxins to immunoRNases. *Curr Pharm Biotechnol*. 2008;9:210-214.

3. Krauss J, Arndt MA, Dubel S, Rybak SM. Antibody-targeted RNase fusion proteins (immunoRNases) for cancer therapy. *Curr Pharm Biotechnol*. 2008;9:231-234.

4. Baynes JW, Wold F. Effect of glycosylation on the in vivo circulating half-life of ribonuclease. *J Biol Chem*. 1976;251:6016-6024.

5. ALEKSANDROWICZ J, URBANCZYK J, OSTROWSKA A, SIERKO J. Further research on the activity of ribonucleases in the blood and urine of patients suffering from proliferative hemocytopathia. *Blood*. 1958;13:652-664.

6. Ardelt W, Ardelt B, Darzynkiewicz Z. Ribonucleases as potential modalities in anticancer therapy. *Eur J Pharmacol*. 2009;625:181-189.

7. TELFORD IR, KEMP JF, TAYLOR EF, YEAMAN MW. Effect of ribonuclease on survival of ascites tumor bearing mice. *Proc Soc Exp Biol Med*. 1959;100:829-831.

8. Newton DL, Ilercil O, Laske DW, Oldfield E, Rybak SM, Youle RJ. Cytotoxic ribonuclease chimeras. Targeted tumoricidal activity in vitro and in vivo. *J Biol Chem*. 1992;267:19572-19578.

9. Saxena SK, Rybak SM, Winkler G, et al. Comparison of RNases and toxins upon injection into Xenopus oocytes. *J Biol Chem*. 1991;266:21208-21214.

10. Shapiro R. Cytoplasmic ribonuclease inhibitor. *Methods Enzymol*. 2001;341:611-628.

11. Lee FS, Vallee BL. Structure and action of mammalian ribonuclease (angiogenin) inhibitor. *Prog Nucleic Acid Res Mol Biol*. 1993;44:1-30.

12. Dickson KA, Haigis MC, Raines RT. Ribonuclease inhibitor: structure and function. *Prog Nucleic Acid Res Mol Biol*. 2005;80:349-374.

13. Turcotte RF, Lavis LD, Raines RT. Onconase cytotoxicity relies on the distribution of its positive charge. *FEBS J*. 2009;276:3846-3857.

14. Zwolinska M, Smolewski P. Onconase: a ribonuclease with antitumor activity. *Postepy Hig Med Dosw (Online)*. 2010;64:58-66.

15. Altomare DA, Rybak SM, Pei J, et al. Onconase responsive genes in human mesothelioma cells: implications for an RNA damaging therapeutic agent. *BMC Cancer*. 2010;10:34-2407-10-34.

16. Ardelt B, Ardelt W, Darzynkiewicz Z. Cytotoxic ribonucleases and RNA interference (RNAi). *Cell Cycle*. 2003;2:22-24.

17. Rybak SM. Antibody-onconase conjugates: cytotoxicity and intracellular routing. *Curr Pharm Biotechnol*. 2008;9:226-230.

18. Wu Y, Saxena SK, Ardelt W, et al. A study of the intracellular routing of cytotoxic ribonucleases. *J Biol Chem*. 1995;270:17476-17481.

19. Zhao HL, Xue C, Du JL, et al. Sustained and cancer cell targeted cytosolic delivery of Onconase results in potent antitumor effects. *J Control Release*. 2012;159:346-352.

20. Choi JH, Jang JY, Joung YK, Kwon MH, Park KD. Intracellular delivery and anti-cancer effect of self-assembled heparin-Pluronic nanogels with RNase A. *J Control Release*. 2010;147:420-427.

21. Chang CH, Gupta P, Michel R, et al. Ranpirnase (frog RNase) targeted with a humanized, internalizing, anti-Trop-2 antibody has potent cytotoxicity against diverse epithelial cancer cells. *Mol Cancer Ther*. 2010;9:2276-2286.

22. Chang CH, Sapra P, Vanama SS, Hansen HJ, Horak ID, Goldenberg DM. Effective therapy of human lymphoma xenografts with a novel recombinant ribonuclease/anti-CD74 humanized IgG4 antibody immunotoxin. *Blood*. 2005;106:4308-4314.

23. Newton DL, Hansen HJ, Mikulski SM, Goldenberg DM, Rybak SM. Potent and specific antitumor effects of an anti-CD22-targeted cytotoxic ribonuclease: potential for the treatment of non-Hodgkin lymphoma. *Blood*. 2001;97:528-535.

24. Chen W, Zheng M, Meng F, et al. In situ forming reduction-sensitive degradable nanogels for facile loading and triggered intracellular release of proteins. *Biomacromolecules*. 2013;14:1214-1222.

25. Maier K, Martin I, Wagner E. Sequence Defined Disulfide-Linked Shuttle for Strongly Enhanced Intracellular Protein Delivery. *Mol Pharm*. 2012.

26. Choi SH, Park TG. G-CSF loaded biodegradable PLGA nanoparticles prepared by a single oil-in-water emulsion method. *Int J Pharm*. 2006;311:223-228.

27. Rajapaksa TE, Stover-Hamer M, Fernandez X, Eckelhoefer HA, Lo DD. Claudin 4-targeted protein incorporated into PLGA nanoparticles can mediate M cell targeted delivery. *J Control Release*. 2010;142:196-205.

28. Taha MA, Singh SR, Dennis VA. Biodegradable PLGA85/15 nanoparticles as a delivery vehicle for Chlamydia trachomatis recombinant MOMP-187 peptide. *Nanotechnology*. 2012;23:325101-4484/23/32/325101. Epub 2012 Jul 23.

29. Diwan M, Elamanchili P, Lane H, Gainer A, Samuel J. Biodegradable nanoparticle mediated antigen delivery to human cord blood derived dendritic cells for induction of primary T cell responses. *J Drug Target*. 2003;11:495-507.

30. Ye M, Kim S, Park K. Issues in long-term protein delivery using biodegradable microparticles. *J Control Release*. 2010;146:241-260.

31. Danhier F, Ansorena E, Silva JM, Coco R, Le Breton A, Preat V. PLGA-based nanoparticles: An overview of biomedical applications. *J Control Release*. 2012;161:505-522.

32. Betancourt T, Byrne JD, Sunaryo N, et al. PEGylation strategies for active targeting of PLA/PLGA nanoparticles. *J Biomed Mater Res A*. 2009;91:263-276.

33. Hassanzadeh-Ghassabeh G, Devoogdt N, De Pauw P, Vincke C, Muyldermans S. Nanobodies and their potential applications. *Nanomedicine (Lond)*. 2013;8:1013-1026.

34. Muyldermans S. Nanobodies: natural single-domain antibodies. *Annu Rev Biochem*. 2013;82:775-797.

35. Oliveira S, Heukers R, Sornkom J, Kok RJ, van Bergen En Henegouwen PM. Targeting tumors with nanobodies for cancer imaging and therapy. *J Control Release*. 2013;172:607-617.

36. Wang Y, Liu P, Du J, Sun Y, Li F, Duan Y. Targeted siRNA delivery by anti-HER2 antibody-modified nanoparticles of mPEG-chitosan diblock copolymer. *J Biomater Sci Polym Ed*. 2013;24:1219-1232.

37. Ruan J, Song H, Qian Q, et al. HER2 monoclonal antibody conjugated RNase-A-associated CdTe quantum dots for targeted imaging and therapy of gastric cancer. *Biomaterials*. 2012;33:7093-7102.

38. Kijanka M, Warnders FJ, El Khattabi M, et al. Rapid optical imaging of human breast tumour xenografts using anti-HER2 VHHs site-directly conjugated to IRDye 800CW for image-guided surgery. *Eur J Nucl Med Mol Imaging*. 2013;40:1718-1729.

39. Samadi N, van Nostrum CF, Vermonden T, Amidi M, Hennink WE. Mechanistic studies on the degradation and protein release characteristics of poly(lactic-co-glycolic-co-hydroxymethylglycolic acid) nanospheres. *Biomacromolecules*. 2013;14:1044-1053.

40. Ghassemi AH, van Steenbergen MJ, Barendregt A, et al. Controlled release of octreotide and assessment of peptide acylation from poly(D,L-lactide-co-hydroxymethyl glycolide) compared to PLGA microspheres. *Pharm Res*. 2012;29:110-120.

41. Ghassemi AH, van Steenbergen MJ, Talsma H, van Nostrum CF, Crommelin DJ, Hennink WE. Hydrophilic polyester microspheres: effect of molecular weight and copolymer composition on release of BSA. *Pharm*

Res. 2010;27:2008-2017.

42. Ghassemi AH, van Steenbergen MJ, Talsma H, et al. Preparation and characterization of protein loaded microspheres based on a hydroxylated aliphatic polyester, poly(lactic-co-hydroxymethyl glycolic acid). *J Control Release*. 2009;138:57-63.

43. Liu Y, Ghassemi AH, Hennink WE, Schwendeman SP. The microclimate pH in poly(d,l-lactide-co-hydroxymethyl glycolide) microspheres during biodegradation. *Biomaterials*. 2012;33:7584-7593.

44. Samadi N, van Steenbergen MJ, vanden Dikkenberg JB, et al. Nanoparticles absed on a hydrophilic polyester with asheddable PEG coating for protein delivery. *In press.*

45. Bollag DM, Rozycki SJ, Edelstein EDS, eds. *Protein Method.* 2nd ed. New York: Willey-Liss; 1996.

46. Leemhuis M, vanNostrum CF, Kruijtzer JAW, et al. Functionalized poly (alpha-hydroxy acid)s via ring-opening polymerization: toward hydrophilic polyesters with pendant hydroxyl groups. *Macromolecules*. 2006;39:3500–3508.

47. Zambaux MF, Bonneaux F, Gref R, Dellacherie E, Vigneron C. Preparation and characterization of protein C-loaded PLA nanoparticles. *J Control Release*. 1999;60:179-188.

48. Dunne M, Corrigan I, Ramtoola Z. Influence of particle size and dissolution conditions on the degradation properties of polylactide-co-glycolide particles. *Biomaterials*. 2000;21:1659-1668.

49. Panyam J, Dali MM, Sahoo SK, et al. Polymer degradation and in vitro release of a model protein from poly(D,L-lactide-co-glycolide) nano- and microparticles. *J Control Release*. 2003;92:173-187.

50. Sah H. A new strategy to determine the actual protein content of poly(lactide-co-glycolide) microspheres. *J Pharm Sci*. 1997;86:1315-1318.

51. Kalnitskey et al. Worthington Biochemical Coprporation (Ribonuleic Acid Assay).

52. Molla MR, Ghosh S. Exploring versatile Sulfhydryl Chemistry in the Chain End of a Synthetic Polylactide. *Macromolecules*. 2012;45(21):8561-8570.

53. Toti US, Guru BR, Grill AE, Panyam J. Interfacial activity assisted surface functionalization: a novel approach to incorporate maleimide functional groups and cRGD peptide on polymeric nanoparticles for targeted drug delivery. *Mol Pharm*. 2010;7:1108-1117.

54. Zhang L, Han L, Qin J, Lu W, Wang J. The use of borneol as an enhancer for targeting aprotinin-conjugated PEG-PLGA nanoparticles to the brain. *Pharm Res*. 2013;30:2560-2572.

55. Patil YB, Toti US, Khdair A, Ma L, Panyam J. Single-step surface functionalization of polymeric nanoparticles for targeted drug delivery. *Biomaterials*. 2009;30:859-866.

56. Gref R, Luck M, Quellec P, et al. 'Stealth' corona-core nanoparticles surface modified by polyethylene glycol #PEG#: influences of the corona #PEG chain length and surface density# and of the core composition on phagocytic uptake and plasma protein adsorption. *Colloids Surf B Biointerfaces*. 2000;18:301-313.

57. Wang M, Thanou M. Targeting nanoparticles to cancer. *Pharmacol Res*. 2010;62:90-99.

58. van de Weert M, Hennink WE, Jiskoot W. Protein instability in poly(lactic-co-glycolic acid) microparticles. *Pharm Res*. 2000;17:1159-1167.

59. Frokjaer S, Otzen DE. Protein drug stability: a formulation challenge. *Nat Rev Drug Discov*. 2005;4:298-306.

60. Erickson HA, Jund MD, Pennell CA. Cytotoxicity of human RNase-based immunotoxins requires cytosolic access and resistance to ribonuclease inhibition. *Protein Eng Des Sel*. 2006;19:37-45.

61. Koopaei MN, Dinarvand R, Amini M, et al. Docetaxel immunonanocarriers as targeted delivery systems for HER 2-positive tumor cells: preparation, characterization, and cytotoxicity studies. *Int J Nanomedicine*. 2011;6:1903-1912.

62. Sun B, Ranganathan B, Feng SS. Multifunctional poly(D,L-lactide-co-glycolide)/montmorillonite (PLGA/MMT) nanoparticles decorated by Trastuzumab for targeted chemotherapy of breast cancer. *Biomaterials*. 2008;29:475-486.

63. Yousefpour P, Atyabi F, Vasheghani-Farahani E, Movahedi AA, Dinarvand R. Targeted delivery of doxorubicin-utilizing chitosan nanoparticles surface-functionalized with anti-Her2 trastuzumab. *Int J Nanomedicine*. 2011;6:1977-1990.

64. Panyam J, Labhasetwar V. Dynamics of endocytosis and exocytosis of poly(D,L-lactide-co-glycolide) nanoparticles in vascular smooth muscle cells. *Pharm Res*. 2003;20:212-220.

65. Furumoto K, Ogawara K, Yoshida M, et al. Biliary excretion of polystyrene microspheres depends on the type of receptor-mediated uptake in rat liver. *Biochim Biophys Acta*. 2001;1526:221-226.

6

Summary and Discussion

1. Summary

During the last two decades pharmaceutical researchers have focused on the development of polymer formulations for protein and peptide drugs. Attention has been focused on the development of macroscopic systems in the form of hydrogels or on polymeric microparticles that release an entrapped protein/peptide for a prolonged time [1-5]. These systems are aimed for local administration and the released bioactive proteins have their target/receptor at extracellular membranes. However, some pharmaceutical proteins have their target intracellularly and therefore systems based on injectable hydrogels or microspheres are not suitable as delivery systems for this class of proteins. For the intracellular delivery of proteins/peptides and particularly for the ones that do not passively pass cellular membranes, polymeric nanoparticles (NPs) are candidate delivery systems. Polymeric NPs have the possibility to accumulate at the aimed site of action via the so-called EPR effect, but are also taken up by the target cell to subsequently release their content intracellularly. Poly(lactic-co-glycolic acid) (PLGA) is one of the most studied biodegradable polymers for drug and protein delivery. However, as pointed out in **Chapter 1** of this thesis some drawbacks are associated with the use of this polymer for the development of protein formulations.

Chapter 1 of this thesis provides a general introduction to therapeutic peptides and proteins, challenges for their intracellular delivery and different technologies applied so far to overcome these issues. A brief description of functionalized polyesters and their attractive features for protein delivery is also provided. In this thesis, PLGHMGA (poly D,L lactic-co-glycolic-co-hyroxymethyl glycolic acid) is investigated as an alternative for PLGA for the design of nanoparticulate protein formulations. Finally, the aims of this thesis are outlined.

In **Chapter 2** we investigated the effect of particle size and PLGA end group on particle degradation behavior as well as on protein loading and release. PLGA particles with different sizes (0.3, 1 and 20 µm) based on acid-terminated PLGA (‘uncapped PLGA’) and ester-terminated PLGA bearing a long aliphatic tail (a dodecanyl end group; ‘capped PLGA’) were prepared and loaded with a model protein (bovine serum albumin, BSA) by a double emulsion solvent evaporation method. It was found that, independent of their size, particles based on capped PLGA showed slower degradation and protein release kinetics than those based on the uncapped polymer, which is probably due to their more hydrophobic nature of the dodecanol-capped PLGA. More importantly, particles based on capped PLGA showed an incomplete BSA release reaching

~70% of the particles payload, while those based on the uncapped PLGA showed a quantitative protein release. An insoluble residue was present till the end of the study (175 days) for BSA loaded particles based on capped PLGA. FTIR analysis of this insoluble residue showed the peaks assigned to BSA as well as peaks originating from PLGA, demonstrating that the residue is a mixture of insoluble protein and polymer degradation products rich in lauryl alcohol (NMR analysis). Therefore, the incomplete release of BSA from particles based on capped PLGA is likely due to hydrophobic interactions between the aliphatic lauryl capping group and the protein. Since many proteins have hydrophobic domains and pockets, similar interactions can be also expected with therapeutic proteins.

In **Chapter 3** we prepared PLGHMGA NPs that are potentially suitable for intracellular delivery of proteins. This chapter reports on the degradation of the particles and the release behaviour of a model protein, bovine serum albumin (BSA), from NPs ranging from 400-700 nm and prepared from polymers of different molecular weights and compositions. The effect of different PLGHMGA concentrations in organic phase used for particle preparation was also studied. Lyophilized particles showed a significant burst release (40-50% of the BSA loading) likely caused by the porosity of the NPs that resulted from sublimation of water, originating from the primary w/o emulsion, during the freeze-drying process. To reduce the burst release, further studies were therefore conducted on non-lyophilized NPs. The NPs showed a continuous mass loss accompanied by a continuous decrease in number average molecular weight indicating that degradation of the NPs is by bulk degradation. The concentration of the polymer in the organic phase used to prepare the NPs had a minor effect on particle degradation rate. More hydrophilic NPs, prepared from PLGHMGA of higher HMG content, showed relatively faster decrease in both molecular weight and dry mass as compared to NPs based polymers with lower HMG contents. This is due to an increased number of pendant hydroxyl groups resulting in an increase in water uptake of the particles. The higher hydration of the polymer matrix in turn enhances the rate of ester bond hydrolysis and also the permeability of the matrices for low molecular weight water-soluble degradation products. Particles based on PLGHMGA with 18% HMG units showed after a burst of around 10-20%, a continuous release of BSA for the next 30 days. Whereas, more hydrophobic particles (based on PLGHMGA with 13% HMG) showed a two phase release pattern characterized by a lag phase of around 40 days followed by a relatively fast and quantitative release of the BSA over the next 20 days. These findings illustrate that release patterns can be effectively modulated by varying the density of pendant hydroxyl groups. Analysis of the water-insoluble nanoparticle residues by ^{1}H NMR revealed a change in copolymer molecular structure which is interpreted as caused by an intramolecular transesterification. A gradual decrease in both HMG (either in its native conformation or as transesterified units) and glycolic content was found, demonstrating that, as expected, HMG and glycolic ester bonds in PLGHMGA are more susceptible to hydrolysis. As mentioned, the NPs studied in **Chapter 3** have a size from 400-700 nm. For the intracellular delivery of therapeutic proteins, however, particles with smaller sizes (100-200 nm) are preferred. Therefore, to reduce the size of the NPs, PEGylated polymers were used.

In **Chapter 4** diblock PEG-PLGHMGA copolymers of two different PEG polymer chain lengths (2000 and 5000 Da) were synthesized and characterized. Placebo and protein loaded NPs were prepared using bare PEG-PLGHMGA, but also by blending PEG-PLGHMGA and PLGHMGA (10-50%). Bovine serum albumin and lysozyme were used as model proteins. PEG-PLGHMGA, due to its amphiphilicity and surface active properties, enabled the preparation of PEGylated NPs without using a surfactant in the external water phase. It was observed that particle properties like zeta potential, morphology, size and PDI were significantly influenced by the PEG-PLGHMGA content and the molecular weight of the PEG chain. A substantial decrease in both size and particle surface charge was observed for NPs containing PEG-PLGHMGA with higher PEG weight fraction and longer PEG chain length. However, the protein encapsulation efficiency in nanoparticles formulated without using surfactant was very low, and the low amount of entrapped protein was rapidly released in about one day. Protein incorporation and release properties of PEGylated PLGHMGA NPs were improved using PVA (polyvinyl alcohol) as surfactant in the preparation protocol. It was observed that BSA and lysozyme were both efficiently encapsulated in the NPs prepared using PVA as surfactant. The presence of PVA at the interface of the organic and aqueous phase perhaps acts as barrier for protein diffusion, not only during particle formation, but also during release from the solidified NPs. Also, more uniform sized NPs were formed in the presence of PVA. The size of the particles prepared with PVA was around 240-280 nm and PDI was < 0.1 which were not profoundly influenced by the PEG content. PEG is not only expected to be present at the particle surface but is also present in the bulk of the particles because of the good compatibility of PEG and PLGHMGA, as demonstrated by DSC analysis. The presence of the hydrophilic PEG in the matrix results in greater water absorbing, thereby in increasing the hydrolysis kinetics of the polymers and thus the degradation rate of the particles. Particularly the ester bond that connects the PEG and PLGHMGA block is very susceptible for hydrolysis.

Surprisingly, particle degradation and consequently the protein release kinetics were nearly similar and independent of PEG-PLGHMGA content and the molecular weight of PEG. These marginal differences could be explained by the almost complete removal of PEG (based NMR analysis) from the degrading NPs in 5 days.

In **Chapter 5** we evaluated the suitability of PEG-PLGHMGA NPs for targeted intracellular delivery of a therapeutic protein. Ribonucleases are small (10–28 kDa) basic proteins which are able to catalyze the degradation of cytosolic RNAs. Therefore these proteins have raised attention in the biopharmaceutical and medical field for use as novel anti-cancer therapeutics. The Her2 (or EGFR2; human epidermal growth factor receptor 2) receptor is overexpressed in aggressive types of breast cancer cells and has become in recent years an important target for therapy. Very recently, functional nanobodies (nanobodies are the variable domains of heavy chain only antibodies present in Camelidae and some sharks) have been developed and the 11A4 nanobody demonstrated specific binding to the Her2 receptor. Therefore, in **Chapter 5** PEGylated PLGHMGA NPs and decorated with a Her2 specific nanobody were developed for targeted intracellular delivery of RNase A. PEGylated particles loaded with RNase were analyzed for their release behavior. It was shown that the particles released the protein in 10-12 days and an enzymatic assay showed that the bioactivity of the released RNase was fully preserved. Further, surface-functionalizable NPs were prepared by addition of 10% of PEG-PLGA with a reactive maleimide group at the PEG terminal end. Dot blot analysis confirmed successful conjugation to C-terminal cysteine of nanobody implying the presence of PEG-PLGA and thus functional maleimide group at the surface of NPs. Cellular binding assay of nanobody-conjugated NPs labelled with a fluorescent dye showed a substantial higher binding to as well as uptake by Her2 over-expressing cancer cells (Skbr3) than NPs without nanobody. The cytotoxic activity of RNase-loaded and nanobody conjugated NPs was compared to that of free RNase, non-conjugated RNase-loaded NPs, and empty NPs, as controls. The results showed that both empty NPs and free RNase (up to a concentration of 100 µM) did not affect cell viability of Skrb3 cells whereas non-conjugated NPs showed toxicity which led to 75% of cell death at highest concentration of RNase (28 µM; IC_{50}: 15 µM). Importantly, nanobody conjugated NPs loaded with RNase exhibited a much stronger cytotoxicity resulting in death of 90% of the cells at highest concentration tested (28 µM, IC_{50}: 5 µM). These results demonstrate that RNase A was released intracellularly where it could catalyze the degradation of cytosolic RNAs resulting in cell killing. The cytotoxic effect of the RNase-loaded NPs was due to either the release of

RNase from the particles in the endosomes which subsequently destabilizes these cellular compartments resulting in its translocalization into the cytosol, or due to destabilization of the endosomes by particles followed by release of the entrapped enzyme in the cytosol, or to a combination of both.

2. Perspectives and Conclusions

The hydrophilic functionalized polyester PLGHMGA is an attractive polymer for the design of NPs loaded with therapeutic peptides or proteins. In summary:

1) Safe/simple methods for protein encapsulation

On lab scale, PLGHMGA NPs are easy to formulate to NPs with high loading of proteins by a simple double emulsion method. The preparation methods used for particles preparation appeared to be compatible with proteins. Circular dichroism analysis of BSA showed that the secondary structure of the released protein was fully preserved. Also, an enzymatic activity assay on released RNase demonstrated that enzymatic activity of this protein was fully retained.

2) Tailorable protein release

As described in Chapter 3 different release patterns (sustained and delayed) can be achieved by modulating the density of pendant hydroxyl group in the copolymer. In this chapter we reported on protein-loaded NPs with a size of 0.3-1 µm which are suitable to target dendritic (and other antigen presenting cells) for vaccination purposes [6]. Modern vaccine development has concentrated on the use of delivery systems releasing antigens in a sustained manner. These systems induce greater immune responses than other systems with immediate antigen release [7]. It can also avoid the risk of tolerance. Systems with delayed protein release can substitute the need of several boosting administrations typically required to induce protective immunity.

3) Surface modification and targeting to specific organs or cells

Covering the surface of NPs with the poly(ethylene glycol) is one of the most commonly used strategies to increase the circulation half-life of i.v. injected NPs. It has been reported that the benefit of PEG to increase circulation half-life may compromise the internalization by target cells. As described in Chapter 4, PEGylated PLGHMGA NPs could easily be prepared from mixtures of PEG-PLGHMGA and PLGHMGA. Further optimization of the PEGylated PLGHMGA systems might be required to prolong their circulation time and avoid uptake by reticuloendothelial system (RES). This can be achieved by modulating PEG surface density and thickness simply by varying the amounts of PEG-PLGHMGA and also PEG molecular weight used in nanoparticle formulation. Chapter 4 shows that PEG-PLGHMGA NPs underwent shedding of PEG in around 5 days. This is likely due to greater hydrophilicity of the PLGHMGA matrix and thus a greater water-absorbing capacity that results in a relatively rapid hydrolysis of the ester bond that connects that PEG and PLGHMGA block. This PEG shedding is attractive for the design of polymeric particulate nanocarriers. Given the PEG shedding kinetics (around 5 days) such systems will likely remain sufficiently long in the circulation to accumulate in e.g. tumors at sufficient levels. The PEG coating cleavage on the other hand is fast enough to allow cellular binding and internalization within a few days. These systems are therefore attractive for targeting tumors. Nevertheless, further *in vivo* studies are required to prove this concept. In Chapter 5 we report on Her2 targeted PEGylated PLGHMGA NPs loaded with therapeutic protein (RNase A) which showed considerable cytotoxic effect (IC_{50}:5µM) when compared to non-targeted NPs (IC_{50}:15 µM) and free RNase (up to 100 µM). These results demonstrate that targeting with PLGHMGA nanoparticle formulations conjugated to a nanobody leads to enhanced uptake of NPs. Future studies of this system should be focused on their in vivo evaluation in suitable animal model. Also Mechanistic studies focused on the cellular uptake and processing of the NPs are recommended.

4) Worm like micelles

This thesis deals with the development of NPs based on (PEGylated) PLGHMGA suitable for (intracellular) delivery of proteins. But these NPs also have interesting features for the delivery of low molecular weight/hydrophobic drugs. In Chapter 4 we reported that amphiphilic PEG-PLGHMGA containing ~ 10-16 % w of PEG self-assembled into a mixture of spherical, rod and cylindrical shape. The assembly of amphiphilic diblock copolymers into differently shaped nanostructures depends on weight fraction of the hydrophilic block as well as on the applied processing route (e.g., solvent exchange, film rehydration, pH switch, etc.). Worm micelles have long been reported to form using short-chain amphiphiles ($\leq$1000 g/mol) that have a high critical micelle concentration (CMC). Classical worm micelles are rather unstable and upon dilution, such as injection into the body, they tend to disassemble. In contrast, the worm micelles that are formed from larger amphiphiles have a higher stability. Worm-like micelles can be used as carriers for hydrophobic drugs and they provide important advantages, such as higher drug loading, longer circulation time and even better tumor penetration and therefore higher anti-tumor activity, over spherical formulations (8). Chapter 4 shows that worm shaped micelles were formed from PEG-PLGHMGA of > 10 kg/mol. This is an interesting finding that warrants further investigation.

Conclusions

A novel functionalized polyester, named as PLGHMGA, was first designed and synthesized in our department and its controlled biodegradability and characteristics were thoroughly investigated [9]. In the thesis of Amir Ghassemi [10-12], the potential of the polymers for the development of sustained release microsphere formulations was demonstrated. In present thesis, the feasibility for use of PLGHMGA NPs for the intracellular and targeted delivery of a therapeutic protein has been demonstrated. Yet, further studies should be conducted to investigate the suitability of these systems for i.v administration and tumor therapy.

References

1. Langer R, Folkman J. Polymers for the sustained release of proteins and other macromolecules. Nature 1976;263(5580):797-800.

2. Wu F, Jin T. Polymer-based sustained-release dosage forms for protein drugs, challenges, and recent advances. AAPS PharmSciTech 2008;9(4):1218-1229.

3. Crotts G, Park TG. Protein delivery from poly(lactic-co-glycolic acid) biodegradable microspheres: release kinetics and stability issues. J Microencapsul 1998;15(6):699-713.

4. Yu L, Li K, Liu X, Chen C, Bao Y, Ci T, et al. In vitro and in vivo evaluation of a once-weekly formulation of an antidiabetic peptide drug exenatide in an injectable thermogel. J Pharm Sci 2013;102(11):4140-4149.

5. Yu L, Xu W, Shen W, Cao L, Liu Y, Li Z, et al. Poly(lactic acid-co-glycolic acid)-poly(ethylene glycol)-poly(lactic acid-co-glycolic acid) thermogel as a novel submucosal cushion for endoscopic submucosal dissection. Acta Biomater 2013.

6. Joshi VB, Geary SM, Salem AK. Biodegradable particles as vaccine delivery systems: size matters. AAPS J 2013;15(1):85-94.

7. Demento SL, Cui W, Criscione JM, Stern E, Tulipan J, Kaech SM, et al. Role of sustained antigen release from nanoparticle vaccines in shaping the T cell memory phenotype. Biomaterials 2012;33(19):4957-4964.

8. Dalhaimer P, Engler AJ, Parthasarathy R, Discher DE. Targeted worm micelles. Biomacromolecules 2004 ;5(5):1714-1719.

9. Leemhuis M, vanNostrum CF, Kruijtzer JAW, Zhong ZY, tenBreteler MR, Dijkstra PJ, et al. Functionalized poly (alpha-hydroxy acid)s via ring-opening polymerization: toward hydrophilic polyesters with pendant hydroxyl groups. Macromolecules 2006;39:3500–3508.

10. Ghassemi AH, van Steenbergen MJ, Barendregt A, Talsma H, Kok RJ, van Nostrum CF, et al. Controlled release of octreotide and assessment of peptide acylation from poly(D,L-lactide-co-hydroxymethyl glycolide) compared to PLGA microspheres. Pharm Res 2012;29(1):110-120.

11. Ghassemi AH, van Steenbergen MJ, Talsma H, van Nostrum CF, Crommelin DJ, Hennink WE. Hydrophilic polyester microspheres: effect of molecular weight and copolymer composition on release of BSA. Pharm Res 2010;27(9):2008-2017.

12. Ghassemi AH, van Steenbergen MJ, Talsma H, van Nostrum CF, Jiskoot W, Crommelin DJ, et al. Preparation and characterization of protein loaded microspheres based on a hydroxylated aliphatic polyester, poly(lactic-co-hydroxymethyl glycolic acid). J Control Release 2009;138(1):57-63.

Appendices

Nederlandse samenvatting

Acknowledgments

Cirrriculm Vitae

List of Publications

Nederlandse samenvatting

Farmaceutische onderzoekers hebben gedurende de laatste twee decennia gewerkt aan de ontwikkeling van op polymeren gebaseerde formuleringen van eiwitten en peptiden. De aandacht was met name gericht op de ontwikkeling van macroscopische systemen in de vorm van hydrogelen of polymere microdeeltjes die het ingesloten eiwit/peptide gedurende een lange tijd afgeven. Deze systemen zijn bedoeld voor lokale toediening en de afgegeven bioactieve eiwitten binden aan de receptor die aanwezig is op het celmembraan. Sommige farmaceutische eiwitten zijn echter intracellulaire actief en dientengevolge zijn deze injecteerbare systemen, gebaseerd op hydrogelen en microdeeltjes, niet geschikt voor de afgifte van deze klasse van eiwitten. Voor de intracellulare afgifte van eiwitten/peptiden, en in het bijzonder voor die niet-passief cellulaire membranen passeren, zijn polymere nanodeeltjes kandidaat-afgiftesystemen. Polymere nanodeeltjes bezitten de mogelijkheid om te accumuleren op hun beoogde plaats van werking via het zogenaamde EPR effect, maar zij worden ook opgenomen door de doelcel om vervolgens hun inhoud intracellulair af te geven. Polymelkzuur-co-glycolzuur (of PLGA) is één van de meest bestudeerde polymeren voor de afgifte van farmaca en eiwitten. Er zijn echter, zoals uiteengezet in **Hoofdstuk 1** van dit proefschrift, enkele nadelen verbonden aan het gebruik van dit polymeer voor de ontwikkeling van eiwitformuleringen.

Hoofdstuk 1 van dit proefschrift geeft een algemene inleiding betreffende therapeutische peptiden en eiwitten, uitdagingen voor hun intracellulaire afgifte en verschillende technologieën die tot op heden toegepast zijn om deze kwesties aan te pakken. Er wordt ook een korte beschrijving van gefunctionaliseerde polyesters en hun aantrekkelijke eigenschappen voor eiwitafgifte wordt ook gegeven. In dit proefschrift wordt polymelkzuur-co-glycolzuur-co-hydroxymethylglycolzuur (PLGHMGA) als een alternatief voor PLGA voor het ontwerp van nanodeeltjes als eiwitformuleringen bestudeerd. Tenslotte worden de doelen van dit proefschrift geschetst.

In **Hoofdstuk 2** onderzochten we het effect van de deeltjesgrootte en PLGA -eindgroep op de afbraak van de deeltjes alsmede op de eiwitbelading en -afgifte. PLGA deeltjes met verschillende afmetingen (0.3, 1 and 20 mm) gebaseerd op zuur-getermineerd PLGA (‘’uncapped’’ PLGA) en ester getermineerd PLGA met een lange alifatische staart (een dodecanyl eindgroep; ‘’capped’’ PLGA) zijn gemaakt en beladen met een modeleiwit (runderserum albumine, BSA) met behulp van een dubbelemulsie verdampingsmethode.

Er werd gevonden dat, onafhankelijk van hun afmeting, deeltjes gebaseerd op ʻʻcappedʼʼ PLGA een langzamere degradatie en eiwitafgiftekinetiek vertoonden dan die gebaseerd op ʻʻuncappedʼʼ PLGA, hetgeen waarschijnlijk veroorzaakt wordt door de hydrofobe eigenschappen van dodecanol getermineerd PLGA. Nog belangrijker is dat deeltjes die gebaseerd zijn op ʻʻcappedʼʼ PLGA een onvolledige afgifte van het ingesloten BSA vertoonden (70 % van de belading), terwijl de op ʻʻuncappedʼʼ PLGA gebaseerde deeltjes het eiwit volledig afgaven. Een onoplosbaar residu was aanwezig tot het einde van de studie (175 dagen) voor de BSA beladen deeltjes gebaseerd op ʻʻcappedʼʼ PLGA. Infrarood spectroscopische analyse van dit onoplosbaar residu lieten pieken zien die toegeschreven kunnen worden aan BSA alsmede aan die van PLGA. Dit toont aan dat het residu een mengsel is van onoplosbaar eiwit en degradatieproducten van het polymeer, die verrijkt zijn in dodecanol (NMR analyse). De incomplete afgifte van BSA uit deeltjes gebaseerd op ʻʻcappedʼʼ PLGA kan derhalve toegeschreven worden aan hydrofobe interacties tussen de alifatische dodecanol groep en het eiwit. Omdat veel eiwitten hydrofobe domeinen en holtes bezitten, kunnen dergelijke interacties ook verwacht worden met therapeutische eiwitten.

In **Hoofdstuk 3** hebben we PLGHMGA nanodeeltjes vervaardigd die potentieel geschikt zijn voor de intracellulaire afgifte van eiwitten. Dit hoofdstuk rapporteert over de degradatie van deze deeltjes en het afgiftegedrag van een modeleiwit, runderserum albumine (BSA), van nanodeeltjes met een afmeting tussen de 400 en 700 nm en vervaardigd met polymeren van verschillende molecuulmassa en samenstellingen. Er is ook gekeken naar het effect van verschillende concentraties van PLGHMGA in de organische fase die gebruikt werden voor de deeltjesvervaardiging op de eigenschappen van de deeltjes. Gevriesdroogde deeltjes vertoonden een significante initiële afgifte (“burst”, 40-50% van de BSA belading) dat waarschijnlijk toegeschreven kan worden aan de porositeit van de nanodeeltjes, veroorzaakt door sublimatie van water afkomstig van de primaire water-in-olie emulsie gedurende het vriesdroogproces. Teneinde de ʻʻburstʼʼ te reduceren werden verdere studies uitgevoerd met niet-gevriesdroogde nanodeeltjes. De nanodeeltjes vertoonden een continue verlies van massa die vergezeld werd door een continue afname in aantal gemiddelde molecuulmassa, hetgeen duidt dat de afbraak van de deeltjes plaatsvindt door bulkdegradatie. De concentratie van het polymeer in de organische fase die gebruikt werd om de deeltjes te vervaardigen, had een gering effect op de snelheid waarmee de deeltjes afbreken. Hydrofielere nanodeeltjes, vervaardigd van PLGHMGA met een hoger hydroxymethylglycolzuur gehalte, lieten een snellere afname in zowel molecuulmassa als drooggewicht zien in vergelijking met nanodeeltjes gebaseerd op polymeren met een lager hydroxymethylglycolzuur gehalte. Dit valt toe te schrijven aan een toenemend gehalte van hydroxyl zijgroepen in het polymeer dat resulteert in een toename in wateropname van de deeltjes. De sterkere hydratatie van de polymeermatrix op zijn beurt verhoogt de snelheid van hydrolyse van de estergroepen en ook de doorlaatbaarheid van de matrices voor laag moleculair gewicht en wateroplosbare degradatieproducten. Deeltjes die gebaseerd waren op PLGHMGA met 18% hydroxymethylglycolzuur eenheden vertoonden na een ‘’burst’’ van ongeveer 10-20% een continue afgifte gedurende 30 dagen. Hydrofobere deeltjes (gebaseerd op PLGHMGA met 13% hydroxymethylglycolzuur) vertoonden een twee-fase afgiftepatroon dat gekenmerkt werd door een lag fase van ongeveer 40 dagen gevolgd door een relatief snelle en volledige release van BSA gedurende de daaropvolgende 20 dagen. Deze vindingen illustreren dat afgiftepatronen effectief kunnen worden gemoduleerd door de dichtheid van hydrofiele zijgroepen te variëren. Analyse van de wateronoplosbare residuen van de nanodeeltjes met proton NMR spectroscopische analyse bracht een verandering in de moleculaire structuur van het copolymeer aan het licht welke veroorzaakt bleek te zijn door een intramoleculaire transesterificatie. Een geleidelijke afname in zowel hydroxymethylglycolzuur (in zijn natieve conformatie of als getransesterificeerde eenheden) als glycolzuur gehalte werd gevonden, hetgeen aantoont dat, zoals verwacht, de hydroxymethylglycolzuur en glycolzuur esterbindingen in PLGHMGA gevoeliger zijn voor hydrolyse. Zoals opgemerkt, de nanodeeltjes die bestudeerd zijn in Hoofdstuk 3 hebben een grootte van 400-700 nm. Kleinere deeltjes met een afmeting tussen de 100 en 200 nm zijn echter gewenst om therapeutische eiwitten intracellulair af te geven. In Hoofdstuk 4 werden diblock PEG-PLGHMGA copolymeren met twee verschillende PEG molecuulmassa’s gesynthetiseerd en gekarakteriseerd. Placebo en eiwit-beladen nanodeeltjes werden vervaardigd gebruikmakend van uitsluitend PEG-PLGHMGA, maar ook door PEG-PLGHMGA te mengen met PLGHMGA. BSA en lysozym werden als modeleiwit gebruikt. De amfifiliciteit en oppervlakteactieve eigenschappen van PEG-PLGHMGA stelden ons in staat om gepegyleerde nanodeeltjes te vervaardigen zonder gebruik te maken van een oppervlakteactieve stof in de externe waterfase. Er werd waargenomen dat eigenschappen van de deeltjes, zoals de zeta-potentiaal, morfologie en grootte, aanzienlijk werden beïnvloed door het diblock PEG-PLGHMGA gehalte en de molecuulmassa van PEG. Een aanzienlijk afname in zowel afmeting als in oppervlaktelading werd waargenomen voor nanodeeltjes die PEG-PLGHMGA bevatten met een hogere gewichtsfractie van PEG en langere PEG ketens. Echter, de eiwit-encapsuleringefficientie in de nanodeeltjes, vervaardigd zonder gebruik te maken van een oppervlakteactieve stof, was zeer laag, en de geringe hoeveelheid opgesloten eiwit werd zeer snel en in ongeveer één dag afgegeven.

De insluiting van het eiwit en de afgifte-eigenschappen van gepegyleerde PLGHMGA nanodeeltjes werden verbeterd door gebruik te maken van polyvinyl alcohol (PVA) in het bereidingsprotocol. Er werd waargenomen dat BSA en lysozym efficiënt werden ingebouwd in de nanodeeltjes vervaardigd met PVA als oppervlakteactieve stof. De aanwezigheid van PVA op het grensvlak van de organische en water-fase fungeert waarschijnlijk als barrière voor eiwitdiffusie, niet alleen gedurende de vorming van de deeltjes maar ook gedurende de afgifte vanuit de vast geworden deeltjes. Ook werden uniformere deeltjes gevormd in de aanwezigheid van PVA. De grootte van de deeltjes vervaardigd met PVA was tussen de 240 en 280 nm en werd niet in sterke mate beïnvloed door het PEG gehalte. Van PEG kan verwacht worden dat het aanwezig zal zijn op het oppervlak van de deeltjes, maar dat het ook aanwezig is in de bulk van de deeltjes, vanwege de goede verenigbaarheid van PEG met PLGHMGA, zoals DSC analyse aantoonde. De aanwezigheid van het hydrofiele PEG in de matrix resulteert in een grotere waterabsorptie, waardoor de hydrolysekinetiek van de polymeren, en dus de afbraaksnelheid van de deeltjes, versneld wordt. In het bijzonder is de esterbinding die het PEG en PLGMHGA block met elkaar verbindt, zeer gevoelig voor hydrolyse. Het was verrassend te constateren dat de afbraak van de deeltjes en dientengevolge de eiwitafgiftekinetiek nagenoeg onafhankelijk waren van het PEG-PLGHMGA gehalte en de molecuulmassa van PEG. Deze marginale verschillen konden worden verklaard door de bijna volledige verwijdering van PEG uit de degraderende nanodeeltjes in 5 dagen.

In **Hoofdstuk 5** beoordeelden we de geschiktheid van gepegyleerde PLGHMGA nanodeeltjes voor doelgerichte intracellulaire afgifte van een therapeutisch eiwit. Ribonucleasen zijn kleine basische eiwitten die in staat zijn de afbraak van cytosolair RNA te katalyseren. Dientengevolge hebben deze eiwitten de aandacht in het biomedische en farmaceutische veld getrokken om gebruikt te worden als nieuwe anti-kanker therapeutica. De Her 2 (of humane epidermale groeifactor; EGFR2) receptor is sterk vertegenwoordigd in agressieve types borstkankercellen en is in recente jaren een belangrijk doel voor therapie geworden. Functionele nanolichamen (dit zijn de variabele domeinen van zware keten antilichamen aanwezig in kameelachtigen en sommige haaien) zijn zeer recent ontwikkeld en van het 11A4 nanolichaam is aangetoond dat het specifiek bindt aan de Her2 receptor. Zodoende zijn in Hoofdstuk 5 van dit proefschrift gepegyleerde PLGHMGA nanodeeltjes, voorzien van een Her2 specifiek nanolichaam, ontwikkeld voor de doelgerichte intracellulaire afgifte van RNase. Gepegyleerde deeltjes beladen met RNase werden geanalyseerd voor hun afgiftegedrag. Aangetoond werd dat de deeltjes het eiwit in 10-12 dagen afgaven en een enzymatische meting liet zien dat de biologische activiteit van het eiwit volledig behouden was. Nanodeeltjes die op hun oppervlak gefunctionaliseerd kunnen worden, werden vervaardigd door toevoeging van 10% PEG-PLGA met een reactieve maleimide groep aan het uiteinde van de PEG-keten. Eiwitanalyse bevestigde de succesvolle conjugatie aan de C-terminale cysteine van het nanolichaam hetgeen de aanwezigheid van PEG-PLGA en dus de functionele maleimide groepen op het oppervlakte van de nanodeeltjes impliceert. Een cellulair bindingsexperiment toonde een aanzienlijk hogere binding voor deze nanodeeltjes aan en ook verhoogde opname door kanker cellen met her2 receptoren (Skbr3) dan voor nanodeeltjes zonder nanolichaam. De cytotoxische activiteit van de RNase-beladen en nanolichaam-geconjugeerde nanodeeltjes werd vergeleken met die van vrij Rnase, niet-geconjugeerde RNase-beladen nanodeeltjes en lege nanodeeltjes. De resultaten zowel lege nanodeeltjes als vrij RNase (tot een concentratie van 100 µM) de levensvatbaarheid van de Skb3 cellen niet beïnvloeden, terwijl niet-geconjugeerde nanodeeltjes toxisch waren en leidden tot 75 % celdood bij de hoogste concentratie RNase (28 µM; IC_{50}: 15 µM). En wat nog belangrijker is, nanolichaam-geconjugeerde nanodeeltjes vertoonden een veel sterkere cytotoxiciteit welke resulteerde in 90% celdood bij de hoogste geteste concentratie (28 µM, IC_{50}: 5 µM). Deze resultaten toonden aan dat RNase intracellulair werd afgegeven alwaar het de afbraak van cytosolair RNAs katalyseert dat resulteert in celdoding. Het cytotoxische effect van de RNase-beladen nanodeeltjes is toe te schrijven aan de afgifte van RNase uit de nanodeeltjes in het endosoom dat vervolgens deze cellulaire compartimenten destabiliseert, hetgeen resulteert in translocatie in het cystosol, of vanwege destabilisatie van de endosomen door de deeltjes gevolgd door afgifte van het ingesloten enzym in het cytosol, of door een combinatie van beide processen.

Acknowledgments

My research journey as a PhD has come to its end. It was not an easy road, full of ups and downs and probably the most challenging part of my life. Every moment of my PhD journey has been shared with many people. Herewith, I would like to thank them all who in one way or another helped me to get to this day.

First of all, I would like to express my special appreciation and thanks to my promotor Professor dr. Wim Hennink. I would like to thank you for accepting me into your group and allowing me to grow as a research scientist and demanding a high quality of work in all my endeavors. Your scientific fatherhood and taking good care of my research path will remain as an asset for my entire professional life!

I would also like to gratefully and sincerely thank my co-promotor Dr. Rene van Nostrum whose immense knowledge as well as positive, encouraging attitude was a great aid to shape my interests and ideas. Dear Rene, thank you for your guidance, understanding, patience, and most importantly your presence and support in my most difficult time of doing PhD.

I was very lucky to have Dr. Maryam Amidi as my second co-promotor. Dear Maryam, I cannot thank you enough for all the great efforts you have made to smooth my PhD path. Thank you for sharing your learning experiences, generosity of time to discuss scientific things and your emotional supports and practical tips and advice not only in science but also in my life.

I wish to thank Dr. Tina Vermonden, who was very supportive throughout my PhD project. Dear Tina, thank you for being such a nice person, always willing to help and share some words in times of need.

I am grateful to members of my thesis reading committee, Prof. dr. H. Schellekens, Prof. dr. J. Feijen, Prof. dr. W. Frijlink, Prof. dr H. Vromans and Prof. dr. W. Jiskoot, for investing their precious time to read and offer their invaluable comments.

I would also like to express my gratitude to Prof. dr. Dinarvand and Prof. dr. Atyabi who are my inspiration for my future scientific career.

Dear Robbert Jan and Enrico, I would also like to thank you for the scientific discussions and your challenging questions, which made me further contemplating my research.

Dear Gert, I appreciate your friendly attention and recommendation for my future career.

All the results described in this thesis were accomplished with the help and support of Biopharmacy’s tecnicians and collaborators.

Special thanks goes to Mies whose presence in the lab area was always exciting and fun, and a “daily lab work routine tiredness killer”! Dear Mies, thank you for your always being ready to help, sometimes even without being asked.

Dear Joep, I would like to thank you for being such a friendly person and your very useful tips in my work.

Thank you Louis and Georgi for being around and your help.

I would also like to thank Dr. J. Kemmink for his assistance in taking many NMR spectrums.

Dear Sabrina, I was fortunate to have the chance to work with you. I am very grateful for our scientific discussions and your very precious help in my last and most stressful days of PhD. Thank you for your useful comments on my manuscript, answering my questions and especially delivering them within few hours during Christmas holidays, when almost everyone was very difficult to reach.

In addition, I would like to thank Marta, whose without help and nanobody!, the 5th chapter of my thesis could not be created.

Thanks to friends and my colleagues who made the lab a friendly environment for working.

My dear Iranian friends: Sima, Mazda and Farshad, Fariba and Amir, Mehrnoush and Ali, Sulmaz and Hamid, Mohadeseh, Negar, Neda, Nazila, Nahid, Afrouz, thank you for the nice talks and good times.

I would like to thank my dear Sulmaz K. with whom I really had a joyful time during my first year of PhD and also travel to US. Dear Sulmaz, your company and being always by my side is very precious to me.

I would like to thank Merel, Filis, Rachel, Yang and Luis, Sohail, Andhyk, Burcin, Kristel, Reka, Dandan and Yinan, Jan Jaap, Erik T., Luann, Jos, Meriem, Audry, Shima, Paul and Kimberly simply

for being around, for sharing some thoughts every now and then, and for always being friendly. I wish you all good luck and success in your future career.

Thank you former Utrecht people: Isil and Afrouz (I enjoyed all the adventures in Hawaii with you!), Markus, Sytze and Niels, Emmy, Melody, Anastasia, Grzegorz, Amir. V. and Roy.

I had the chance to supervise a few highly motivated students: Michael, Andreia, Samir and Anna.

Anna, thank you for being such a great reliable person to whom I could not only talk about running experiments but also about my problems and excitements. Through the whole year of challenging the inevitable ups and downs of “PLGA experiments”, working late nights and weekends (sometimes even without me being there...) did not seem to bother you. You were even always around to lend a hand with my experiments, I appreciate that more than you know. I would also like to thank my first teachers in Utrecht University, Amir G. and Hajar.

I would like to thank Roy and Erik, who have given me great friendship and support for making my thesis ready.

Dear Roy, thank you for your sincere help and guidance.

Dear Erik, special thanks to you for your generous offer to help; for the cover design and providing me with the InDesign software to layout my thesis. If it had not been for your help, I would have faced many problems to make everything ready on time. I am very impressed by your computer skills, by the way.

Dear Barbara, I am grateful to your kind assistance and your supportive words.

I have very special friends to thank, going back to my pre-PhD days: Azadeh and Mahta, Asal, Nazanin, Fati and Narges.

I was lucky enough to get to know some very nice family friends here: Manizheh joon and agha Rasoul, Neda and Arash, Noushin and Payam, that I would like to thank them all for their moral supports and all the fun time.

Finally, I want to thank my parents I am deeply indebted to for their support, encouragement and their wise advices and endless love.

My wonderful brother and sister in-law: Reza and Nafiseh, thank you for always being there for me.

I would like to thank my in-laws family for their spiritual supports especially my father in-law, who was my inspiration to persue my studies.

My aunty Habbibeh joon and my dear cousin Bahareh, thank you very much for all your kind supports you have given me.

Yaser jan, where would I be without you? You deserve my greatest gratitude, and lots of love and respect. I am very happy that living in The Netherlands gave me this opportunity to get to know you more. I really deeply appreciate your calm, kind and caring nature. Thank you for all your unconditional support, and for putting up with me when I am being impossible and grumpy. I hope that we stay together forever.

Curriculum vitae:

Neda Samadi was born on February 5th 1978 in Tehran, Iran. After finishing high school, she passed the National Academic Entrance Exam for Medical Sciences to study pharmacy at the Faculty of Pharmacy Tehran University of Medical Sciences. Her Pharm D. research project entitled: “ Synthesis of Piracetam, a pharmaceutical raw material in lab scale” was conducted under the supervision of Prof. A. Shafiee. Neda successfully completed her Pharmacy Doctorate Degree (Pharm. D) in 2002. After one year of training she was appointed as an expert of biopharmaceutical products (Vaccine quality assurance and GMP Inspection Expert) at the Ministry of Health, Tehran, Iran. In 2007, she was awarded a scholarship from Tehran University to continue with her studies under the supervision of Prof. Wim Hennink, Dr. Rene van Nostrum, Dr. Maryam Amidi and Dr. Tina Vermonden. Neda started her PhD project in 2009 entitled “Biodegradable nanoparticles based on aliphatic polyesters; towards targeted intracellular delivery of protein therapeutics” the results of which are presented in this thesis.

List of Publications

N. Samadi, C. F. van Nostrum, T. Vermonden T, M. Amidi, W. E. Hennink. Mechanistic studies on the degradation and protein release characteristics of poly(lactic-co-glycolic-co-hydroxymethylglycolic acid) nanospheres. Biomacromolecules, 14(4):1044-1053 (2013).

N. Samadi, A. Abbadessa, A. Di Stefano, C.F. van Nostrum, T. Vermonden, S. Rahimian, E. A. Teunissen, M.J. van Steenbergen, M. Amidi, W.E. Hennink. The effect of lauryl end-group capping on protein release and degradation of poly(D,L-lactic-co-glycolic acid) particles. Journal of Controlled Release, 172(2):436-43 (2013).

N. Samadi, M. J. van Steenbergen, J. B. vanden Dikkenberg, T. Vermonden, C. F. van Nostrum, M. Amidi, W. E. Hennink. Nanoparticles based on a hydrophilic polyester with a sheddable PEG coating for protein delivery. Accepted for publication.

N. Samadi, M. M. Kijanka, S. Oliveira, T. Vermonden, C. F. van Nostrum, M. Amidi, P. M. P. van Bergen en Henegouwen, W.E. Hennink. Nanobody-targeted and RNase-loaded nanoparticles based on a hydrophilic polyester aimed for cancer therapy. Manuscript in preparation.